

**CARDIOPROTECTION BY HIGH DENSITY LIPOPROTEIN IS MEDIATED BY
THE SCAVENGER RECEPTOR CLASS B TYPE 1**

**CARDIOPROTECTION BY HIGH DENSITY LIPOPROTEIN IS MEDIATED BY
THE SCAVENGER RECEPTOR CLASS B TYPE 1**

By Kristina Durham, BSc, MSc

A thesis submitted to the School of Graduate Studies in Partial Fulfilment of the
Requirements for the Degree Doctorate of Philosophy

McMaster University © Copyright by Kristina Durham, August 2016

McMaster University Doctor of Philosophy (2016) Hamilton, Ontario (Medical Sciences)

TITLE: Cardioprotection by High Density Lipoprotein is Mediated by the Scavenger
Receptor Class B Type 1

AUTHOR: Kristina Durham, BSc (University of Waterloo), MSc (University of
Waterloo)

SUPERVISOR: Professor Bernardo Trigatti

NUMBER OF PAGES: 186

Lay Abstract

High density lipoproteins are known to protect against cardiac stress and cardiovascular disease. The scavenger receptor class B type I is a high affinity high density lipoprotein receptor, though its role in mediating the protective effects of high density lipoprotein on the heart has yet to be thoroughly examined. We have shown that high density lipoprotein protects against different types of cardiomyocyte death induced by various stressors on the heart, and that in each case, high density lipoprotein requires the scavenger receptor class B type I to trigger downstream cardioprotective signaling through phosphoinositide 3-kinase, and protein kinase B.

Abstract

Cardiovascular disease and cancer are the leading causes of death in Canada and are a major burden to the health of developed societies. Three quarters of all cardiovascular related deaths are due to ischemic heart disease and heart attack.

Doxorubicin is an effective and commonly used chemotherapeutic that has deleterious side effects including cardiotoxicity and heart failure, thereby limiting its long term use.

In a recent study both reconstituted and native high density lipoprotein particles provided protection against doxorubicin-induced cell death *in vitro*, and a number of studies have implicated high density lipoprotein in protection against myocardial ischemia. As high density lipoprotein provides protection to cardiomyocytes undergoing cardiotoxic stress, or ischemic stress, we postulate that it may be a notable target for protection against the deleterious effects of cardiac stress. The scavenger receptor class B type I is a high-affinity high density lipoprotein receptor, and its role in facilitating high density lipoprotein mediated signaling in the cardiomyocyte has yet to be assessed. Here we have evaluated whether increasing high density lipoprotein protects cardiomyocytes and the heart against cardiotoxic or ischemic stress, and the signaling mechanisms involved.

We have shown that increasing plasma high density lipoprotein attenuates the cardiotoxic effects of doxorubicin, and that high density lipoprotein protects isolated cardiomyocytes against necrosis induced by simulated ischemia. Our findings presented here demonstrate a critical role for cardiomyocyte scavenger receptor class B type 1 in facilitating high density lipoprotein mediated protection. We have also identified phosphoinositide 3-

kinase and protein kinase B as downstream mediators in the cardioprotective signaling cascade by high density lipoprotein and the scavenger receptor class B type I.

Acknowledgements

This thesis could not have been possible without the support of those around me. I give my sincerest thanks to those who have played a role in my life the past four years- both within and outside of the lab. You have all played a hand in shaping me into the scientist that I am today.

I would first like to express my gratitude to my supervisor, Dr. Bernardo (Dino) Trigatti. Your expertise, guidance, and patience have helped guide me throughout this process. With most of the experimental techniques that I used being new to the lab, I appreciate having had your guidance in developing and validating these protocols. I especially admire your vast knowledge, skill for writing, and love of science. It is from you that I have learned the important skill of critical thinking.

I would like to thank my committee members, Dr. Greg Steinberg, and Dr. Judy West-Mays for sharing their time, expertise, and encouragement over the past four years.

To my parents, Scott and Laurie, who have supported me in more ways than they can imagine throughout this journey. I am so grateful for your continued encouragement, and willingness to go out of your way to help me with absolutely anything that I needed.

Ryan- thank you for supporting me in my decision to pursue a long path as a 'professional student'. You have always encouraged me to be ambitious in my professional goals and your continued support in this is truly beyond compare.

To those who have been a part of the Trigatti lab, and those friends at McMaster-
I thank you for making my time here so enjoyable, especially to Melissa for your
continued support with the animal work, and for just being a great co-worker! I have
been fortunate to work with and make friends with very positive and encouraging people,
and feel privileged to have spent the past four years at McMaster.

Table of Contents

Lay Abstract.....	iii
Abstract	iv
List of Tables and Figures.....	xii
List of Abbreviations and Symbols.....	xvi
Chapter 1. General Introduction	1
1.1. Cardiac Health and Stress	1
1.2. Cardiac Stress; Doxorubicin Induced Cardiotoxicity	1
1.3. Mechanisms of DOX Cardiotoxicity	2
1.4. Mechanisms of DOX Cardiotoxicity: Role of Top-2 β	4
1.5. Mechanisms of DOX Cardiotoxicity: Cardiomyocyte Atrophy	5
1.6. Cardiac Stress: Myocardial Ischemia.....	7
1.7. Role of Calcium Overload in Myocardial Ischemic Injury and DOX Cardiotoxicity	8
1.8. Role of Oxidative Stress in Myocardial Ischemic Injury and DOX Cardiotoxicity	9
1.9. Lipoproteins	11
1.10. HDL Composition and Classes.....	11
1.11. HDL Biogenesis.....	13

1.12.	HDL Remodelling.....	14
1.13.	Cardioprotective Nature of HDL	15
1.14.	PI3K/AKT- A Cardioprotective Signaling Pathway.....	17
1.15.	Scavenger Receptor Class B Type I.....	21
1.16.	Intracellular Signaling by HDL through SR-B1	24
1.17.	Rationale for the Role of SR-B1 in HDL Mediated Cardioprotection	25
1.18.	Simulation of Myocardial Ischemia.....	27
1.19.	Overview of Mouse Strains Used in Experimentation	27
1.20.	Overall Context and Objectives	29
Chapter 2. Aims and Hypotheses of Thesis.....		31
Chapter 3. HDL Requires SR-B1, PI3K and AKT1 to Protect Against Doxorubicin Induced Cardiotoxicity.....		33
3.1.	Preface.....	33
3.2.	Abstract.....	33
3.3.	Introduction.....	35
3.4.	Results.....	36
3.5.	Discussion.....	43
3.6.	Methods.....	48

3.7.	Figures.....	55
3.8.	References.....	77
Chapter 4. Therapeutic Administration of ApoA1 Protects Against Doxorubicin Induced Cardiomyocyte Apoptosis..... 83		
4.1.	Preface.....	83
4.2.	Abstract.....	83
4.3.	Introduction.....	84
4.4.	Results.....	86
4.5.	Discussion.....	88
4.6.	Methods.....	90
4.7.	Figures.....	94
4.8.	References.....	98
Chapter 5. HDL protects cardiomyocytes against necrosis induced by simulated ischemia, through SR-B1, PI3K, and AKT1/2 100		
5.1.	Preface.....	100
5.2.	Abstract.....	100
5.3.	Introduction.....	101
5.4.	Results.....	103
5.5.	Discussion.....	106

5.6.	Methods.....	109
5.7.	Figures.....	113
5.8.	References.....	119
Chapter 6.	Limitations, and Future Directions	125
Chapter 7.	Conclusions.....	133
Chapter 8.	References.....	134

List of Tables and Figures

Chapter 1

Figure 1.1 Structure of DOX.	4
Figure 1.2 Mechanisms of DOX induced cardiotoxicity.	6
Figure 1.3 Basic depiction of HDL.	13
Figure 1.4 Cardioprotective Targets of AKT.	21
Figure 1.5 Depiction of HDL binding to SR-B1.	23
Table 1.1 Information Pertaining to Mouse Models.	29
Figure 1.6 Proposed mechanism of HDL mediated protection against the cardiac stressors DOX and OGD.	30

Chapter 3

Figure 3.1 Mice overexpressing ApoA1 are resistant to DOX induced cardiotoxicity. ..	55
Figure 3.2 Mice lacking SR-B1 are not protected against DOX induced cardiotoxicity when ApoA1 is overexpressed.	57
Figure 3.3 Treatment of mice lacking SR-B1 with DOX leads to exacerbated cardiomyocyte apoptosis.	58
Figure 3.4 SR-B1 is required for protection of HIVCM and NMCM against DOX induced apoptosis <i>in vitro</i>	59
Figure 3.5 Hearts lacking SR-B1 are more sensitive to DOX induced apoptosis in the presence of wild type HDL.	61

Figure 3.6 Overexpression of ApoA1 increases activation of AKT under stressed conditions whereas knockout of SR-B1 abolishes this effect of ApoA1 overexpression.	62
Figure 3.7 Protection by HDL against DOX induced apoptosis requires PI3K, and AKT.	63
Figure 3.8 Protection by HDL against DOX-induced apoptosis requires AKT1 and AKT2.	65
Supplementary Figure 3.1 Plasma ApoA1 and HDL-C levels.	66
Supplementary Figure 3.2 Plasma ApoA1 and HDL-C levels.	67
Supplementary Figure 3.3 SR-B1 expression levels do not differ in ApoA1 ^{+/+} and ApoA1 ^{Tg/Tg} heart homogenates following 5 weekly injections of saline or DOX.	68
Supplementary Figure 3.4 Immunofluorescent staining of SR-B1 in SR-B1 ^{+/+} or SR-B1 ^{-/-} NMCM or HIVCM.	68
Supplementary Figure 3.5 HDL but not LDL protects HIVCM against DOX-induced cell death.	69
Supplementary Figure 3.6 NMCM isolated from litters born to parents on chow diet and probucol diet respond to DOX and HDL similarly.	71
Supplementary Figure 3.7 Host macrophages (SR-B1 ^{+/+}) are present in both SR-B1 ^{+/+} and ^{-/-} transplanted hearts.	72
Supplementary Figure 3.8 Activation of AKT by HDL.	73
Supplementary Figure 3.9 AKT inhibition by LY294002 and AKT Inh V.	73

Supplementary Figure 3.10 Female mice lacking SR-B1 have exacerbated cardiomyocyte apoptosis following a single injection of DOX.....	74
Supplementary Table 3.1 Physical Characteristics of Mice.	74
Supplementary Table 3.2 Physical Characteristics of Mice	75
Supplementary Table 3.3 Physical Characteristics of Mice	75
Supplementary Table 3.4 List of siRNAs	75
Supplementary Table 3.5 List of Primary Antibodies	76
Supplementary Table 3.6 List of Secondary Antibodies	76
<u>Chapter 4</u>	
Figure 4.1 Experimental timeline.	94
Figure 4.2 IP injection of ApoA1 increases plasma ApoA1 levels.	95
Figure 4.3 Increasing ApoA1 by injection protects against the apoptotic effect of a single DOX injection.	96
Figure 4.4 AKT is activated in an ApoA1 and stress dependent manner at Ser473.....	97
Table 4.1 Animal Characteristics.....	97
<u>Chapter 5</u>	
Figure 5. 1 HDL protects against OGD-induced necrosis of HIVCM	113
Figure 5.2 4 hrs of OGD induced necrosis of cardiomyocytes.....	115
Figure 5.3 SR-B1 is required for HDL mediated protection of NMCM against OGD-induced necrosis.....	116
Figure 5.4 SR-B1 is required for HDL-mediated protection of HIVCM against OGD-induced necrosis, and activation of AKT.....	117

Figure 5.5 PI3K, AKT1, and AKT2 are required for HDL mediated protection of
HIVCM against OGD-induced necrosis. 118

List of Abbreviations and Symbols

$\pm dP/dt$	Rate of pressure development and decline
ABCA1	ATP-binding cassette transporter A1
ABCG1	ATP-binding cassette transporter G1
AKT	Protein Kinase B
AMPK	AMP activated protein kinase
Apo	Apolipoprotein
BAD	Bcl-2 associated death promoter
BAX	Bcl-2 associated X protein
Bcl-2	B-cell lymphoma 2
Ca ²⁺	Calcium
CAD	Coronary artery disease
CETP	Cholesterylester transfer protein
CHD	Coronary heart disease
CHF	Congestive heart failure
CHO	Chinese hamster ovary cells
CON	Control
CSA	Cross sectional area
cTNT/cTNI	Cardiac troponin T/I
CVD	Cardiovascular disease
DHCR24	3 β -hydroxysteroid- Δ 24 reductase

DMEM	Dulbecco's Modified Eagle Medium
DOX	Doxorubicin
DXZ	Dexrazoxane
EL	Endothelial lipase
eNOS	Endothelial nitric oxide synthase
ER	Endoplasmic reticulum
ERK	Extracellular signal regulated kinases
FBS	Fetal bovine serum
FC	Free cholesterol
FOXO	Forkhead box transcription factor
FPLC	Fast protein liquid chromatography
GLUT4	Glucose transporter type 4
GSH	Glutathione
GSK-3 β	Glycogen synthase kinase 3 beta
HBSS	Hank's balanced salt solution
HDL	High density lipoprotein
HIVCM	Human immortalized ventricular cardiomyocytes
HL	Hepatic lipase
HO-1	Heme oxygenase-1
IDL	Intermediate density lipoproteins
i.p.	Intraperitoneal

IR	Ischemia reperfusion
IRI	Ischemia reperfusion injury
K ⁺	Potassium
LAD	Left anterior descending
LCAT	Lecithin-cholesterol acyltransferase
LDL	Low density lipoprotein
LDLR	Low density lipoprotein Receptor
LVEDP	Left ventricular end diastolic pressure
LVESP	Left ventricular end systolic pressure
MAPK	Mitogen activated protein kinase
M199	Media 199
MI	Myocardial infarction
MnSOD	Manganese superoxide dismutase
mTOR	Mammalian target of rapamycin
mTORC2	Mammalian target of rapamycin Complex 2
Na ⁺	Sodium
NCLPDS	Neonatal calf lipoprotein deficient serum
NMCM	Neonatal mouse cardiomyocytes
O ₂	Oxygen
OGD	Oxygen glucose deprivation
PBS	Phosphate Buffered Saline

PDK1	Phosphoinositide-dependent protein kinase 1
PDZK1	PDZ domain containing 1
PH	Pleckstrin Homology
PI3K	Phosphoinositide 3-kinase
PIP2	Phosphatidylinositol (4,5) bisphosphate
PIP3	Phosphatidylinositol (3,4,5) trisphosphate
PKC	Protein kinase C
PTEN	Phosphatase and tensin homolog
RCT	Reverse cholesterol transport
rHDL	Reconstituted HDL
ROS	Reactive oxygen species
S1P	Sphingosine 1-phosphate
S1PR	Sphingosine 1-phosphate receptor
Ser473	Serine 473
SERCA2a	Sarcoendoplasmic reticulum calcium ATPase 2a
siRNA	Silencing RNA
SR	Sarcoplasmic reticulum
SR-B1	Scavenger receptor class B type I
Src	Proto-oncogene tyrosine-protein kinase Src

STAT3	Signal transducer and activator of transcription 3
Thr308	Threonine 308
Top-2 β	Topoisomerase 2 β
TUNEL	Terminal deoxynucleotidyl transferase dUTP nick end labelling
UPR	Unfolded protein response
UV	Ultraviolet
VLDL	Very low density lipoprotein
WT	Wild-type

Chapter 1. General Introduction

1.1. Cardiac Health and Stress

The heart, a vital organ of life, faces the obstacle of functional recovery following injury caused by stressors such as myocardial ischemia or drug induced cardiotoxicity. The heart is severely limited in its ability to regenerate cardiomyocytes as their proliferative capacity is low (1). Although researchers have identified cardiomyocytes being replaced in the adult heart, due to low capacity for regeneration the heart is unable to compensate for severe cardiomyocyte loss due to myocardial ischemia or cardiotoxicity (2, 3). Following cardiac injury the heart cannot replace dead myocardium, and so it attempts to replace lost tissue with fibrotic deposition, or hypertrophic remodelling (4). Ultimately, loss of cardiomyocytes compromises cardiac contractility and can lead to heart failure (4). The obstacle of limited regeneration highlights the importance of protecting the heart against the initial cardiac stress and thereby preventing cardiomyocyte loss.

1.2. Cardiac Stress; Doxorubicin Induced Cardiotoxicity

Cancer is a leading cause of death in developed societies (5). The two most commonly used anthracycline-based chemotherapeutics for both children and adults are doxorubicin (DOX) and daunorubicin. Terminal half life of DOX in humans is 24-48 h, and for a single dose of 60mg/m^2 , the peak plasma concentration is 2-6 $\mu\text{g/mL}$ (6, 7). DOX's pleiotropic use is highlighted by its ability to treat tumors of both solid and hematologic origin (8), though anthracycline therapeutics including DOX are limited in their long-term use due to dose-dependent cardiotoxicity (9). The cardiotoxic side effects range from less severe asymptomatic left ventricular dysfunction, to problematic

arrhythmias and severe symptomatic congestive heart failure (CHF) (8, 9). The estimated cumulative percentage of patients with CHF was 5% in patients receiving a cumulative DOX dose of $400\text{mg}/\text{m}^2$, which increased to 26% at a dose of $550\text{mg}/\text{m}^2$, and 48% at $700\text{mg}/\text{m}^2$ (9). Onset of cardiac dysfunction typically occurs within the first year following the termination of chemotherapy in adults, though in survivors of childhood cancer, onset can be delayed by 4-20 years (10-12). In fact, survivors of childhood cancer now represent a new, vast, group of adults at risk of developing premature cardiovascular disease (CVD).

1.3. Mechanisms of DOX Cardiotoxicity

DOX enters tissues and cells by passive diffusion across the plasma membrane. DOX is a tetracyclic quinoid aglycone, with an amino sugar (see Figure 1.1). Its quinone moiety acts as an electron acceptor, and following cellular uptake DOX can undergo redox cycling, resulting in production of reactive oxygen species (ROS) and oxidative stress (13). DOX can reportedly bind to the cytoplasmic proteasome, which assists in the translocation of DOX to the nucleus by an ATP-dependent nuclear pore-mediated mechanism (14), where DOX can interact with DNA and induce DNA strand breaks (15). Additionally, DOX binds anionic membrane phospholipids and more specifically, cardiolipin- a major cardiomyocyte mitochondrial inner membrane phospholipid, with high affinity (16). At the mitochondria, cardiolipin plays an integral role in mediating and stabilizing components of the electron transport chain, and therefore affects energy metabolism (17). It remains to be tested whether DOX binding to cardiolipin causes defects in energy metabolism or structural changes to the mitochondrial membrane.

At the cellular level, DOX initiates its deleterious effects from within the cytoplasm, mitochondria, and nucleus, and promotes suppression of protein synthesis, ultrastructural changes, alterations to energy metabolism, and alterations in cellular signaling (18). These deleterious effects can cause cardiomyocyte death, atrophy, and impaired cardiac function (18). DOX-induced cardiomyocyte death occurs mainly by way of apoptosis, however; autophagy and necrosis have also been implicated (19, 20). Although interrelated and complex, the mechanisms of DOX-induced cardiotoxicity can be grouped into three subsets; oxidative stress, formation of the topoisomerase 2 beta (Top-2 β)-DOX-DNA cleavage complex, and dysregulation of intracellular calcium (Ca²⁺) release. Research demonstrates that these mechanisms are activated in a cooperative and concerted manner to induce cardiomyopathy. Similar mechanisms also play a role in cardiac injury induced by myocardial ischemia, which will be discussed later in this introduction.

Therapeutic strategies developed for protection against DOX cardiotoxicity have yielded mixed results, leaving dose modification as the most effective approach. Although not endorsed worldwide, dexrazoxane (DRZ) is currently the only United States Food and Drug Administration, and Health Canada approved drug for use in combination with DOX to limit cardiotoxicity in adults (21). DRZ acts as an iron chelator, interferes with ROS production, can bind to Top-2 β to inhibit complex formation with DOX, and also reduce Top-2 β expression (22-24). A recent systematic review found an association of DRZ with reduced risk of cardiovascular complications, but increased risk of secondary malignant neoplasms in children receiving chemotherapy

(25). Given these results, Health Canada cautions against use of DRZ in children, as well as in elderly populations with reduced cardiac, hepatic, or renal function.

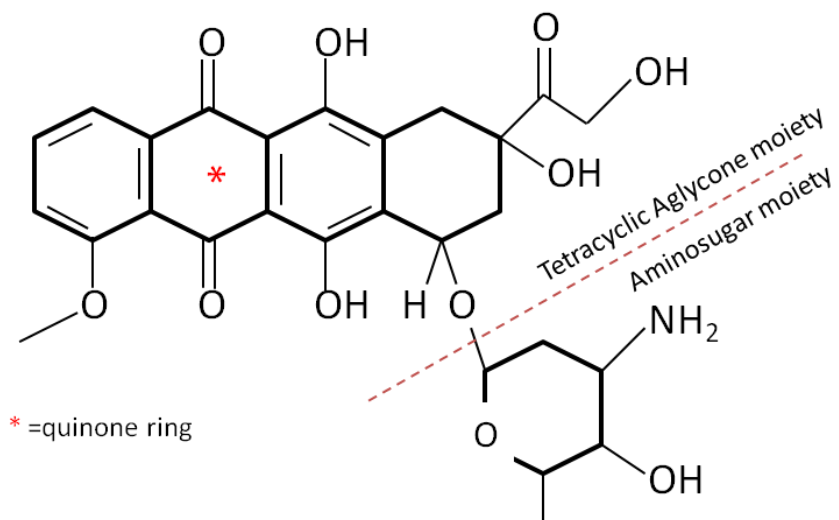


Figure 1.1 Structure of DOX.

DOX is comprised of a tetracyclic aglycone moiety and an aminosugar. Redox cycling occurs at the quinone ring indicated by a red star. Modified from National Institutes of Health, National Center for Biotechnology Information, PubChem, 2016.

1.4. Mechanisms of DOX Cardiotoxicity: Role of Top-2 β

Recently, Top-2 β was identified as a molecular mediator of DOX cardiotoxicity. Top-2 β is found in both the nucleus and mitochondria, and is an important mediator of DNA topology (15). Top-2 β alters the topology of DNA by catalyzing the breaking and rejoining of DNA in order to allow for strands to pass by one another (15). DOX directly binding to Top-2 β and DNA forms the Top-2 β —DOX—DNA cleavage complex (26). By binding to Top-2 β , DOX reportedly induced DNA strand breaks and disrupts

rejoining of DNA, resulting in cell death (27). The potential for crosstalk between mechanisms should be noted as chronic DOX exposure alters expression of genes involved in mitochondrial function and oxidative metabolism, which are improved by cardiomyocyte specific deletion of Top-2 β (26).

1.5. Mechanisms of DOX Cardiotoxicity: Cardiomyocyte Atrophy

A hallmark feature of DOX cardiotoxicity is myofibril structural disarray, and atrophy- a reduction in cardiomyocyte cross sectional area (CSA), and these ultrastructural changes to the myocardium appear well before clinical manifestations (28). Given that cardiomyocyte size is related to overall force generation during contraction, reduced cardiomyocyte CSA in diseased states will eventually manifest as a reduction in cardiac function, as in the case of DOX-cardiotoxicity (29). The ubiquitin proteasome is a critical regulator of cardiomyocyte size, and does so by tagging proteins for degradation (30). Atrogin-1 is a muscle specific ubiquitin lygase that facilitates atrophic signaling in cardiomyocytes by promoting protein degradation (30). DOX upregulates Atrogin-1 in cardiomyocytes in a p38-mitogen activated protein kinase (MAPK) dependent manner leading to degradation of contractile proteins, and reduction in cardiomyocyte size (31).

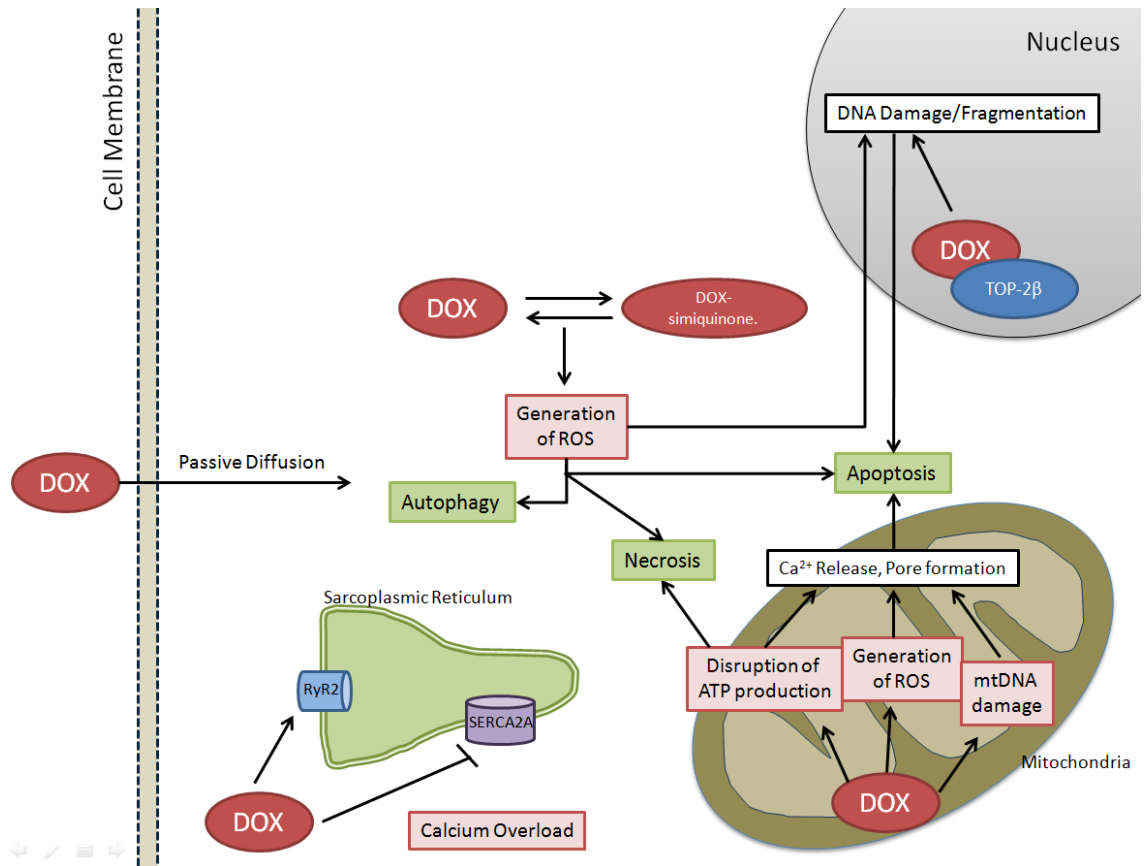


Figure 1.2 Mechanisms of DOX induced cardiotoxicity.

DOX enters the cell by passive diffusion, and within the cytoplasm undergoes redox cycling resulting in the generation of ROS, and oxidative stress. Oxidative stress is known to contribute to activation of autophagic, necrotic, and apoptotic pathways of cell death. DOX can promote Ca^{2+} overload by inhibiting SERCA2a and transiently enhancing the activity of RyR2. DOX can bind cardiolipin, a major inner mitochondrial membrane lipid. At the mitochondria DOX promotes damage to mitochondrial DNA (mtDNA), disruption of mitochondrial function and therefore ATP production, and promotes the generation of ROS, all of which can contribute to initiation of cell death. Adapted from Burrige, PW, et al. Human induced pluripotent stem cell-derived

cardiomyocytes recapitulate the predilection of breast cancer patients to doxorubicin-induced cardiotoxicity. 2016. *Nature Medicine*. 22, 547–556.

1.6. Cardiac Stress: Myocardial Ischemia

Cardiovascular disease (CVD) is a leading cause of death and a major burden to the healthcare systems of developed societies (32). Three quarters of all cardiovascular related deaths are due to ischemic heart disease and heart attack (32). Partial or complete occlusion in one or more areas of the coronary tree renders an ischemic myocardial environment, which if left un-perfused, results in myocardial infarction due to irreversible death of cardiomyocytes (33). Non-infarcted areas must compensate for the lack of contractile activity of infarcted tissue and over time increased demand on the non infarcted tissue may lead to detrimental functional changes such as hypertrophy, and can lead to heart failure (33); therefore it is of utmost importance to prevent or limit the amount of cardiomyocyte loss.

Obstruction of blood flow at the myocardium causes a block in the supply of oxygen (O₂) and nutrients to the myocardium, in addition to inhibiting the clearance of cardiac metabolites. This can alter cellular homeostasis and result in cardiomyocyte death by way of necrosis, programmed necrosis (necroptosis), apoptosis, and autophagy (34-36). The form of death that a cardiomyocyte undergoes is dependent on several factors including the magnitude and duration of the ischemic event, and location of the cardiomyocyte with respect to the ischemic environment (35, 37).

Under normoxic conditions, 60-70% of energy in the heart is derived from aerobic oxidation of fatty acids (38). Cellular homeostasis largely relies on regulation of energetic ATP supply; and under ischemic conditions- when cellular O₂ levels are low,

the cardiomyocyte relies heavily on anaerobic ATP production (39, 40). ATP production by anaerobic metabolism is inefficient in comparison to aerobic metabolism in the cardiomyocyte, and is paired with the production of inorganic phosphate, lactate, and H^+ which accumulate in and around an ischemic cardiomyocyte, and ultimately increases pH (36, 41). Inefficient ATP synthesis reduces or inhibits the function of ATP-dependant pumps, and as a consequence promotes intracellular accumulation of sodium and depletion of potassium (34, 41). Imbalances in the ionic state across cellular membranes lead to membrane swelling and rupture, and further impairs regulation of cytoplasmic Ca^{2+} , the implications of which will be discussed below (34, 41).

1.7. Role of Calcium Overload in Myocardial Ischemic Injury and DOX Cardiotoxicity

Ca^{2+} overload is a mechanism of both DOX cardiotoxicity and myocardial ischemic injury. Ca^{2+} release from the sarcoplasmic reticulum (SR) is required for cardiac contraction, and it is therefore of importance to regulate its release and uptake by the SR (42). Inability of the SR to take up Ca^{2+} or increased release of Ca^{2+} would lead to consistently high cytoplasmic levels, resulting in impaired relaxation of the cardiac muscle (42). Regardless of the initiating cardiac stress (cardiotoxic drug or ischemia), a rise in cytosolic Ca^{2+} leads to non cycling actin-myosin cross bridges, membrane rupture (a hallmark feature of necrosis), and cellular damage caused by activation of Ca^{2+} dependent phospholipases, proteases, and calpain (a mediator of apoptosis) (34). Physiologically these detrimental cellular changes manifest as arrhythmias, or myocardial contracture (42).

The ryanodine receptor 2 (RyR2) and the sarcoendoplasmic reticulum ATPase 2a (SERCA2a) regulate calcium release and uptake from the SR, and thereby contribute to coordination of the cardiomyocyte contractile cycle. Both DOX, and doxorubicinol- a metabolite of DOX, can bind and inhibit SERCA2a as well as bind RyR2 and in a biphasic effect enhance and then inhibit RyR2 activity (43, 44). Given the role of RyR2 in mediating calcium release from the SR, and SERCA2a in transporting calcium from the cytosol to the SR, DOX and doxorubicinol promote accumulation of cytoplasmic Ca^{2+} (43, 44). In the case of myocardial ischemia, a rise in cytosolic Ca^{2+} occurs due to lack of ATP required for normal function of SERCA2a and other ATP dependent Ca^{2+} pumps (34). Overall, Ca^{2+} overload can be induced by both cardiotoxic and ischemic stress and leads to death and dysfunction of cardiomyocytes.

1.8. Role of Oxidative Stress in Myocardial Ischemic Injury and DOX Cardiotoxicity

Redox signaling is a crucial component of normal and pathophysiological responses of cells. The cardiomyocyte is armed with several classes of enzymes to combat ROS including, but not limited to, superoxide dismutase (SOD), glutathione (GSH), catalase, and peroxidases (45). Changes to the cellular redox state through alterations in the balance between oxidant and reductant levels can trigger signaling cascades that lead to an outcome of cell proliferation, differentiation, or death (46). Reaction of free radicals with oxygen (O_2) can spur chain reactions with some amino acids, peptides, and proteins to yield hydroperoxides (34, 46). Hydroperoxides are key species in protein damage, and can initiate DNA strand breaks, both of which promote cardiomyocyte death and dysfunction (34, 46).

Oxidative stress is a factor involved in both DOX cardiotoxicity and myocardial ischemic injury. In the ischemic cardiomyocyte, ROS contribute to dysfunction of the mitochondria, activation of apoptosis, and Ca^{2+} overload (46). Oxidative stress activates apoptosis by opening the mitochondrial permeability transition pore and subsequent release of pro-apoptotic proteins (46). In addition, ROS have been reported to contribute to ischemia-induced dysfunction of mitochondrial respiration and oxidative phosphorylation (47). ROS also contribute to defective Ca^{2+} handling by impairment of SERCA activity, thereby reducing Ca^{2+} transport into the SR, and exacerbating Ca^{2+} overload within the ischemic cell (48, 49).

Upon cellular uptake, DOX readily undergoes redox cycling between its quinone and semiquinone forms thereby generating substantial amounts of ROS (13). Additionally, DOX increases accumulation of iron within the mitochondria, leading to further ROS production (50). Paired with production of ROS, DOX treatment reduces the activity and expression of matrix manganese SOD (MnSOD) and GSH peroxidase (51), further promoting oxidative stress. Given the high levels of ROS associated with DOX-treatment and reduction in antioxidant expression, one would hypothesize antioxidant therapy may be useful for cardioprotection against DOX. Administration of antioxidants such as vitamin E, or N-acetylcysteine to dogs yielded inconsistent results (52, 53). In a prospective randomized clinical trial, N-acetylcysteine was ineffective in protecting against anthracycline induced cardiotoxicity (53, 54). Overall, antioxidant therapies have proved ineffective in their protection against DOX cardiotoxicity, possibly due to the deleterious effects of DOX aside from ROS generation, and currently no clear

guidelines or worldwide accepted therapies exist for preventing or treating DOX cardiotoxicity.

1.9. Lipoproteins

Lipoproteins are diverse biological particles that provide a means of transport for lipids such as cholesterol and triglycerides, between cells, tissues, and other lipoproteins (55). Plasma lipoproteins are separated into classes based on their density, size, and relative content of cholesterol, triglycerides, and apolipoproteins (55). These classes include: chylomicrons, very-low-density lipoproteins (VLDL), intermediate density lipoproteins (IDL), low density lipoproteins (LDL), and high density lipoproteins (HDL) (55). At its most basic form, a lipoprotein consists of apolipoproteins and a monolayer of phospholipids and cholesterol which encapsulates a hydrophobic core that is rich in triglycerides and cholesteryl esters. The proteome of lipoprotein classes and subclasses are diverse in nature, and can include apolipoproteins, enzymes, lipid transfer proteins, acute phase proteins, and proteinase inhibitors, among others (56).

1.10. HDL Composition and Classes

Clinical and basic research has demonstrated that unlike other lipoproteins, HDL has unique anti-oxidative, anti-apoptotic, and anti-inflammatory properties. HDL is often referred to as ‘good cholesterol’ by the non-scientific community due to these cytoprotective properties. HDLs are distinguishable from other lipoprotein classes based on their small particle size (5-11nm), density (1.063-1.21g/ml), and their apolipoprotein (Apo) content –the major apolipoprotein being ApoA1 (57). ApoA1 constitutes up to ~70% of the total protein content of HDL, and its major function is to provide a point of interaction between HDL and cellular receptors (57). Other apolipoproteins that are

carried by HDL, but in smaller proportions, include ApoAII, ApoD, ApoCs, ApoE, and ApoM among others (57). HDL composition is dynamic with many subfractions existing within the class of lipoproteins referred to as HDL. Initially, in 1954, two subclasses of HDL were separated by ultracentrifugation and identified as HDL2- HDL that was relatively lipid-rich, and HDL3- HDL that was relatively protein-rich (58). The HDL2 subclass is comprised of HDL that are lower in protein (43% of weight) and higher in cholesterol (23% of weight) than HDL3 (58% protein, 14% cholesterol) (59). These two classes were further divided based on their particle size by non-denaturing gel electrophoresis into HDL3c (7.2-7.8nm), HDL3b (7.8-8.2nm), HDL3a (8.2-8.8nm), HDL2a (8.8-9.7nm), and HDL 2b (9.7-12.0nm) (60). HDL particles can also be divided into alpha-migrating (including HDL2a-c and HDL3a-c) and pre-beta-migrating particles (unlipidated ApoA1 or discoidal HDL- phospholipidated ApoA1). Alpha and pre-beta-migrating HDL differ in their surface charge and therefore electrophoretic mobility (61). Given the complexity of what we refer to as HDL, it is important to appreciate that subgroups may differ in their function.

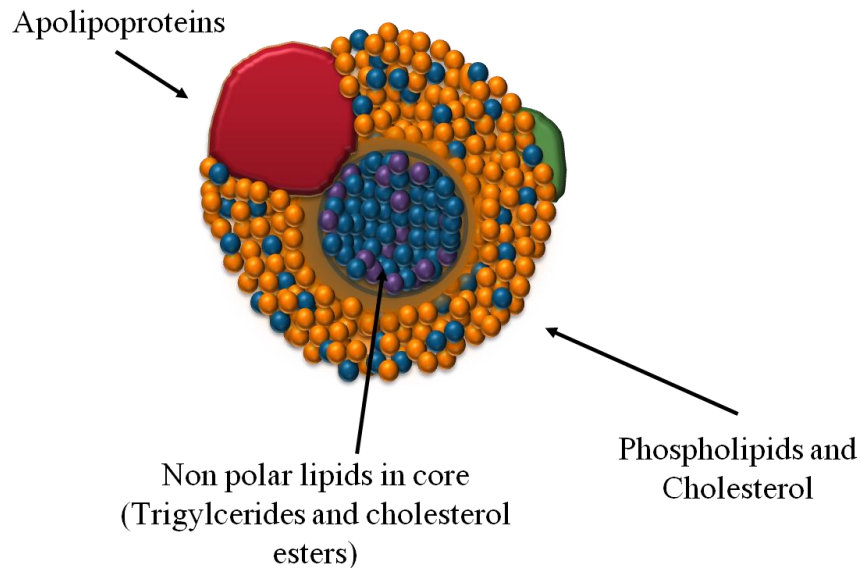


Figure 1.3 Basic depiction of HDL.

Apolipoproteins, the backbone of lipoproteins, phospholipids, and cholesterol encapsulate a core rich in triglycerides and cholesterol esters. Modified from Kingwell, BA., et al. 2014. HDL raising therapies: progress, failures, and future. *Nature Reviews Drug Discovery*. 13:445-464.

1.11. HDL Biogenesis

The biogenesis and remodeling of HDL is a complex process and requires apolipoproteins, enzymes, cellular receptors, and lipid transfer proteins to co-ordinate the production and remodeling of HDL. Biogenesis of HDL is initiated by synthesis and secretion of ApoA1 largely by the liver and intestine into the plasma and mesenteric lymph (62). Next, lipid-free ApoA1 interacts with ATP-binding cassette transporter A1 (ABCA1). In general, ATP-binding cassette transporters (ABCs) are integral for the ATP-dependent transfer of substrates across membranes (63). ABCA1 facilitates the

transfer of cellular phospholipids and cholesterol to ApoA1, and leads to the conversion of lipid-free ApoA1 to discoidal HDL particles (64). ABCA1 is abundantly expressed in macrophages, liver, intestines, and brain tissue (64, 65). Next, discoidal HDL are converted to spherical particles by the esterification of free cholesterol by lecithin-cholesterol acyltransferase (LCAT) (66). LCAT associates with discoidal HDL, and upon activation by ApoA1, catalyzes the transfer of the 2-acyl group of phosphatidylcholine or phosphatidylethanolamine to cholesterol to form a cholesterol ester (66). Cholesterol esters comprise the core of spherical HDL, and following esterification and movement to the core are replaced in the shell of the particle by unesterified cholesterol that is constantly being picked up from other cells or tissues (66).

1.12. HDL Remodelling

There are numerous ways in which HDL particles are remodeled and catabolized by plasma and membrane proteins, giving rise to dynamic subfractions that differ in size, shape, composition, and function. Membrane receptors including ATP-binding cassette transporter G1 (ABCG1) and SR-B1 promote movement of lipids between cells and HDL, and plasma proteins such as cholesteryl ester transfer protein (CETP) assist in movement of lipids between lipoproteins. ABCG1 facilitates cellular efflux of cholesterol and phospholipids to spherical HDL (67). SR-B1 is a critical membrane receptor expressed in hepatocytes, macrophages, steroidogenic tissues, and other cell types that promotes bi-directional movement of unesterified cholesterol between tissues and HDL, in addition to mediating selective uptake of cholesteryl esters, triglycerides, and phospholipids from HDL to cells (68-70). It is of note that unlike ABCs, SR-B1 mediated movement of cholesterol from cells to HDL is a passive and energy

independent process, and does not require internalization or degradation of the particle (71). SR-B1 will be discussed in greater detail below.

Other plasma proteins contribute to HDL remodelling. Cholesteryl esters can undergo direct transfer from HDL to VLDL and LDL via CETP, a plasma protein (72). Transfer of cholesteryl esters by CETP requires equimolar transport of triglycerides in the opposite direction (VLDL or LDL to HDL) (72). The triglyceride and phospholipid cargo on HDL can also be modified by hepatic lipase (HL) and endothelial lipase (EL) which hydrolyze triglycerides and phospholipids, promoting a reduction in HDL size, and dissociation of ApoA1 from the particle (73, 74). In summary, there are many cellular, plasma, and lipoprotein-associated mediators of HDL composition, that contribute to the dynamic nature of HDL composition, and likely affect HDL function.

1.13. Cardioprotective Nature of HDL

A number of clinical studies have demonstrated an inverse correlation between plasma levels of HDL and risk of CVD (32, 75, 76). More broadly, HDL is recognized as a protective factor both clinically and experimentally in the protection against atherosclerosis (77, 78), myocardial ischemic injury and infarction (79-83), and *in vitro* DOX-induced cardiomyocyte apoptosis (84). Mechanisms by which HDL protects against various forms of cardiac stress are under intense investigation.

HDL may provide protection against myocardial ischemic injury in two ways; indirectly for example, by limiting atherosclerotic plaque formation and therefore prevention of myocardial ischemia or other peripheral effects, or directly by inducing protective signaling on the cardiomyocyte. It is conceivable that HDL would reach the cardiomyocyte in order to bind and initiate protective signaling given that interstitial

HDL levels are approximately 25% of their plasma levels (85), and HDL can transcytose the endothelial layer (86). The cardioprotective mechanisms of HDL in response to myocardial ischemia will be discussed in detail below, though to date there are only two brief reports of the ability of HDL to protect against DOX-induced cardiomyocyte apoptosis in *in vitro* systems (84, 87).

Early research has described the protective effects of HDL against atherosclerosis and the manifestation of myocardial ischemic injury. Infusion of ApoA1 or HDL precursors into mice and rabbits increased plasma HDL levels, and reduced the development of atherosclerosis (88, 89). The effects of HDL on ischemia using experimental systems to induce ischemia *in vivo* (ligation of the left anterior descending (LAD) coronary artery) or *ex vivo* (stopping perfusion of a Langendorff perfused heart) without the requirement of atherosclerosis have been tested (79, 81). Preconditioning of the *ex vivo* heart with reconstituted HDL or ApoA1 complexed with phospholipids improves cardiac function and prevents release of creatine kinase (a marker of cardiomyocyte necrosis) following ischemia/reperfusion (79). The cardioprotective nature of HDL is supported by *in vivo* experimental evidence reporting that following LAD coronary artery ligation, adenovirus mediated gene transfer of ApoA1 in a low density lipoprotein receptor knockout mouse (LDLR^{-/-}) significantly protects against a decline in cardiac function, reduces infarct size, and improves survival (81). Additionally, the endogenous levels of ApoA1 correlate with infarct size following LAD ligation in mice, where mice lacking one (heterozygous) or two (homozygous) copies of the ApoA1 gene are increasingly sensitive to myocardial infarction (90). Thus, these models provide evidence that HDL protects hearts directly, and not only by attenuating

atherosclerotic plaque development (79-81, 83) Regardless of the experimental model of ischemia, HDL consistently provides protection against cardiomyocyte death and cardiac dysfunction.

Cell types other than cardiomyocytes participate in formation of an infarct following ischemia. Endothelial cells play a role in attracting circulating cells to the site of injury (91). Once bound to ligands on the endothelial cell, circulating immune cells can infiltrate the underlying tissue. Infiltrating cells, responsible for clearance of dead cardiomyocytes, release pro-inflammatory, pro-oxidant, and proteolytic molecules and enzymes (91). HDL mediates NO and prostanoid production in endothelial cells following ischemia/reperfusion, which in turn promotes vasodilation and inhibition of cell adhesion molecules thereby reducing circulating cell adhesion to the endothelial layer (92). Others have reported intravenous administration of ApoA1 10 minutes prior to ischemia prevented production of the inflammatory cytokines tumor necrosis factor α (TNF- α), and interleukin-6, reduced leukocyte infiltration into the heart, and reduced infarct size (93, 94). Lastly, HDL protects isolated cardiomyocytes from hypoxia-reoxygenation induced cell death (95), though the role of cardiomyocyte SR-B1 in mediating HDL protection against ischemia-induced cardiomyocyte death has not been tested.

1.14. PI3K/AKT- A Cardioprotective Signaling Pathway

The phosphoinositide 3-kinase (PI3K) and protein kinase B (AKT) pathway is reportedly a major mediator of cardioprotective effects of ApoA1. Co-administration of a PI3K inhibitor (Wortmannin) with ApoA1 abolishes the protective effects of ApoA1 on

infarct size (94). These data suggest the importance of the PI3K/AKT pathway in mediating the protective effects of ApoA1, and therefore HDL.

PI3K and its downstream effector AKT are central to and main determinants of cardiomyocyte survival and function (96). Activation of PI3K and AKT leads to inhibition of cardiomyocyte death, and activation of AKT preserves function in surviving cardiomyocytes (97, 98). Several classes of PI3K exist and include Class IA and B (the most studied and understood), Class II, and Class III which differ in their structure and substrate specificity (99). PI3K is activated either directly by cell surface receptors or by signaling molecules such as Src family protein tyrosine kinases. For example, Class IA PI3K has been reported to be activated by both G-coupled protein receptors (GPCRs) and non-receptor tyrosine kinases, whereas IB were reported to be activated by GPCRs exclusively (99). In the case of SR-B1, Src has been reported to bind to SR-B1 to in turn activate PI3K (100, 101). Activated PI3K generates phosphatidylinositol (3,4,5) trisphosphate (PIP3) which serves as a membrane docking site for proteins that express pleckstrin homology (PH) domains, including AKT and phosphoinositide-dependent protein kinase 1 (PDK1) (102).

Three isoforms of AKT (AKT1, AKT2, AKT3) exist and exhibit ~80% homology although they are encoded by different genes (103). AKT1, AKT2, AKT3 have varied tissue expression where AKT1 has been reported to be widely expressed, AKT2 being highly expressed in muscle and adipocytes, and AKT3 having the most limited distribution being mainly expressed in the brain and testes (103). The major isoforms of AKT are reported to be present in the heart are AKT1 and AKT2 (103). *In vitro* studies reported the three isoforms having similar substrates, however; studies in genetically

modified mice have identified distinct roles of the AKT isoforms (96). Studies evaluating AKT1 null mice have reported reduced fetal and postnatal growth and greater sensitivity to cellular apoptosis (104, 105). Mice lacking AKT2 grow normally, but exhibit deficiencies in glucose homeostasis (106). Knockout of AKT3 reduced brain size but does not affect body weight or glucose homeostasis (107). Although common substrates exist for the three isoforms of AKT, it appears they also have non-redundant functions.

Once recruited to the membrane PDK1 phosphorylates AKT at Thr308, leading to partial activation, and phosphorylation at Ser473 by mammalian target of rapamycin complex 2 (mTORC2) leads to full enzymatic activity of AKT (102, 108, 109). The activity of PI3K is antagonized by phosphatase and tensin homolog (PTEN), whose lipid phosphatase activity reduces the cellular pool of PIP3 by converting PIP3 back to phosphatidylinositol (4,5) bisphosphate (PIP2) (110). AKT is dephosphorylated by the protein phosphatase 2A (PP2A) (111).

Downstream targets of AKT include cell growth, cell survival, anti-inflammatory and metabolic effectors, as depicted in Figure 1.4. Upon activation, AKT phosphorylates forkhead box transcription factor (FOXO) 3a, thereby leading to nuclear exclusion and reduced transcription of pro-apoptotic molecules (112). AKT mediated phosphorylation and activation of endothelial nitric oxide synthase (eNOS) leads to enhanced nitric oxide (NO)-release (113, 114). In the myocardium, release of NO results in inotropic and chronotropic events, such as enhancement of ventricular relaxation and decreased myocardial oxygen consumption, reduced inflammation (115). AKT also affects cell growth by phosphorylation and inhibition of glycogen synthase kinase 3β (GSK-3 β), a

negative regulator of cardiomyocyte hypertrophy (116, 117), and by activating mammalian target of rapamycin (mTOR), a positive regulator of protein synthesis and therefore cell growth (118, 119).

Targeting AKT has been demonstrated to protect against DOX cardiotoxicity, and myocardial ischemic injury. Constitutively active AKT expression negatively regulates DOX-induced upregulation of Atrogin-1 (31), and adenovirus mediated delivery of constitutively active AKT1 to the myocardium inhibited DOX-induced reductions in cardiac function and prevented a DOX-induced decline in cardiac weight (120). Transgenic expression or adenoviral mediated gene transfer of AKT leads to increased SERCA2a expression, a central regulator of calcium mobilization, and promotes preservation of cardiac contractility under stressed conditions (121-123). Under oxidative stress, AKT mediates uptake of glucose by activation of the glucose transporter GLUT4 (124), and inhibition of GSK-3 β by AKT leads to increased cardiac glycogen synthesis, an effect which is known to precondition the heart against ischemic injury (125, 126). Taken together, the downstream effectors of PI3K and AKT highlight the importance of this pathway in cardiomyocyte and cardiac health, function, and survival.

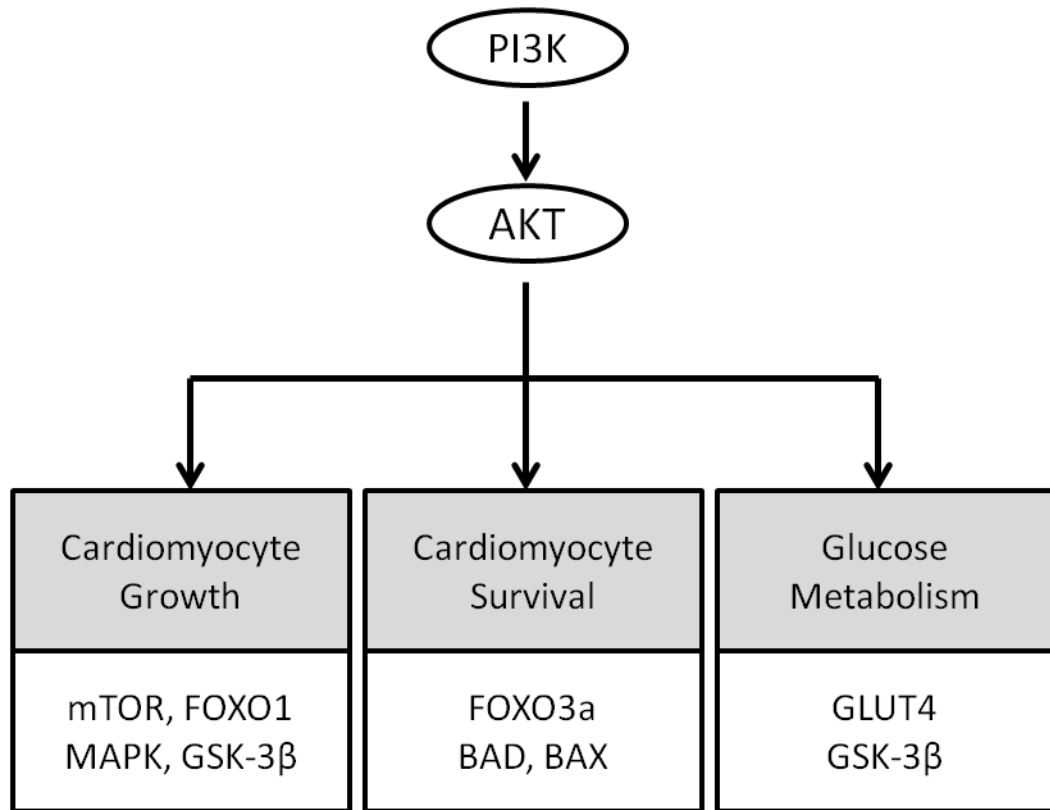


Figure 1.4 Cardioprotective Targets of AKT.

Activation of PI3K, and AKT results in the modulation of cardioprotective pathways. Pathways include targets for cardiomyocyte growth, cardiomyocyte survival, and glucose metabolism. Modified from Matsui, T., and Rosenzweig, A. 2005. Convergent signal transduction pathways controlling cardiomyocyte survival and function: the role of PI 3-kinase and Akt. *J Mol Cell Cardiol* 38:63-71.

1.15. Scavenger Receptor Class B Type I

Scavenger receptors are able to bind a range of ligands and have diverse functions including, but not limited to, clearance of apoptotic cells and pathogens (127). Different structural classes of scavenger receptors have been described and have little sequence

similarities (127). SR-B1 belongs to the class B family of scavenger receptors, and is encoded by the SCARB1 gene on chromosome 5 in mice, and chromosome 12 in humans (69). SCARB1 encodes a 509 amino acid protein that becomes fatty acylated and N-glycosylated (69). SR-B1 is comprised of an extracellular ligand binding domain, two transmembrane domains, and cytoplasmic amino and carboxy terminal domains (70, 128, 129). Within the ligand binding domain of class B scavenger receptors exists a cluster of α helices giving rise to a hydrophobic tunnel through its core (130). SR-B1 is reported to cluster within cholesterol rich domains of the plasma membrane such as caveoli, at least in some cell types (129). SR-B1 is expressed in cells of both hematopoietic (ex. macrophages, platelets), and non-hematopoietic origin (ex. steroidogenic cells, hepatocytes, and endothelial cells) (70, 131). SR-B1 protein has been reported in heart tissue but it is unclear if this is due to expression in cardiomyocytes, endothelial cells, or other resident cells of the heart (70).

SR-B1 binds a number of ligands including HDL, LDL, VLDL, apoptotic bodies via phosphatidyl serine, and chemically modified proteins including maleylated albumin, and acetylated LDL (69, 70, 132). Despite its many ligands, the major function of SR-B1 is thought to be its binding to HDL and the ability to facilitate exchange of lipids between cells and bound HDL. Recent research, however; has reported other roles of SR-B1 including mediating cellular uptake of the Hepatitis C virus, and macrophage efferocytosis (100, 133). By mediating lipid exchange, SR-B1 plays an integral role in reverse cholesterol transport (RCT), where cholesterol is collected by HDL from various tissues, and offloaded at hepatic and steroidogenic tissues (134). RCT represents a mechanism for protection against atherosclerosis by removing cholesterol from the

arterial wall (135). SR-B1 binds to ApoA1 on HDL (136), and mediates the movement of phospholipids, triglycerides, vitamins, and unesterified cholesterol to/from HDL particles (70, 137-139). Unlike other lipoprotein receptors, SR-B1 does not appear to internalize and degrade the lipoprotein, but allows for internalization and selective lipid uptake from the lipoprotein to the cell, followed by re-secretion of HDL (70, 140, 141). Based on the literature, we identified a lack in knowledge of what role SR-B1 has in cardiomyocytes, and hypothesized that SR-B1 could play an integral role in facilitating HDL signaling in the cardiomyocyte given that it has been reported in cardiac tissue.

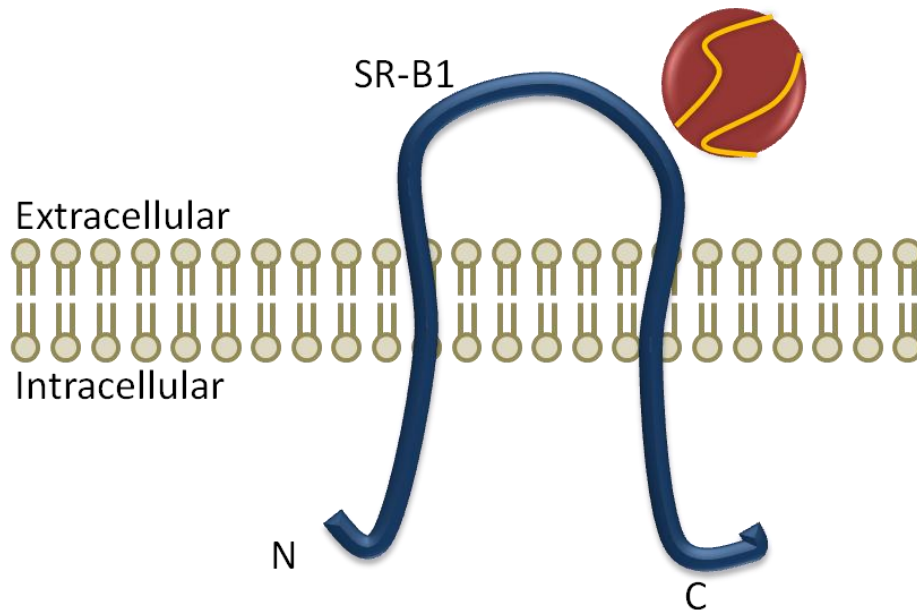


Figure 1.5 Depiction of HDL binding to SR-B1.

SR-B1 is a plasma membrane receptor with two transmembrane domains and an extracellular loop where ligands such as HDL, other lipoproteins, and vitamin E can bind. The intracellular N and C terminal domains of SR-B1 are depicted. Modified from Al-Jarallah, A., and Trigatti, B. 2010. A role for the scavenger receptor, class B type I in high density lipoprotein dependent activation

of cellular signaling pathways. *Biochimica et Biophysica Acta (BBA) - Molecular and Cell Biology of Lipids*. 12: 1239-1234.

1.16. Intracellular Signaling by HDL through SR-B1

Our lab and others have demonstrated that SR-B1 mediates HDL-initiated signaling in model cell lines (Chinese hamster ovary cells), macrophages, hematopoietic stem cells, and endothelial cells, among others (142-150). We have extrapolated from findings in these cell types to propose mechanisms through which SR-B1 may signal in the cardiomyocyte. HDL signaling through SR-B1 triggers activation of a number of intracellular targets including AMP-activated protein kinase (AMPK), PI3K, AKT, and ERK1/2 (148, 149, 151) by uptake of lipids (including ceramide, estrogen, and sphingosine 1-phosphate) from HDL (142-145). Conversely, in endothelial cells, intracellular signaling can be induced by the interaction of ApoA1 or reconstituted HDL that contains only ApoA1 and phospholipids, suggesting lipid transport from HDL may not be the only method for signal transduction to occur (152).

Our lab has demonstrated a role for the HDL/SR-B1/PI3K/AKT pathway in initiating macrophage migration, and protection against macrophage apoptosis (153-155). Recent evidence also demonstrated the role of the SR-B1/PI3K pathway in mediating macrophage efferocytosis (100). In brief, following introduction of apoptotic cells to macrophages, SR-B1 activated macrophage PI3K through the non-receptor tyrosine kinase Src (100). Macrophages lacking SR-B1 have defective efferocytosis and were reported to contribute to the generation of increased atherosclerotic plaque size (100).

Binding of HDL to SR-B1 increases the expression of heme oxygenase-1 (HO-1) in human coronary artery endothelial cells, an effect which is downstream of PI3K and

AKT (152). HO-1 reportedly protects against cardiac injury following ischemia (156, 157), and advocates a mechanism by which SR-B1 could mediate HDL induced cardiomyocyte protection. Additionally, the anti-inflammatory and anti-adhesive effects of HDL (93, 94, 158) could be mediated by SR-B1, as HDL activates eNOS in an SR-B1 dependent manner (148, 159). By stimulating NO production by eNOS, SR-B1 facilitates vascular smooth muscle relaxation, endothelial cell migration, and attenuation of monocyte cell adhesion (148, 159). In the myocardium, release of NO is cardioprotective, and initiates enhancement of ventricular relaxation and preserves myocardial oxygen consumption (115). Additionally, HDL can mediate hypoxia-induced angiogenesis in coronary artery endothelial cells via SR-B1 (160, 161), and promote differentiation of peripheral blood monocytes into endothelial progenitor cells via a PI3K/AKT/NO pathway (162). Alternatively, in endothelial cells, SR-B1 activates AMPK through calcium/calmodulin dependent protein kinase (CAMK) which in the context of perivascular electric injury leads to endothelial cell migration and carotid artery reendothelialization (163).

Clearly SR-B1 plays an integral role in mediating the signaling cascades initiated by HDL in macrophages and endothelial cells. Given that many of these targets (PI3K, AKT, AMPK, eNOS) are also components of protective pathways in cardiomyocytes, we hypothesize that SR-B1 may also mediate protective signaling by HDL in the cardiomyocyte.

1.17. Rationale for the Role of SR-B1 in HDL Mediated Cardioprotection

Mice lacking SR-B1 provide rational for the importance of SR-B1 in mediating cardioprotection by HDL. In mouse models of atherosclerosis, atherosclerotic lesions

typically do not form spontaneously in the coronary arteries without genetic modification or long term high fat diet feeding. Coronary artery atherosclerosis and non-lethal myocardial fibrosis can be induced in LDLR apolipoproteins E double knockout (LDLR/ApoE dKO) mice by feeding mice a high fat diet for a prolonged period of time (164). Interestingly, when SR-B1 is knocked out in mice also lacking ApoE (SR-B1/ApoE dKO), and these animals are fed a normal chow diet, mice exhibit occlusive coronary artery atherosclerosis and extensive myocardial infarction, cardiac conductance abnormalities, and reduced heart function, resulting in death at a very young age (165). Of significance is the striking phenotype of extensive and lethal myocardial infarction when SR-B1 is knocked out on an atherogenic strain (ApoE^{-/-}, ApoE-hypomorphic, or LDLR^{-/-}) while on a normal or high fat/high cholesterol diet (165-167). We therefore hypothesized that the effects of SR-B1 may extend beyond its role in atherosclerosis, such as to facilitate protection against clinical manifestations including myocardial infarction.

Importantly, we have evidence that HDL activates cardiomyocyte AKT in a PI3K dependent manner (94, 168), and more specifically, the activation of this pathway is downstream of SR-B1 in other cell types (148, 152, 155, 159). Our current understanding of whether HDL could 1) protect the heart against DOX-induced cardiotoxicity *in vivo*, and 2) whether HDL requires SR-B1 for protecting the heart against various stressors such as cardiotoxic drugs or myocardial ischemia, is lacking. We hypothesize, based on the ability of HDL to protect isolated cardiomyocytes against apoptosis *in vitro* (84), and the fact that PI3K/AKT signalling protects against cardiac stress (96) and is a cellular pathway downstream of HDL/SR-B1 in other cell types (148,

152, 155, 159), that 1) HDL protects against DOX-induced cardiotoxicity, could be a notable target for protection against DOX-induced cardiotoxicity, and 2) SR-B1 mediates protective signaling by HDL in cardiomyocytes. Thus, here we evaluate the role of SR-B1 and downstream mediators PI3K and AKT in the protective signaling by HDL against oxygen glucose deprivation (OGD)-induced cardiomyocyte death.

1.18. Simulation of Myocardial Ischemia

Mice are resistant to coronary artery atherosclerosis-a major initiating factor of human myocardial ischemia (34). Because of this, experimental myocardial ischemia has to be initiated in mouse models by manipulation of genetics or diet to promote the development of coronary artery atherosclerosis, or induced by surgically ligating the LAD coronary artery (169). In response to the difficulty of generating mice with coronary artery atherosclerosis and control of myocardial ischemia, in addition to the skill required to perform ligation of the coronary artery, researchers can gain mechanistic insight using methods of simulated ischemia. These methods include stopping perfusion of an isolated perfused heart for a given time period to induce global ischemia, or *in vitro* simulation of ischemia in isolated cardiomyocytes by limiting (hypoxia) or eliminating (anoxia) O₂ and/or energy producing substrates such as glucose (170).

1.19. Overview of Mouse Strains Used in Experimentation

Genetically modified mice were used for experimentation throughout this dissertation. These mice will be briefly discussed here. Detailed information regarding the supplier, catalogue number, and background strain can be found in Table 1.1 below.

The SR-B1^{-/-} mouse was generated by Dr. Monty Krieger and colleagues, and first reported in the literature in 1997 (134). Targeted mutagenesis of the first exon and 554

bases of intron 1 and insertion of a neomycin resistance cassette resulted in total body deficiency of SR-B1 (134). The SR-B1^{-/-} mouse was important in demonstrating the role of SR-B1 in RCT. Mice deficient in SR-B1 had increased HDL particle size with no difference in plasma ApoA1 suggesting that the large, cholesterol rich HDL were an effect of impaired hepatic clearance of HDL-C, and not an increase in number of HDL particles (134). Homozygous male mice are fertile, but homozygous female mice are infertile, though female infertility is corrected by feeding of a diet rich in probucol, and allows for breeding of homozygotes (171). Probuco1 is an anti-oxidant and cholesterol lowering drug that has been applied clinically as a therapeutic for CVD, and when fed to SR-B1^{-/-} mice, restores HDL-C levels and fertility (171).

The ApoA1^{Tg/Tg} mice were generated by Dr. Rubin and colleagues, and were first reported in the literature in 1991 (172). Mice were generated by transgenic insertion of the human ApoA1 gene under the control of its own promoter. ApoA1^{Tg/Tg} mice reportedly express ~245mg/dl human ApoA1 in plasma, have two fold higher plasma HDL-C, and a substantial post-transcriptional decrease in endogenous mouse ApoA1 (112 to 6.5mg/dl) (172). Mice homozygous for the transgenic insert are viable, fertile and normal in size. SR-B1^{-/-}ApoA1^{Tg/Tg} mice were generated in-house by crossing ApoA1^{Tg/Tg} and SR-B1^{-/-} mice.

Table 1.1 Information Pertaining to Mouse Models

ANIMAL CODE	GENETICS	GENTEIC BACKGROUND	SOURCE	Mouse Code/Origin
ApoA1 ^{+/+} OR SR-B1 ^{+/+}	Wild- type mouse	C57Bl/6	Bred in house	C57Bl/6J, JAX
SR-B1 ^{-/-}	Replacement of the entire coding region of the first exon and an additional 554 bases of intron 1 with a neomycin cassette	C57Bl/6J	Bred in house, back crossed 10 generations onto C57Bl/6J	B6;129S2- <i>Scarb1</i> ^{tm1Kri} /J, Krieger Lab
ApoA1 ^{Tg/Tg}	Transgenic insertion of the human apolipoprotein A-I gene including the promoter.	C57Bl/6J	Bred in house	C57BL/6-Tg(APOA1)1Rub/J, JAX
ApoA1 ^{Tg/Tg} SR-B1 ^{-/-}	Cross between ApoA1 ^{Tg/Tg} and SR-B1 ^{-/-} mice	C57Bl/6J	Crossed and bred in house	See above.

1.20. Overall Context and Objectives

The major objective of this thesis is to characterize the mechanism of HDL mediated protection against cardiac injury and cell death induced by DOX and OGD. We aim to determine whether SR-B1, and downstream signaling through PI3K and AKT are involved in HDL mediated protection of cardiomyocytes. Here we have also assessed whether raising HDL by overexpression of ApoA1 or injection of ApoA1 can protect the heart against DOX-induced cardiotoxicity. We conclude that increasing plasma HDL attenuates the cardiotoxic effects of DOX, and that HDL protects isolated cardiomyocytes against OGD-induced necrosis. Beyond this, our findings demonstrate a critical role for SR-B1 in cardiomyocytes by facilitating HDL mediated protection. We have also identified PI3K and AKT as downstream mediators in the cardioprotective signaling cascade by HDL and SR-B1.

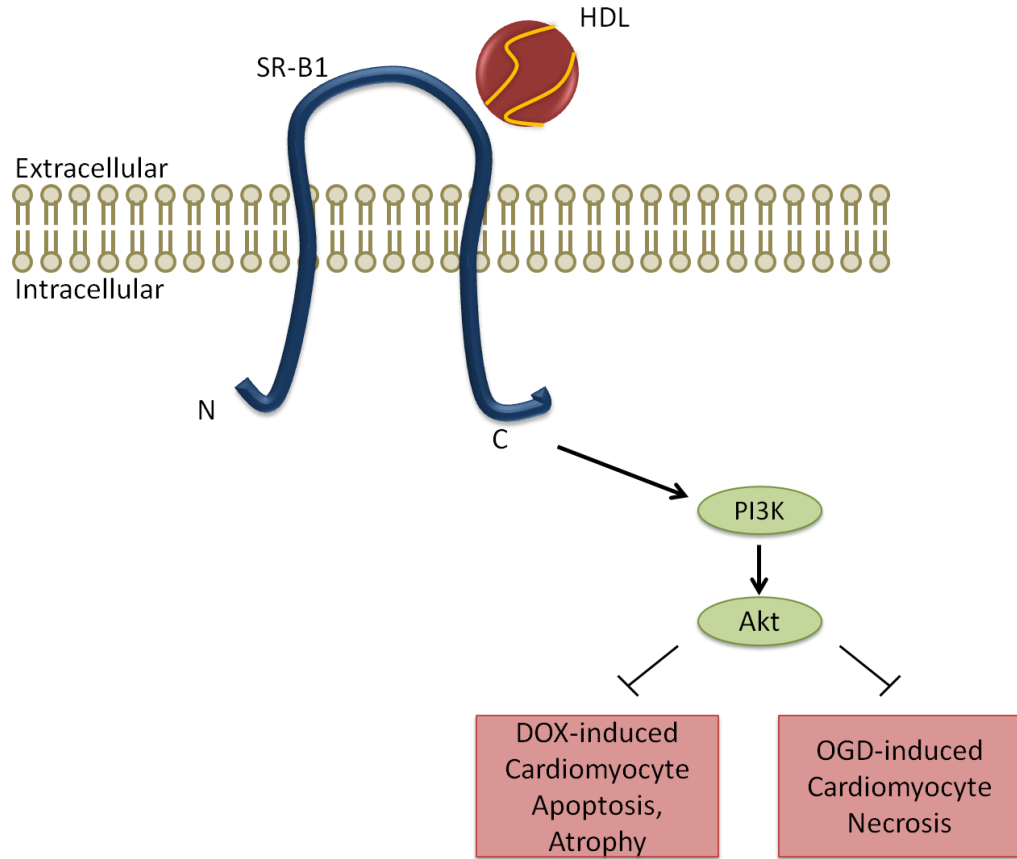


Figure 1.6 Proposed mechanism of HDL mediated protection against the cardiac stressors DOX and OGD. SR-B1 depiction modified from Al-Jarallah, A., and Trigatti, B. 2010. A role for the scavenger receptor, class B type I in high density lipoprotein dependent activation of cellular signaling pathways. *Biochimica et Biophysica Acta (BBA)- Molecular and Cell Biology of Lipids*. 12: 1239-1234.

Chapter 2. Aims and Hypotheses of Thesis

The objectives of this thesis are three-fold.

Aim 1. Evaluate whether increasing plasma HDL by overexpression of ApoA1 protects against DOX-induced cardiotoxicity, and to determine whether SR-B1, PI3K, and AKT mediate the protective effect of HDL against DOX-cardiotoxicity and/or cardiomyocyte apoptosis.

Hypotheses of Aim 1: I hypothesize that:

1. Increased plasma HDL will provide protection against DOX-induced *in vivo* cardiotoxicity, in an SR-B1 dependant manner.
2. SR-B1, PI3K, and AKT are required for HDL mediated protection against DOX-induced cardiomyocyte apoptosis.

Aim 2. To evaluate the effects of therapeutic injection of ApoA1 in an acute model of DOX-induced cardiotoxicity in mice.

Hypotheses of Aim 2: I hypothesize that:

1. Therapeutic injection of ApoA1 will protect against the cardiomyocyte apoptosis and atrophy caused by a single injection of DOX.
2. Therapeutic injection of ApoA1 will induce activation of AKT in the hearts.

Aim 3. To evaluate the role of SR-B1/PI3K/AKT in mediating HDL-induced cardiomyocyte protection against OGD-induced necrosis.

Hypotheses of Aim 3: I hypothesize that:

1. OGD will induce necrosis of cardiomyocytes.
2. HDL will protect against OGD-induced necrosis.

3. HDL requires SR-B1, PI3K, and AKT for protection against cardiomyocyte death induced by OGD.

Chapter 3. HDL Requires SR-B1, PI3K and AKT1 to Protect Against Doxorubicin Induced Cardiotoxicity

Author List: Kristina Durham, Christy Mak, Cyrus Thomas, Melissa MacDonald, Bernardo Trigatti

3.1. Preface

In this manuscript we aimed to 1) determine whether overexpression of ApoA1 and therefore an increase in plasma HDL protects against the deleterious cardiotoxic side effect of DOX, and 2) evaluate the mechanisms involved in protection. Specifically, we identified the contribution of SR-B1, PI3K, and AKT to the cardioprotective effects of HDL.

This project was initiated by Kristina Durham and Dr. Bernardo Trigatti. Experiments were designed by Kristina Durham with guidance from Dr. Bernardo Trigatti. Kristina Durham conducted all experiments with the exceptions of Figure 3.2 and Supplementary Figure 3.2 which were designed by Kristina Durham, and carried out by Christy Mak under the supervision of Kristina Durham, and Figure 3.1D-F, which was also designed, supervised, and analyzed by Kristina Durham, but carried out by Cyrus Thomas. All data were interpreted by Kristina Durham with guidance from Dr. Bernardo Trigatti. This manuscript was written by Kristina Durham with guidance and editing from Dr. Bernardo Trigatti. This manuscript has been submitted to AJP-Heart and Circulation and is currently undergoing revisions.

3.2. Abstract

Doxorubicin is a widely used chemotherapeutic though its use is severely limited due to its deleterious cardiotoxic side effect that can lead to heart failure. HDL has been

shown to protect cardiomyocytes *in vitro* against doxorubicin-induced apoptosis. The scavenger receptor class B type I (SR-B1) is a high affinity HDL receptor that mediates cytoprotective signaling by HDL through AKT. Here we assess whether increased HDL levels can protect against DOX-induced cardiotoxicity in mice, *in vivo*, and in cardiomyocytes in culture, and explore the intracellular signaling mechanisms involved.

Mice with increased levels of HDL, through overexpression of human ApoA1 (ApoA1^{Tg/Tg}) and control wild type mice with normal levels of HDL (ApoA1^{+/+}) were treated chronically with doxorubicin. Following treatment, ApoA1^{+/+} mice displayed cardiac dysfunction as evidenced by reduced LVESP, and reduced \pm dP/dt. In contrast, left ventricular function was maintained following doxorubicin treatment in ApoA1^{Tg/Tg} mice. Histological analysis revealed reduced cardiomyocyte cross-sectional area and increased cardiomyocyte apoptosis following doxorubicin treatment in ApoA1^{+/+} mice. ApoA1^{Tg/Tg} mice, on the other hand, were protected against doxorubicin-induced cardiomyocyte atrophy and apoptosis. Similar *in vivo* analyses revealed overexpression of ApoA1 does not protect against doxorubicin-induced cardiotoxicity when SR-B1 is knocked out, and that SR-B1 is required for HDL mediated protection of cardiomyocytes against doxorubicin-induced apoptosis *in vitro*. Using neonatal mouse cardiomyocytes and human immortalized ventricular cardiomyocytes in combination with genetic knockout, inhibitors, or siRNA mediated knockdown, we demonstrate that SR-B1, PI3K, and AKT1 are required for HDL mediated protection against doxorubicin-induced cardiomyocyte apoptosis.

Our findings illustrate the protective effect of ApoA1 against doxorubicin cardiotoxicity *in vivo* and demonstrate the roles of SR-B1, PI3K, and AKT as mediators

in the protective effect, and will have important implications both for our understanding of how the protective properties of HDL extend beyond effects on atherosclerotic plaque, and also for understanding the role of SR-B1 in mediating HDL induced protection of cardiomyocytes.

3.3. Introduction

Cancer is a leading cause of death in developed societies and is a major burden to the health care system (1). Doxorubicin (DOX) is a widely used and effective cancer treatment, though its long term use is severely limited by its dose-dependent and deleterious side effects including cardiotoxicity and congestive heart failure (1). At the cellular level, DOX promotes suppression of protein synthesis, ultrastructural changes, alterations to energy metabolism, and cardiomyocyte death, which together manifest physiologically as a reduction in cardiac function (2). A major therapeutic goal of cardiology is to prevent cardiomyocyte death caused by an insult such as DOX, as current treatments are limited in their ability to repair or replace dead myocardium. A potential avenue for promoting cardiomyocyte protection against DOX is through high density lipoprotein (HDL). In a recent study both reconstituted and native HDL particles provided protection against DOX-induced cell death *in vitro* (3), though whether this translates to *in vivo* protection is yet to be determined. Here we assess whether increasing plasma apolipoprotein A1 (ApoA1), the major apolipoprotein and precursor of HDL, protects against DOX-induced cardiomyocyte atrophy and apoptosis, and cardiac dysfunction.

Mechanisms by which HDL protects against other forms of cardiac stress have been linked to its anti-inflammatory and anti-oxidative signaling, as well as its role in

reverse cholesterol transport (RCT) (4-6). The scavenger receptor class B type I (SR-B1) is a high affinity HDL receptor that is a key player in RCT, and mediates bidirectional flux of lipids between cells and lipoproteins. Additionally, binding of HDL to SR-B1 initiates intracellular signaling in macrophages, endothelial and other cells (7-13). Intracellular signaling by HDL or ApoA1 complexed with phospholipids, through SR-B1 triggers activation of phosphoinositide 3-kinase (PI3K), protein kinase B (AKT), and extracellular signal regulated kinases (ERK) 1 and 2 (11, 12, 14, 15). Although the signaling initiated through SR-B1 has yet to be studied in the cardiomyocyte, the signaling cascades known to be initiated in other cell types through SR-B1 are also involved in cardioprotection (16). In light of the protective effects of HDL against DOX-induced cardiomyocyte apoptosis *in vitro*, and the protective signaling induced by HDL through SR-B1 in other cell types, we investigated the signaling mechanisms involved in HDL mediated protection against DOX-induced cardiotoxicity and cardiomyocyte apoptosis.

3.4. Results

ApoA1^{Tg/Tg} mice are protected against DOX-induced cardiac dysfunction, cardiomyocyte apoptosis, and atrophy. Overexpression of human ApoA1 led to elevated levels of ApoA1 in plasma as previously described (17), which corresponded to a 3.09 fold increase in HDL cholesterol as compared to ApoA1^{+/+} mice (Supplementary Fig. 3.1). Following treatment, body weight (BW), heart weight (HW), and heart weight to tibial length ratio (HW:TL) were lower in both ApoA1^{+/+} and ApoA1^{Tg/Tg} mice treated with DOX than corresponding saline-treated controls though differences in TL were not statistically significant, suggesting mouse growth was likely not impaired

(Supplementary Table 3.1). There was no effect of ApoA1 overexpression on HW, BW, and TL (Supplementary Table 3.1).

Left ventricular function was analyzed by invasive hemodynamics. No differences in left ventricular function were observed between ApoA1^{+/+} and ApoA1^{Tg/Tg} mice injected with saline (Fig. 3.1A, B). Cardiac dysfunction was observed in ApoA1^{+/+} animals following chronic DOX treatment, as indicated by a reduced rate of pressure development (+dP/dt), an increase in the rate of pressure decline (-dP/dt), and reduction in the left ventricular end systolic pressure (LVESP) (Fig. 3.1B, C). ApoA1^{Tg/Tg} mice were protected against DOX-induced cardiac dysfunction since \pm dP/dt, and LVESP were similar in ApoA1^{Tg/Tg} mice following DOX or control saline-treatment (Fig. 3.1B, C). The preservation of these parameters in DOX-treated ApoA1^{Tg/Tg} but not ApoA1^{+/+} mice demonstrates that ApoA1 overexpression and/or increased HDL protects against DOX-induced cardiac dysfunction.

Histological analysis further confirmed that overexpression of ApoA1 provided protection at the cellular level against DOX-induced cardiomyocyte apoptosis and atrophy. ApoA1^{+/+} hearts displayed a 12.4 fold increase in apoptosis following DOX treatment (0.49 ± 0.7 versus 6.07 ± 0.67 % TUNEL-positive cardiomyocytes, Fig. 3.1D, E). In contrast, hearts from ApoA1^{Tg/Tg} mice treated with either saline or DOX exhibited similar and low levels of cardiomyocyte apoptosis (0.38 ± 0.11 vs. 0.43 ± 0.15 % TUNEL-positive cardiomyocytes, Fig. 3.1D, E). Cardiomyocyte cross sectional area (CSA) was reduced by 26.4% in ApoA1^{+/+} mice whereas it was preserved in ApoA1^{Tg/Tg} mice treated with DOX compared to those treated with saline (Fig. 3.1F, G). Together, this data

suggests that overexpression of ApoA1 protected against DOX-induced cardiomyocyte apoptosis and atrophy.

The cardioprotective effects of overexpressing ApoA1 require SR-B1. To assess the role of SR-B1 in mediating the protective effects of ApoA1 overexpression, we generated SR-B1^{-/-}ApoA1^{Tg/Tg} mice. ApoA1 overexpression in SR-B1^{-/-} mice resulted in elevated plasma ApoA1 levels, and a 3.5 fold increase in HDL cholesterol compared to SR-B1^{-/-}ApoA1^{+/+} (Supplementary Fig. 3.2A, C). Chronic administration of DOX prevented body weight gain in both SR-B1^{-/-}ApoA1^{+/+} and SR-B1^{-/-}ApoA1^{Tg/Tg} mice though body growth as measured by TL was not altered by DOX (Supplementary Table 3.3). DOX-induced a similar reduction in HW:TL in both strains of mice (Supplementary Table 3.3). Overexpression of ApoA1 in SR-B1^{-/-} mice did not mitigate the cardiotoxic effects of DOX. This was evidenced by similar levels of apoptotic cardiomyocytes in DOX treated SR-B1^{-/-}ApoA1^{+/+} and SR-B1^{-/-}ApoA1^{Tg/Tg} mice (6.1 vs. 6.8% apoptotic cardiomyocytes, p>0.05, Fig. 3.2A, B), and similar level of atrophy (25.6 vs. 26.8% reduction in CSA compared to relative saline treated animals, p>0.05, Fig. 3.2C, D).

Lack of SR-B1 in vivo sensitizes cardiomyocytes to DOX-induced apoptosis. Our data demonstrates that overexpression of ApoA1 protects against DOX-induced cardiotoxicity via a pathway that requires the HDL receptor SR-B1. To test whether SR-B1 itself facilitates protection against DOX-induced apoptosis and atrophy under conditions of normal levels of ApoA1, we subjected SR-B1^{-/-} and control SR-B1^{+/+} mice with normal wild-type ApoA1 (ApoA1^{+/+}) to chronic DOX versus saline treatment. Chronic administration of DOX prevented body weight gain in both SR-B1^{+/+} and SR-B1^{-/-} mice

although body growth as measured by TL was not altered by DOX (Supplementary Table 3.3). Similarly, DOX reduced HW to TL ratios to a similar extent in SR-B1^{+/+} and SR-B1^{-/-} mice. No differences in animal characteristics were observed between the two strains following weekly saline injections (Supplementary Table 3.2). DOX treatment increased apoptosis in both SR-B1^{+/+} and SR-B1^{-/-} cardiomyocytes as compared to respective saline treated groups (4.1 vs. 7.2% apoptotic cardiomyocytes Fig. 3.3A, B). On the other hand, DOX reduced cardiomyocyte CSA to a similar extent in SR-B1^{+/+} and SR-B1^{-/-} mice (15.58 and 18.23% reduction relative to saline treated Fig. 3.2C, D). This suggests that the degree of DOX-induced cardiomyocyte apoptosis but not atrophy is increased in the absence of SR-B1 expression.

SR-B1 in cardiomyocytes mediates HDL-dependent protection against DOX-induced apoptosis. We next assessed whether SR-B1 specifically on the cardiomyocyte is required for the cardioprotective effects of HDL against DOX-induced cardiotoxicity. SR-B1 protein expression in hearts (ApoA1^{+/+} and ApoA1^{Tg/Tg} treated with DOX or saline) and cardiomyocytes (neonatal mouse cardiomyocytes [NMCM] from SR-B1^{+/+} mice, and human immortalized ventricular cardiomyocytes [HIVCM]) was confirmed by immunofluorescence labeling and/or western blotting (Supplementary Fig. 3.4, Fig. 3.4C). Treatment of mouse cardiomyocytes with either human HDL (Fig. 3.4) or HDL prepared from wild type mice (not shown) protected SR-B1^{+/+} NMCM against DOX-induced apoptosis (23.7±1.8 vs. 7.7±5.0% TUNEL positive cardiomyocytes, Fig. 3.4A,B). Conversely, HDL did not protect SR-B1^{-/-} NMCM against DOX-induced apoptosis (31.6±5.8 vs. 35.5±8.3 TUNEL positive cardiomyocytes, Fig. 3.4A, B) suggesting that SR-B1 in murine cardiomyocytes is required for HDL mediated

protection against DOX-induced apoptosis. Similarly, DOX-induced apoptosis in HIVCM (1.9 ± 1.0 vs. $43.9 \pm 2.0\%$ TUNEL positive cardiomyocytes, Fig. 3.4E, F), and pretreatment of cells with HDL attenuated this induction (43.9 ± 2.0 vs. $14.6 \pm 0.8\%$ TUNEL positive cardiomyocytes, Fig. 3.4E, F). siRNA mediated knockdown of SR-B1, which resulted in a reduction in SR-B1 protein levels by $\sim 85\%$ (Fig. 3.4C, D), prevented HDL dependent protection of HIVCM against DOX-induced apoptosis (42.1 ± 5.2 vs. $36.3 \pm 1.9\%$ TUNEL positive cardiomyocytes, Fig. 3.4E, F). These data demonstrated that SR-B1 is present in cardiomyocytes and that cardiomyocyte SR-B1 is required for HDL-mediated protection against DOX-induced apoptosis. Deletion of SR-B1 results in expansion of cholesterol in HDL sized particles (18) and this was confirmed in our animals (Fig. 3.5A), raising the possibility that altered HDL metabolism and/or structure in SR-B1 deficient mice, rather than the absence of SR-B1 in cardiomyocytes themselves, may have contributed to the increased DOX-induced apoptosis in hearts from SR-B1^{-/-} mice. To test if the absence of SR-B1 in hearts themselves increased the sensitivity to DOX-induced apoptosis *in vivo*, in a manner predicted by our *in vitro* studies of the effects of knockout or knockdown of SR-B1 in cardiomyocytes in culture, we used an ear pinna heart transplantation model where neonatal hearts of SR-B1^{+/+} and SR-B1^{-/-} were surgically transplanted to opposite ears of an adult wild-type mouse. In this model, hearts become vascularised and display pulsatile activity (19, 20). In this way, hearts of different genotypes (SR-B1^{+/+} and SR-B1^{-/-}) can be tested in the same environment—specifically, in the presence of the same wild-type (SR-B1^{+/+}) HDL. Transplanted recipient mice were treated with a single injection of either saline or 1mg/kg DOX and apoptosis of cardiomyocytes in neonatal hearts transplanted under the ear pinnae was

analyzed one week later. DOX did not induce apoptosis of cardiomyocytes the SR-B1^{+/+} transplants (0.82±0.23 vs. 0.99±0.52% TUNEL positive cardiomyocytes, Fig. 3.5C,D), however; SR-B1^{-/-} transplants displayed 2.21 fold increase in numbers of apoptotic cardiomyocytes (1.78±0.21 vs. 3.95±0.4% TUNEL positive cardiomyocytes, Fig. 3.5C,D) in DOX- versus saline-treated recipients. This suggests that a lack of SR-B1 in the heart, itself, sensitizes cardiomyocytes to DOX-induced apoptosis. In light of a recent report that deletion of SR-B1 in macrophages impairs clearance of apoptotic cells (21), and the well-known presence of tissue macrophages in hearts, we wanted to ensure that the increased levels of cardiomyocyte apoptosis observed in transplanted SR-B1^{-/-} compared to SR-B1^{+/+} hearts was not due to differences in the capacity of macrophages to clear apoptotic cells. Therefore we stained transplanted heart sections for SR-B1 and the macrophage marker CD107b to determine if macrophages in the transplanted hearts were derived from the recipient host. We observed SR-B1-staining in the majority of CD107b⁺ cells in both the SR-B1^{+/+} and SR-B1^{-/-} transplants from recipients treated with either saline or DOX, and that the numbers of CD107b⁺ stained cells increased dramatically in the tissues from mice treated with DOX compared to those from saline-treated mice (Supplementary Fig. 3.7). This suggests that the majority of cardiac macrophages in this system are derived from the host, and express SR-B1 and that there should be no difference in the capacity for clearance of apoptotic cardiomyocytes from the transplanted SR-B1^{+/+} and SR-B1^{-/-} hearts, but rather, that the increased cardiomyocyte apoptosis reflects an increased sensitivity of cardiomyocytes in hearts from SR-B1^{-/-} mice to DOX-induced apoptosis.

AKT is activated in an SR-B1 dependent manner in hearts of mice overexpressing ApoA1 following chronic DOX treatment. Heart homogenates were assessed for the ratio of phosphorylated AKT (pAKT, Ser 473) to total AKT (tAKT) protein levels, indicating the level of activation of AKT. Activation of AKT did not differ between any animals that were treated with saline. Treatment of ApoA1^{+/+} mice with DOX, similarly did not change the levels of AKT phosphorylation. In contrast, ApoA1 overexpressing mice exhibited a 2.9 fold increase in pAKT:tAKT following chronic DOX treatment (Fig. 3.6A, B). Interestingly, when this was repeated in SR-B1^{-/-} mice, ApoA1 overexpression did not lead to elevated DOX-induced pAKT:tAKT; in contrast, DOX treatment resulted in a 49% reduction in pAKT:tAKT in SR-B1^{-/-}ApoA1^{+/+} and a 55% reduction in SR-B1^{-/-}ApoA1^{Tg/Tg} mice (Fig. 3.6C, D). No difference in baseline pAKT:tAKT at baseline (Fig.3.6E,F) were observed between SR-B1^{+/+} and SR-B1^{-/-} hearts. This suggests the absence of SR-B1 expression sensitizes the myocardium to DOX-induced reductions in activated AKT, and that SR-B1 is required for ApoA1^{Tg/Tg} mediated increase in pAKT:tAKT following DOX exposure.

HDL Requires PI3K, AKT1, and AKT2 to induce protection of cardiomyocytes against DOX-induced apoptosis. PI3K is an upstream effector of AKT and is a determinant of cardiomyocyte function and survival. We found that HDL increased activation of AKT between 30min to 24h following treatment of HIVCM (Supplementary Fig. 3.9). To evaluate the role of PI3K and AKT in HDL mediated protection against DOX-induced apoptosis, we inhibited PI3K or AKT, or knocked down AKT1 and AKT2 (the most prominent isoforms in cardiomyocytes (22)) and assessed the effect on HDL mediated protection against DOX-induced apoptosis. Protection by HDL of HIVCM and NMCM

was attenuated by either LY294002- an inhibitor of PI3K, or AKT Inhibitor V-an inhibitor of all AKT isoforms (Fig. 3.7A, B), implicating PI3K and AKT in the protective signaling cascade initiated by HDL. To delineate whether specific isoforms of AKT are involved in HDL mediated protection, we knocked down AKT1, AKT2 or both using siRNA which resulted in ~71% and ~72% reduction in protein levels respectively in NMCM (Fig. 3.8 A/B), and ~70 and ~84% reduction in protein levels respectively in HIVCM (Fig. 3.8D, E). Knockdown of AKT1 completely abolished protection by HDL in NMCM (55.2 ± 14.5 vs. $52.1 \pm 10.9\%$ TUNEL positive cardiomyocytes, Fig. 3.8C). Similarly, when AKT2 was knocked down, HDL could no longer protect NMCM against DOX induced apoptosis (39.6 ± 2.5 vs. $33.9 \pm 11.7\%$ TUNEL positive cardiomyocytes, Fig. 3.8C). Similarly in HIVCM, knockdown of AKT1 abolished protection by HDL (Fig. 3.8 F), and HDL appeared to lose much of its ability to protect cardiomyocytes against DOX-induced apoptosis since HDL pre-treatment reduced apoptosis by only 40% in cells treated with siAKT2 compared to virtually 100% in cells treated with siScram (Fig. 3.8F). Knockdown of both AKT1 and AKT2 did not reduce HDL dependent protection of HIVCM further than knockdown of AKT1 or AKT2 alone (Fig. 3.8C, F).

3.5. Discussion

Cardiotoxicity and chronic heart failure are major side effects of the chemotherapeutic DOX. A recent study of 12 females receiving chemotherapy (7 of which were treated with DOX) indicated these women had reductions in plasma ApoA1 and a corresponding decrease in plasma HDL-C (23). Given the cardioprotective nature of HDL, and the protection afforded to cardiomyocytes against DOX-induced apoptosis *in vitro* (3), we sought to assess whether increasing ApoA1 provides protection against

DOX-induced cardiotoxicity *in vivo*, and to understand the mechanisms involved. Our data is the first to demonstrate that increasing plasma ApoA1 *in vivo* attenuates the cardiotoxic effects of DOX by protecting against cardiomyocyte atrophy and apoptosis, and maintaining cardiac function. As the therapeutic effect of DOX on cancer cells is accompanied by the negative effects on cardiomyocytes, an ideal therapeutic would enhance tumor cytotoxicity while reducing cardiotoxicity. Although the present study was performed in cancer-free mice (in order to avoid confounding variables associated with malignancy), evidence from other studies provides rationale for hypothesizing that the cardioprotective effects of HDL would extend to mice with tumors while allowing DOX to maintain its chemotherapeutic effects. Raising plasma ApoA1 by genetic overexpression or injection of human ApoA1 has been reported to reduce tumor metastasis and improves survival, whereas knockout of ApoA1 enhances tumor growth in multiple mouse tumor models, indicating the importance of ApoA1 in anti-tumorigenic activities (24). Furthermore, encapsulating DOX in HDL enhances its cytotoxic effect on tumors *in vivo* (25). This evidence in combination with our results reinforces the therapeutic potential for ApoA1 or HDL raising therapies during DOX treatment. Future research should employ an animal tumor model to assess the effects of increasing ApoA1 on both the heart and tumor following DOX therapy.

Examination of the intracellular signaling involved in HDL mediated protection against DOX-induced cardiomyocyte apoptosis revealed the importance of SR-B1. Here we have demonstrated that SR-B1 is required for the protective effects of ApoA1 and HDL mediated protection against DOX. Contrary to our results, a recent study by Brinck *et al.*, found that down regulating SR-B1 in rat cardiomyocytes did not alter the effect of

HDL when cells were cultured with HDL and DOX for a period of 20h. As a hydrophobic molecule, DOX is readily incorporated into HDL, altering its effective concentration and/or presentation to cells, which may result in alterations in signaling at the cardiomyocyte. In our *in vitro* experiments, we controlled for this by incubating cells with HDL for 24h, and removing the HDL during incubation with DOX. Our experiments also differ in the species of cardiomyocytes used. In a separate study, ApoA1 induced intracellular signaling through ERK, ACC, and AMPK in L6 myotubes was impaired when SR-B1 was knocked down (26). Overall, our experiments indicate an integral role of SR-B1 in facilitating the protective effects induced by increased ApoA1 against DOX-induced apoptosis and cardiotoxicity.

Up to this point research has focused on the involvement of the sphingosine-1-phosphate (S1P) receptors (S1PR) in the cardioprotective effects of HDL, though the participation of specific S1PR isoforms remains unclear. Circulating S1P is primarily carried by HDL (27), and when applied alone, or as part of reconstituted HDL containing ApoA1 with phospholipids, protects cardiomyocytes against various stresses (3, 28, 29). Tao *et al.*, have implicated S1P₁ and S1P₃ receptors in HDL induced protection of adult mouse cardiomyocytes against hypoxia-reoxygenation (29), whereas Frias *et al.*, shown inhibition of S1P₂ receptor ablates the protection afforded by HDL against DOX-induced apoptosis in neonatal rat ventricular cardiomyocytes (3). The differences may be in part due to the cargo of S1P on the HDL particle, and/or the differences in cardiomyocytes studied. Alternatively, SR-B1, known to mediate the cellular uptake of HDL bound lipids, could mediate the uptake of HDL bound S1P, making it accessible to S1PRs. Overall our data presents a role for SR-B1 in facilitating HDL-induced cytoprotective

signaling, though at this time we cannot rule out co-operative effects of SR-B1 and S1PRs. Further research is required to determine if one or more S1PRs are involved in HDL dependent signaling through SR-B1, or whether SR-B1 mediates signaling by HDL independently of S1PRs (30) in cardiomyocytes. In summary, lack of SR-B1 abolishes the *in vivo* protective effects of overexpressing ApoA1, and negates the *in vitro* HDL mediated protection against apoptosis, which emphasizes the importance of SR-B1 *in vivo* for protection against cardiotoxicity.

For our *in vivo* studies, we elicited a 10-fold increase in plasma ApoA1, and a ~2.5 fold increase in plasma HDL-C levels by overexpressing hApoA1. As HDL raising therapies such as lifestyle modification, small molecule drugs, and ApoA1 mimetics provide more modest increases in HDL levels, future studies should delineate whether smaller increases in plasma ApoA1 provide protection against DOX cardiotoxicity. Chronic DOX treatment induced increased cardiotoxicity despite the ~2-fold higher HDL-C levels in SR-B1^{-/-} mice compared to SR-B1^{+/+} mice. We interpret this to mean that merely increasing HDL-C is not sufficient—rather that HDL function (in this case, signaling via SR-B1 in cardiomyocytes) is the important parameter that confers protection against DOX-induced cardiotoxicity. In the case of SR-B1^{-/-} mice, the absence of SR-B1 in cardiomyocytes prevents cardioprotective signaling by HDL. This is consistent with our observation that neonatal hearts from SR-B1^{-/-} mice were more susceptible to DOX-induced cardiotoxicity than neonatal hearts from SR-B1^{+/+} controls when both were transplanted into wild type recipients.

We further examined the involvement of intracellular components including PI3K and AKT. Contrary to Frias *et al.*, who found LY294002 did not affect the protective

effects of HDL or S1P induced protection of neonatal rat cardiomyocytes (3), we found that inhibition of PI3K by LY294002 mitigated the effects of HDL induced protection in both HIVCM and NMCM. Our results demonstrate that AKT is an important mediator of HDL induced suppression of cardiomyocyte apoptosis evoked by DOX, which is in accord with several other studies reporting that targeting AKT pathways promotes protection against DOX-induced cardiotoxicity (31-34). Further to this, we have demonstrated that AKT1 is required for protection by HDL against DOX-induced apoptosis. Our results are consistent with studies that demonstrate that gene delivery of AKT1 protects against the DOX-induced decline in cardiac function (35), and AKT1 is the major isoform involved in protection against ischemic preconditioning (36).

Our findings presented here illustrate the protective effect of raising ApoA1 levels against DOX-induced cardiotoxicity *in vivo*. Furthermore, we show that the protection afforded by HDL requires SR-B1 and involves a PI3K/AKT1 dependent pathway. Our research will have important implications both for our understanding of how the protective properties of HDL extend beyond effects on atherosclerotic plaque, and also for understanding the role of SR-B1 in mediating HDL induced protection of cardiomyocytes. It may also lead to new insights into therapeutic interventions for anthracycline based chemotherapeutics or other forms of cardiotoxicity.

3.6. Methods

Antibodies and siRNA

Please refer to Supplementary Tables 5 and 6 for a detailed list of all antibodies and siRNAs used in this manuscript.

Chronic DOX Treatment of Animals

All mice were group housed and given free access to normal chow diet and water. Beginning at 7 weeks of age, male mice were given 5 weekly intraperitoneal (IP) injections of 5mg/kg DOX (Toronto Research Chemicals, Toronto, ON, Canada) or 0.9% sterile saline. Blood was collected by tail bleed 24 hours following the fifth injection for plasma cTnI analysis. Organs were snap frozen or perfusion fixed with 10% w/v formalin one week following the fifth injection.

Hemodynamic Measurements and Electrocardiography

One week following the fifth injection, animals were anesthetized by isoflurane and left ventricular pressures in 5 animals per group were measured by inserting a pressure-volume catheter (PVR-1045 or PVR-1035, Millar, Houston, TX) into the left ventricle through the right common carotid artery. Electrocardiography was performed using a 3 lead approach. Data was collected and analyzed with the ADInstruments system and Lab Chart software (ADInstruments, Colorado Springs, CO).

Lipoprotein Profiles

Whole blood collected by cardiac puncture one week following the last injection was centrifuged, and plasma was collected. Plasma from saline treated animals was fractionated by gel filtration FPLC on a Sepharose 6 column (GE Healthcare Life

Sciences, Mississauga, ON, Canada). Cholesterol content in each fraction was assayed by using the Cholesterol Infinity kit (Wako Chemicals USA, Richmond, VA) following manufacturer's instructions. Total cholesterol in HDL sized fractions was quantified by summing cholesterol in fractions 26 to 42 in SR-B1^{+/+} animals, or fractions 18-42 in SR-B1^{-/-} fractions.

Microscopy

Fluorescent and bright field images were captured using a Zeiss Axiovert 200M inverted microscope (Carl Zeiss Canada Ltd. Toronto, ON, Canada), or an Olympus BX41TF microscope (Olympus Canada Inc., Richmond Hill, ON, Canada).

Cardiomyocyte CSA Analysis

Fixed hearts were paraffin embedded and sectioned at 4µm. Sections were deparaffinised, stained with hematoxylin and eosin, and imaged using light microscopy. CSA was determined using ImageJ software by measuring a minimum of 130 cardiomyocytes/heart across three sections of the heart representing the base, midline, and apex. Only round or cuboidal and nucleated cardiomyocytes were included in analyses.

Quantification of Apoptosis

Sections were subjected to antigen revival using by boiling the samples for 5 min in a microwave pressure cooker while incubated in Antigen Unmasking Solution (Vector Laboratories, Burlington, ON, Canada). Apoptosis was assessed using the terminal deoxynucleotidyl transferase-mediated dUTP nick end-labeling (TUNEL) assay according to manufacturer's instructions (Millipore Canada Ltd., Etobicoke, ON, Canada). Sections were co-stained with mouse monoclonal anti cardiac troponin T

antibody (cTnT, Thermo Fisher Scientific Inc., Waltham, MA) using a Mouse on Mouse Kit with biotinylated secondary labeling (Vector Laboratories, Burlington, ON, Canada) and tertiary labeling with streptavidin conjugated AlexaFluor 568 antibody (Life Technologies, Burlington, ON, Canada) to identify cardiomyocytes from other cardiac cells, and nuclei were stained with DAPI. Apoptotic cardiomyocytes were identified as having a TUNEL-positive nucleus that was surrounded by cTnT staining. TUNEL positive nuclei were counted in 4 randomly selected fields per section, from 3 sections per heart representing the base, midline, and apex of the heart. Apoptosis was expressed as a ratio of TUNEL positive cardiomyocyte nuclei to total cardiomyocyte nuclei.

Culture of Neonatal Mouse Cardiomyocytes and Human Immortalized Ventricular Cardiomyocytes

Hearts were isolated from 1-3 day old neonatal mice and placed into ice cold Hank's balanced saline solution (HBSS, Life Technologies, Burlington, ON, Canada). Atrial and aortic appendages were removed and ventricles were washed with fresh ice cold HBSS. The ventricles were then serially digested at 37°C using 0.2mg/mL collagenase type II (Worthington Biochemical Corp., Lakewood, NJ), and 0.6mg/mL pancreatin (Sigma-Aldrich Canada Co., Oakville, ON, Canada) in HBSS. After each digestion, cell suspension was transferred into fetal bovine serum (FBS, Life Technologies, Burlington, ON, Canada) on ice. The cell suspension was centrifuged at 300xg for 10 min at 4°C. The supernatant was removed and the cell pellet was re-suspended in 37°C DMEM/M199 (4:1) supplemented with 10% horse serum, 5% fetal bovine serum (FBS), 100µM bromodeoxyuridine, 100U/mL penicillin, 100µg/L streptomycin, and 0.5mM L-Glutamine (Life Technologies, Burlington, ON, Canada). The cell suspension was transferred to an

uncoated plate for 1h to allow non cardiomyocytes to adhere. The myocyte enriched suspension was then removed for cell counting and plated at 1×10^5 cells/cm² on collagen type I (Life Technologies, Burlington, ON, Canada), coated dishes and incubated in a humid 5% CO₂ incubator at 37°C for 48 hours at which point they were used for experiments. SV40 large T antigen HIVCM were obtained from Applied Biological Materials Inc. (Richmond, BC, Canada). HIVCMs were cultured in Prigrow I media (Applied Biological Materials Inc., Richmond, BC, Canada) and were supplemented with 10% FBS, and 100U/mL penicillin.

DOX Treatment of Cells

In some experiments HIVCMs were transfected with scrambled siRNA, or siRNA against SR-B1, AKT1 or AKT2 either individually or in combination. See Supplementary table 5 for a list of siRNA used. Cells were transfected using Lipofectamine RNAi Max (Life Technologies, Burlington, ON, Canada), 24h prior to the initiation of experimental treatments. In all experiments, HIVCMs, and NMCMS were starved of lipoproteins by incubating for 24h in media containing lipoprotein deficient serum either before all treatments, or in the case of siRNA experiments, 24h following transfection. Next, cells were treated with or without 100µg/mL human HDL (Alfa Aesar, Ward Hill, MA) for 24 hours, and subsequently treated with or without 1µM DOX for 6 hours. In other experiments, cells were treated with 10µM LY294002 (PI3K inhibitor; Cell Signaling Technologies Inc., Danvers, MA) or 3µM AKT Inhibitor V (pan-AKT inhibitor; Millipore Canada Ltd., Etobicoke, ON, Canada), or vehicle (DMSO) 30 min prior to and during HDL treatment.

Cell death analyses

For assessment of apoptosis NCMs and HIVMs were fixed with 4% paraformaldehyde, stained for apoptosis using the TUNEL assay, and co stained with DAPI. NCM were co-immunostained for cTnT (as described above) to identify cardiomyocytes. TUNEL positive cardiomyocytes were imaged by fluorescence microscopy.

Ear Pinna Heart Transplant

Neonatal hearts were transplanted under the ear pinna of an adult recipient according to previous reports (19, 20). Adult SR-B1^{+/+} mice served as recipients for heart transplants, and both ears underwent transplant surgery. 1 day old SR-B1^{+/+} or SR-B1^{-/-} neonates served as heart donors. Recipients were anesthetized under isoflurane/O₂ for the duration of the surgery. Aseptic techniques were followed and a 2mm transverse incision into the epidermis was made on the dorsum of the recipient's ear pinna. Using fine-tip sterile forceps a small pocket between the cartilage and skin was made. Donor neonates were sterilized and decapitated, and their hearts were quickly removed by thoroacotomy and placed in ice cold sterile saline. Aortic and atrial appendages were removed and following a second rinse in ice cold saline, the ventricular portion was inserted into the ear pocket of the recipient. Gentle compression was applied to remove air and seal the pocket. Animals were allowed to recover for one week, at which point the transplanted hearts were visually assessed for spontaneous beating, and the recipient mice with two viable transplants were injected with a single IP injection of 0 or 1 mg/kg DOX. Seven days post injection mice were euthanized and hearts collected from the ear pinna

for histological evaluation of apoptosis using TUNEL, and identification of cardiomyocytes using with cTnT co-staining.

Western Blotting

Hearts or cells were lysed in a buffer containing 20mM Tris-HCl pH 7.5, 150mM NaCl, 1mM Na₂EDTA, 1mM EGTA, 1% Triton, 2.5mM Na₄P₂O₇, 1mM β-glycerophosphate, 1mM Na₃VO₃, with 1μg/mL Pepstatin A, 1mg/mL leupeptin 2μg/mL aprotinin, 50μM p-Amidinophenylmethylsulfonylfluoride (all from Sigma-Aldrich Canada Co., Oakville, ON, Canada). Homogenates or lysates (20-25μg total protein), and plasma (1.5μL) were denatured and separated by SDS-polyacrylamide gel electrophoresis and transferred onto a PVDF membrane. Antibodies were applied following manufacturer's instructions, and visualized using enhanced chemiluminescence (Thermo Fisher Scientific Inc., Waltham, MA). For a list of antibodies used, refer to Supplementary Table 6.

Statistical Analysis

Data are expressed as mean ± standard error of the mean (SEM). Differences are considered statistically significant at P < 0.05. Data was analyzed for statistical significance using GraphPad software (GraphPad Software, Inc., La Jolla, CA). Normality was assessed using the Shapiro-Wilk or D'Agostino-Pearson omnibus test, and equal variance by F test. Data that was normally distributed and showed equal variance were analyzed by Student's *t* test (2-tailed, unpaired) to compare two groups, one way ANOVA to compare more than two groups, and two-way ANOVA to compare data with two or more independent variables. Post hoc analysis of statistically relevant

comparisons were tested using the Tukey test for groups with equal N groups, or the Tukey-Kramer test for groups with unequal N.

3.7. Figures

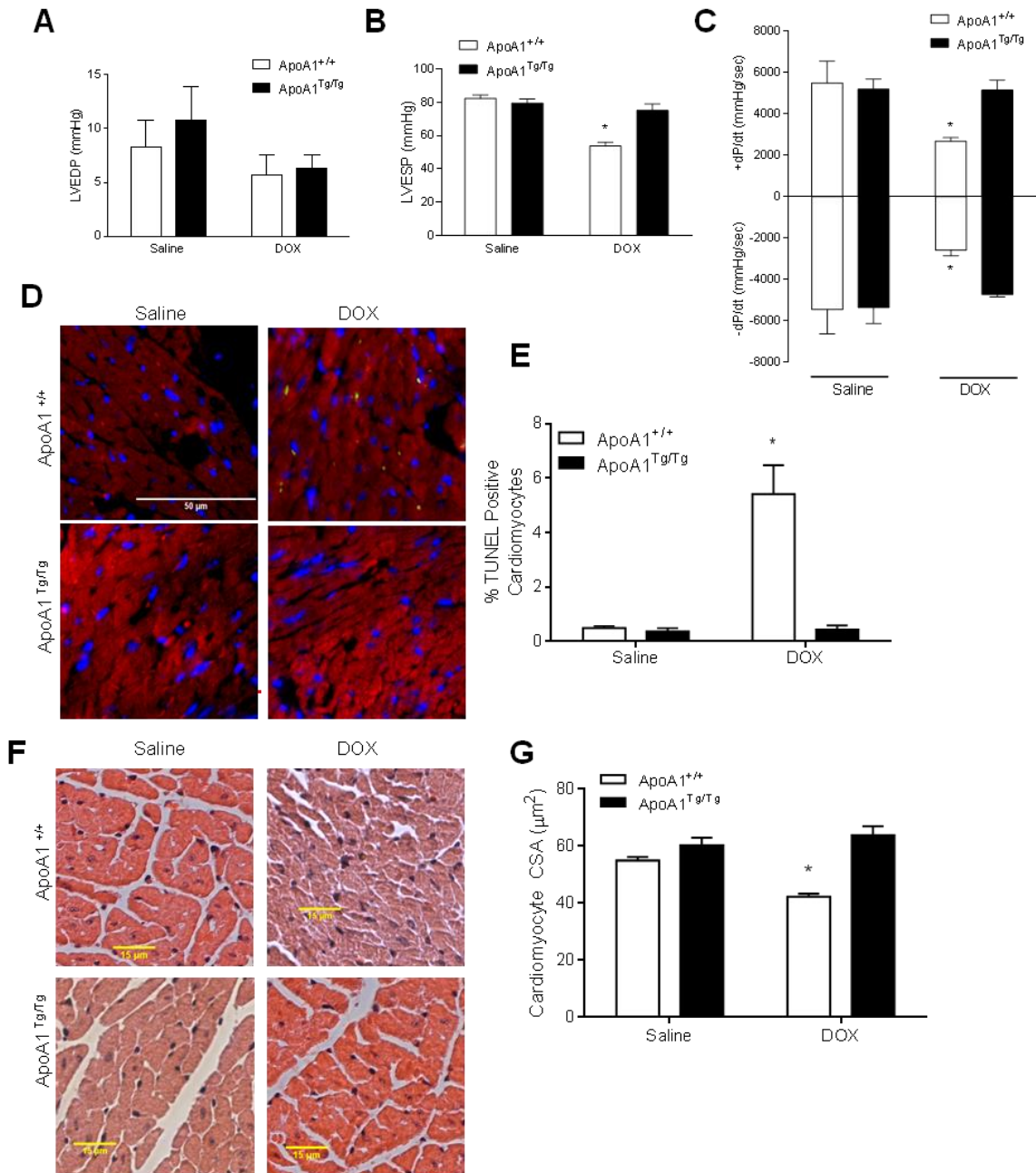


Figure 3.1 Mice overexpressing ApoA1 are resistant to DOX induced cardiotoxicity.

A) Left ventricular end diastolic pressure. N=5 animals/group. B) Left ventricular end systolic pressure. N=5 animals/group. C) Rate of pressure development and decline of the left ventricle. N=5 animals/group. D) Representative images and E) quantification of

TUNEL positive cardiomyocytes. N=7 animals/group. Red= cTnT, Green= TUNEL, Blue=DAPI. Scale bar= 50 μ m. F) Representative images and G) quantification of cardiomyocyte CSA. N=7 animals/group. * p <0.001. Scale bar= 15 μ m. All data represents mean \pm S.E.M. *= p <0.05

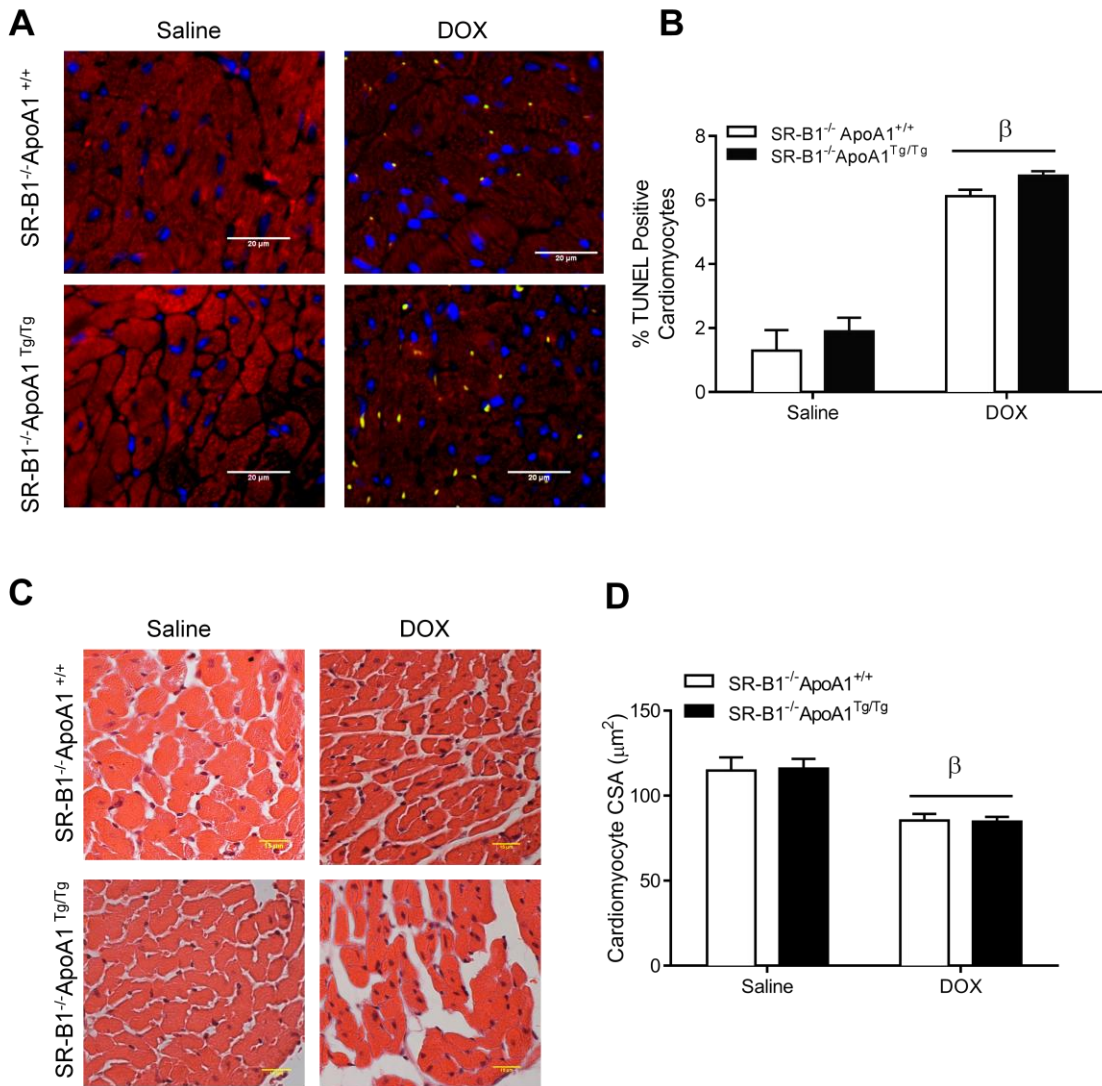


Figure 3.2 Mice lacking SR-B1 are not protected against DOX induced cardiotoxicity when ApoA1 is overexpressed.

A) Representative images and B) quantification of TUNEL positive cardiomyocytes.

N=6-8 animals/group. Red= cTnT, Green= TUNEL, Blue=DAPI. Scale bar=

50µm. C) Representative images and D) quantification of cardiomyocyte CSA.

N=6-8 animals/group. *p<0.001. Scale bar= 15µm. All data represents

mean±S.E.M. *=p<0.05

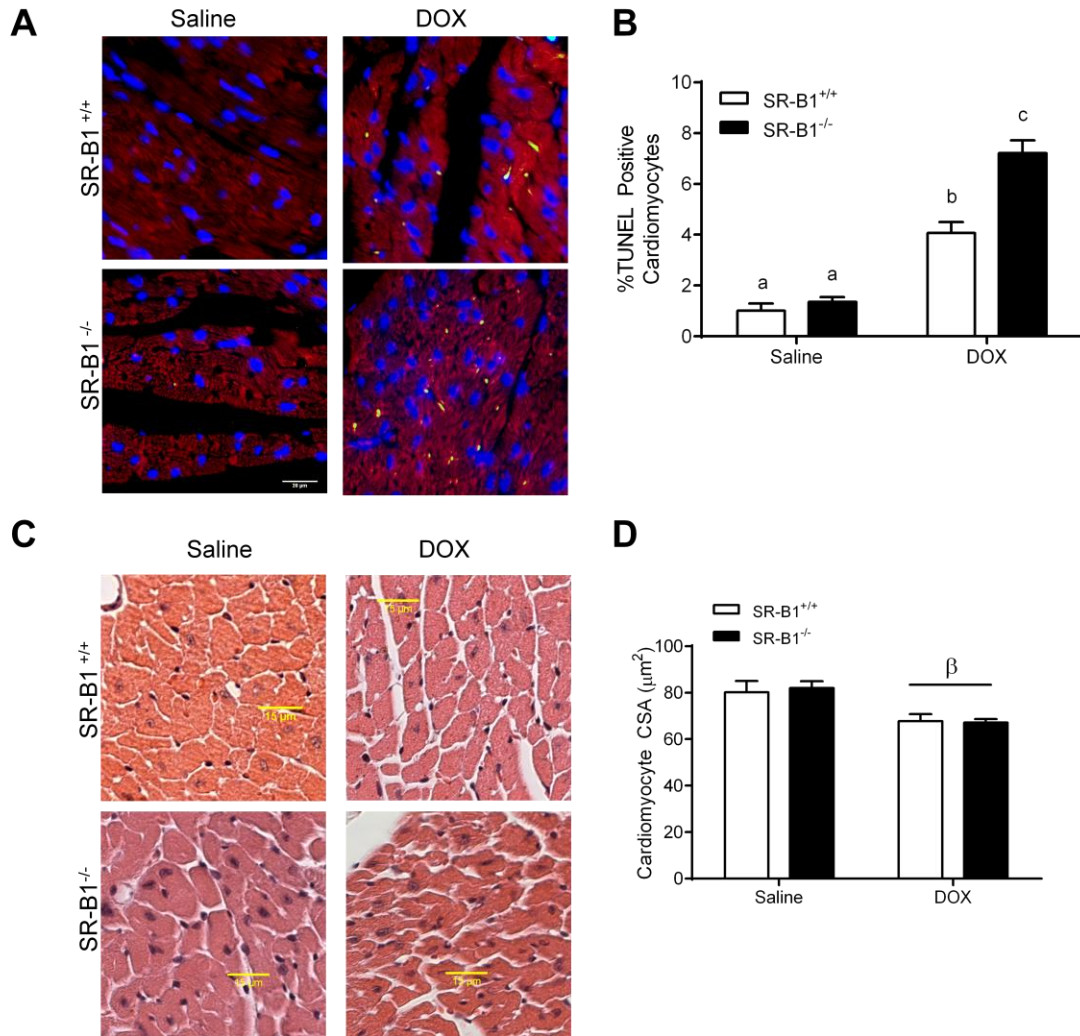


Figure 3.3 Treatment of mice lacking SR-B1 with DOX leads to exacerbated cardiomyocyte apoptosis.

A) Representative images of TUNEL stained heart sections and B) quantification of apoptosis. Red= cTnT, Green= TUNEL, Blue=DAPI. Scale bar= 20µm. N=7-8 animals/group. Dissimilar letters are significantly different $p < 0.05$ C) Representative images and D) quantification of cardiomyocyte CSA in SR-B1^{+/+} and SR-B1^{-/-} hearts treated with saline or DOX n=5 animals/group. β = treatment effect $p < 0.001$. Scale bar= 15µm. All data represents mean±S.E.M..

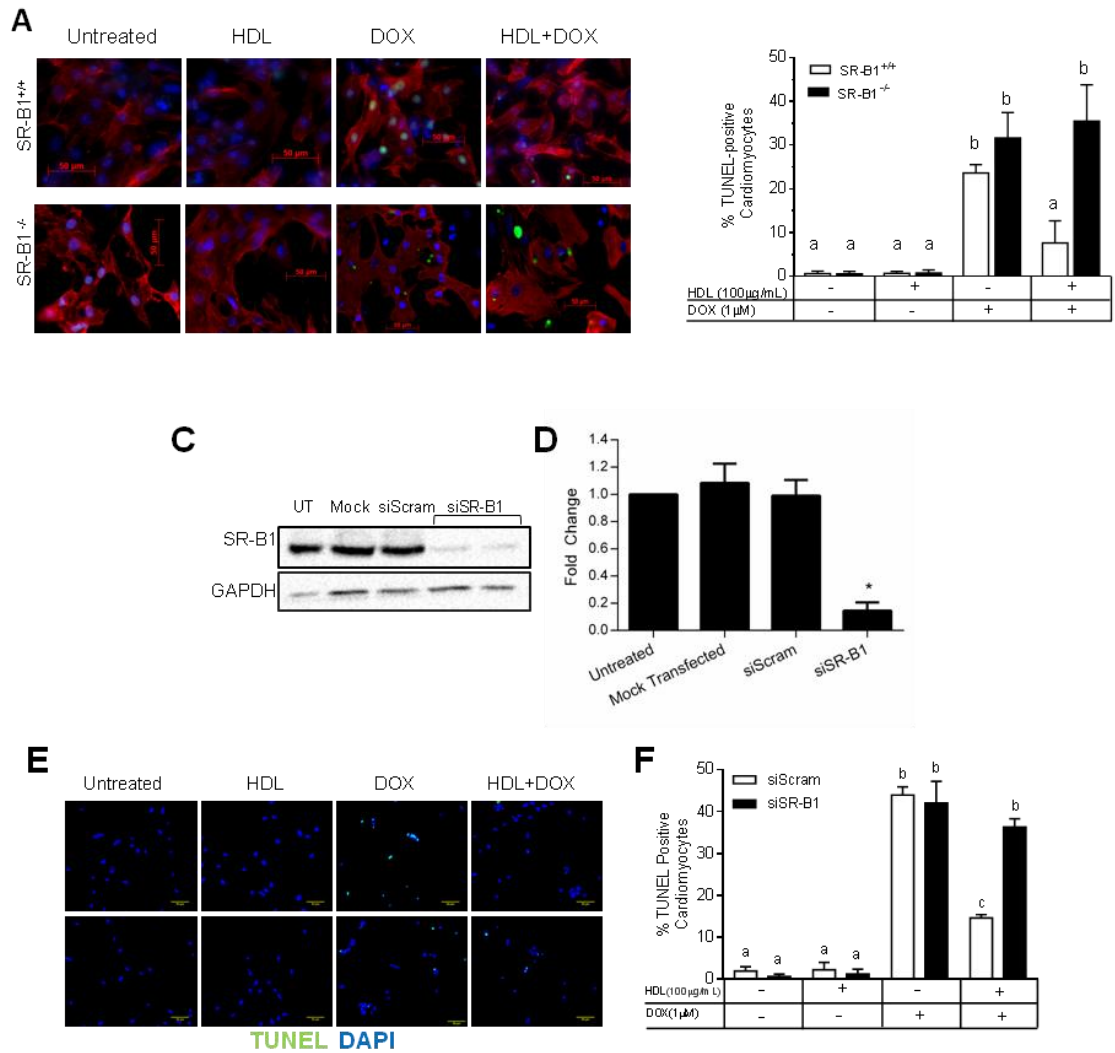


Figure 3.4 SR-B1 is required for protection of HIVCM and NMCM against DOX induced apoptosis *in vitro*.

A) Representative images of TUNEL staining and B) quantification for DOX induced apoptosis of isolated neonatal SR-B1^{+/+} or ^{-/-} cardiomyocytes treated ± human or mouse HDL. Red=cTnT, Green=TUNEL, blue=DAPI. Scale bar= 50µm. N=3 wells/group. C) Representative western blot of HIVCM transfected with scrambled or SR-B1 siRNA, and D) quantification in the bar graph. N=3/group. E) Representative TUNEL staining and F) quantification in the bar graph. N=3/group.

quantification for DOX induced apoptosis of HIVCM treated \pm human HDL.

Green=TUNEL, blue=DAPI. Scale bar= 50 μ m. N=2-3 replicates/group. Dissimilar letters are significantly different, and $*=p<0.01$.

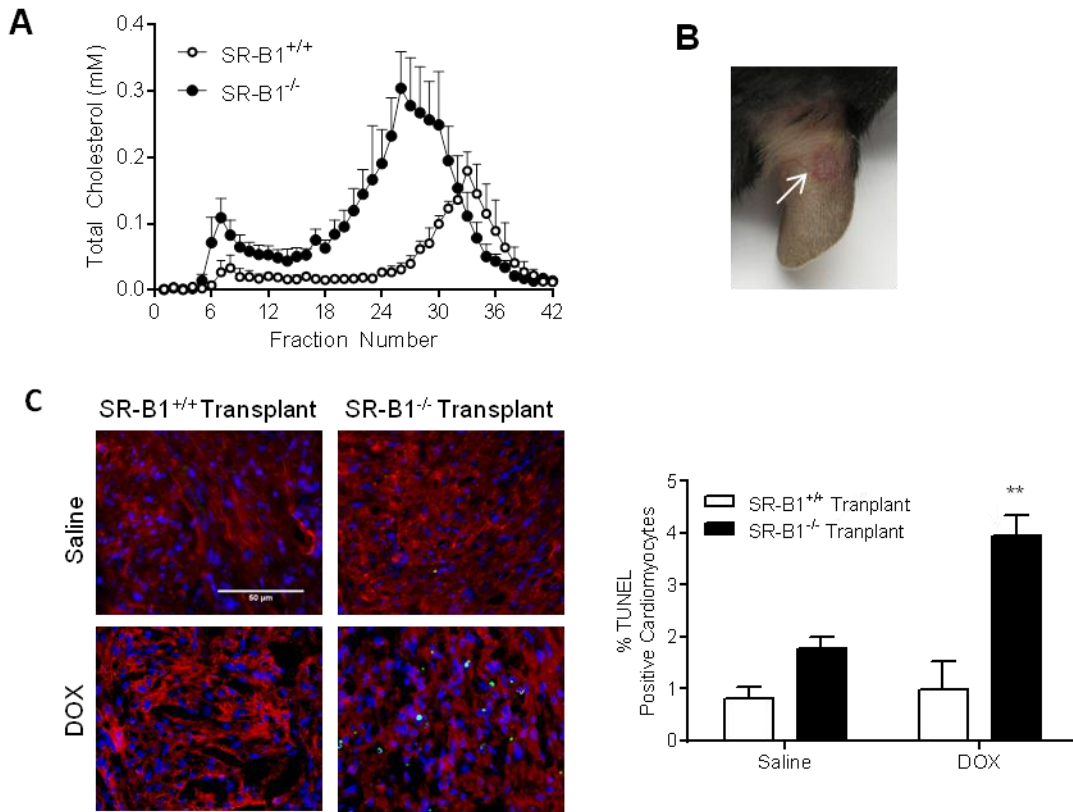


Figure 3.5 Hearts lacking SR-B1 are more sensitive to DOX induced apoptosis in the presence of wild type HDL.

A) Average lipoprotein profiles of SR-B1^{+/+} and SR-B1^{-/-} mice, n=3/group. B)

Representative image of neonatal heart placed under the ear pinna of an adult recipient.

C) Representative images and quantification of TUNEL positive cardiomyocytes in transplanted hearts. N=3-4/group. Red= cTnT, Green= TUNEL, Blue=DAPI. Scale bar= 20µm. All data represents mean±S.E.M., **=p<0.001.

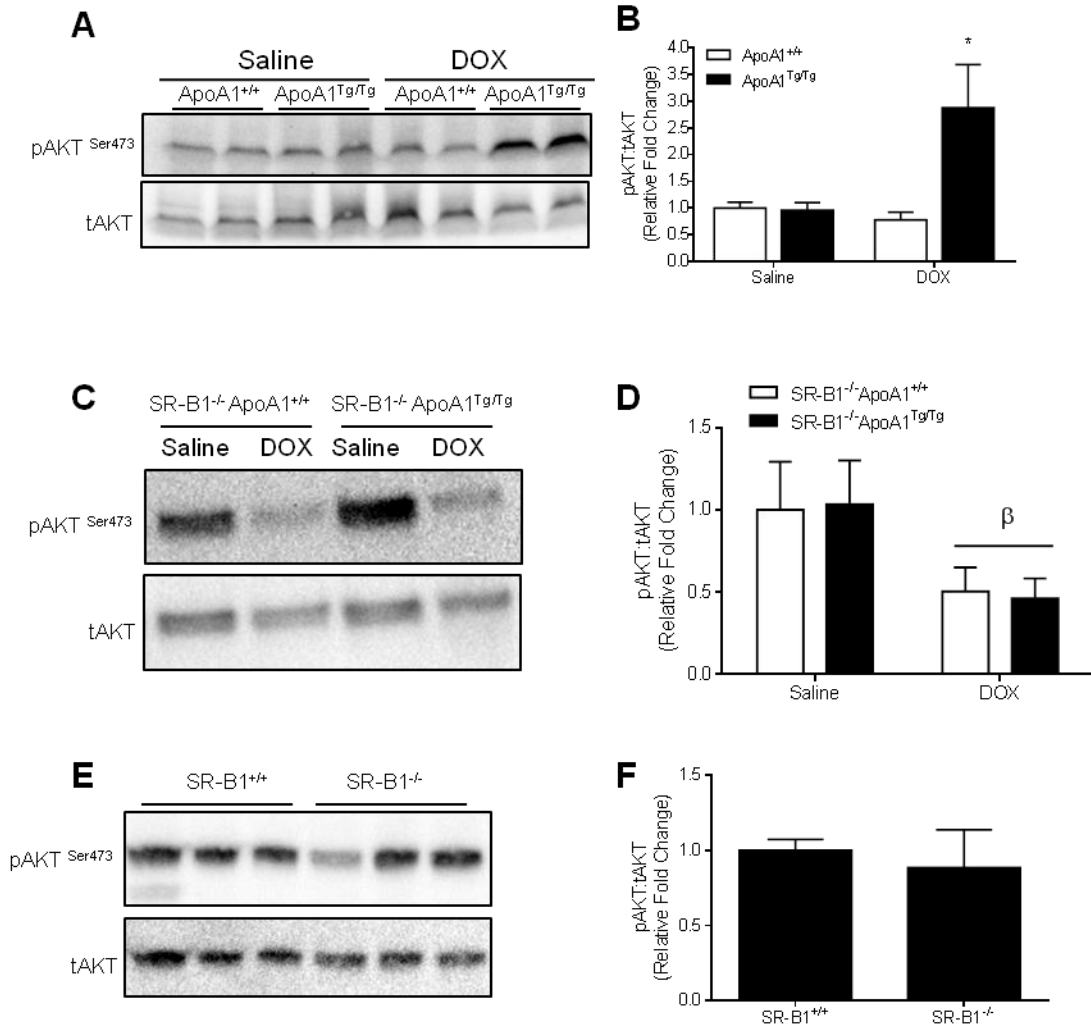


Figure 3.6 Overexpression of ApoA1 increases activation of AKT under stressed conditions whereas knockout of SR-B1 abolishes this effect of ApoA1 overexpression.

A) Representative western blot and B) quantification of ApoA1^{+/+} and ApoA1^{Tg/Tg} heart homogenates from mice treated ±DOX chronically. N=5-6 animals/group. *p<0.01. C) Representative western blot and D) quantification of SR-B1^{-/-} ApoA1^{+/+} and SR-B1^{-/-} ApoA1^{Tg/Tg} heart homogenates from mice treated ±DOX chronically. N=4 animals/group. *p<0.01. E) Representative western blot and F) quantification of SR-B1^{+/+} ApoA1^{+/+} and SR-B1^{-/-} ApoA1^{+/+} heart homogenates.

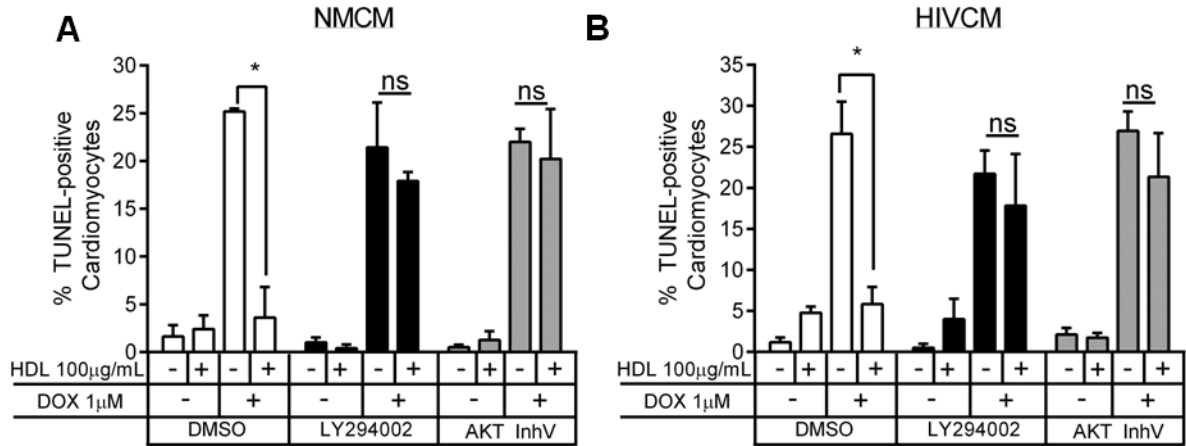


Figure 3.7 Protection by HDL against DOX induced apoptosis requires PI3K, and AKT.

A/B) DOX-induced cell death assessed by TUNEL staining in NMCM (A) and HIVCM (B) treated ±HDL and ±LY294002 to inhibit PI3K, or ±AKT Inhibitor V to inhibit AKT.

*p<0.01. Data represents mean±S.E.M. N=3/group unless otherwise stated.

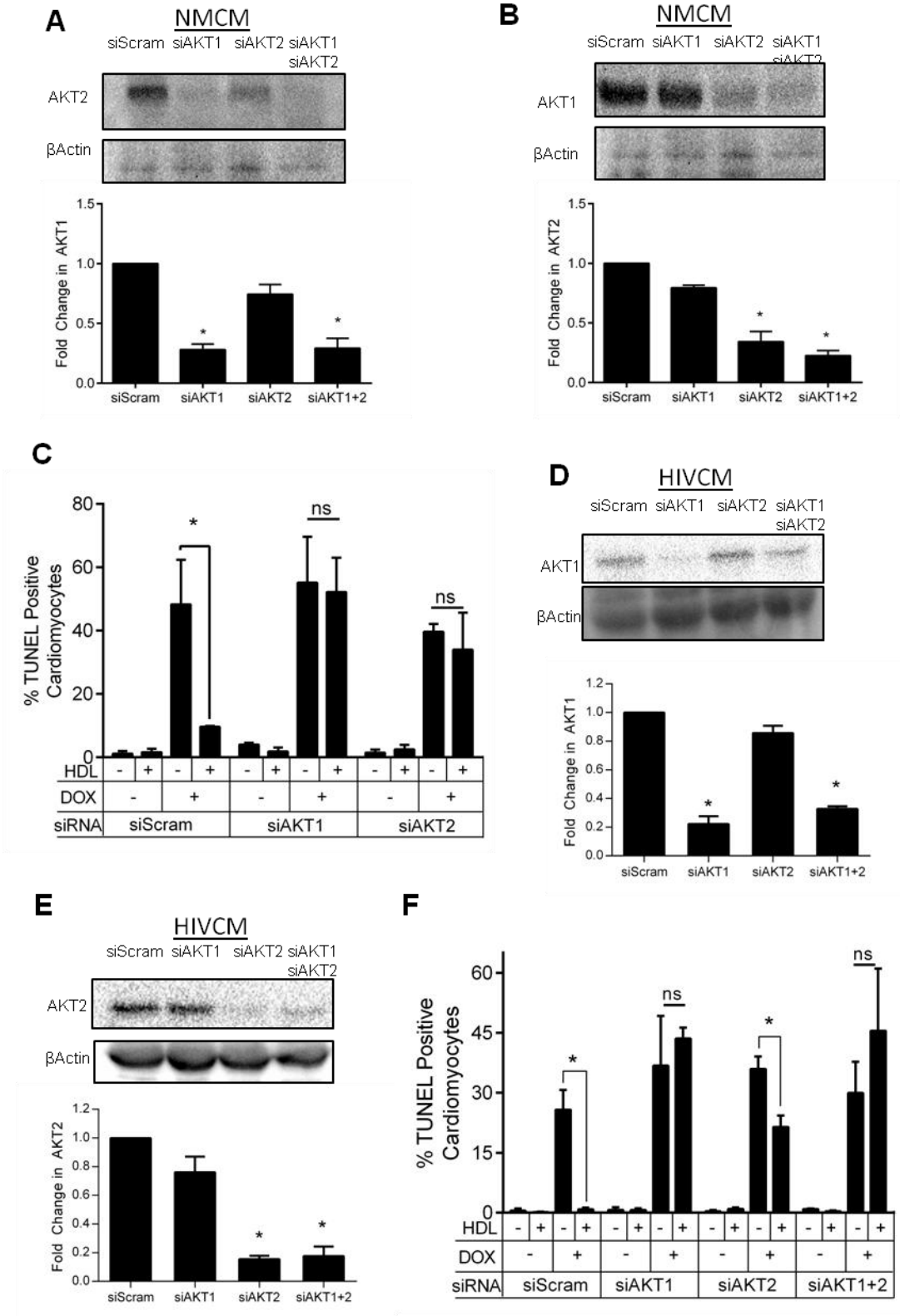
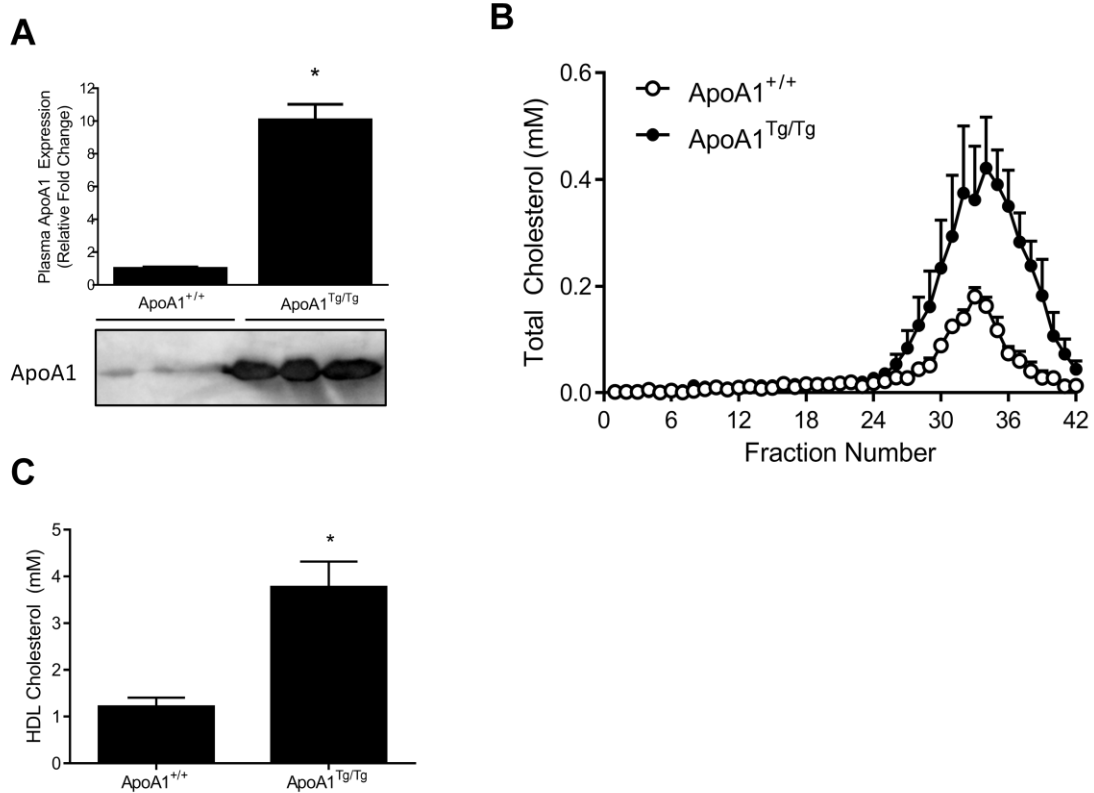


Figure 3.8 Protection by HDL against DOX-induced apoptosis requires AKT1 and AKT2.

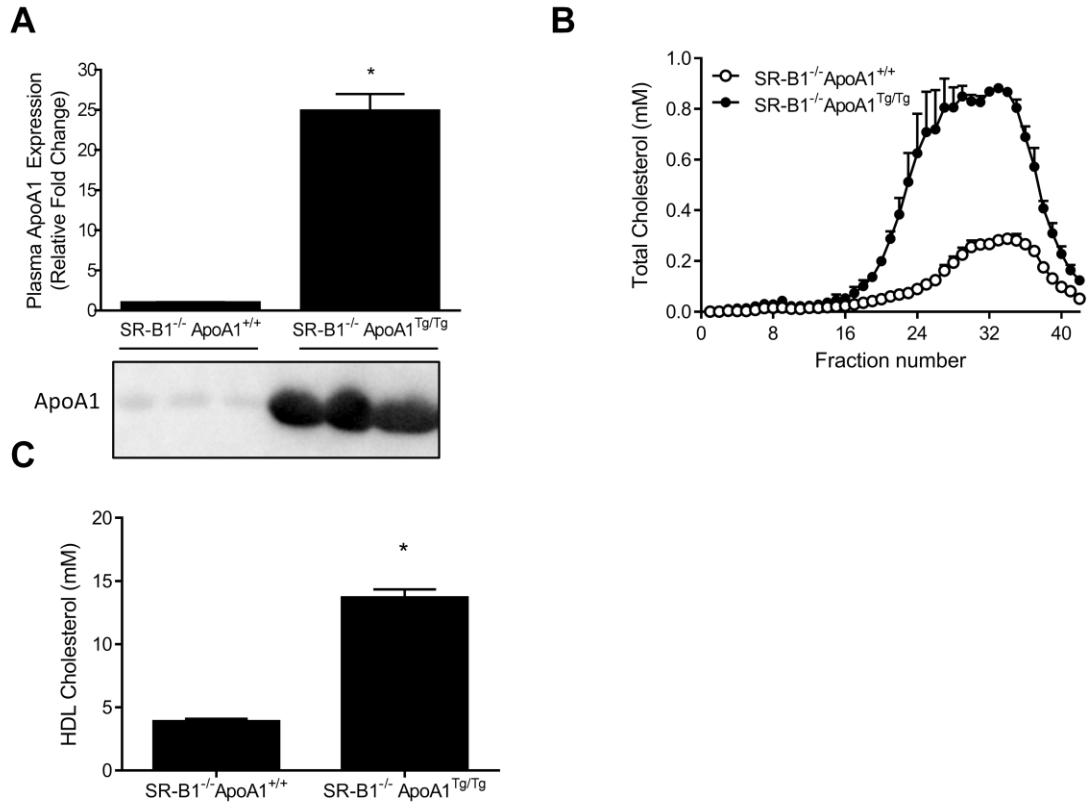
A/B Representative immunoblots and quantification of AKT1 (A) and AKT2 (B) in NMCM transfected with scrambled siRNA or siRNA for AKT1, AKT2, or AKT1 and 2 in combination. C) DOX-induced cardiomyocyte death assessed by TUNEL staining in NMCM transfected with siScram, siAKT1, siAKT2, or siAKT1+2 siRNA and treated \pm HDL * p <0.01. D/E) Representative immunoblots and quantification of AKT1 (D) and AKT2 (E) in HIVCM transfected with scrambled siRNA or siRNA for AKT1, AKT2, or AKT1 and 2 in combination. F) DOX-induced cardiomyocyte death assessed by TUNEL staining in HIVCM transfected with siScram, siAKT1, siAKT2, or siAKT1+2 siRNA and treated \pm HDL * p <0.01. Data represents mean \pm S.E.M. N=3/group unless otherwise stated.



Supplementary Figure 3.1 Plasma ApoA1 and HDL-C levels.

A) Immunoblotting of ApoA1 in plasma from ApoA1^{+/+} and ApoA1^{Tg/Tg} mice. N=3/group. B) Lipoprotein profile of plasma from ApoA1^{+/+} and ApoA1^{Tg/Tg} mice treated with saline. Curve represents averages of 3 and 5 animals/group. C) Quantification of area under the curve of lipoprotein profiles in fractions 26-42.

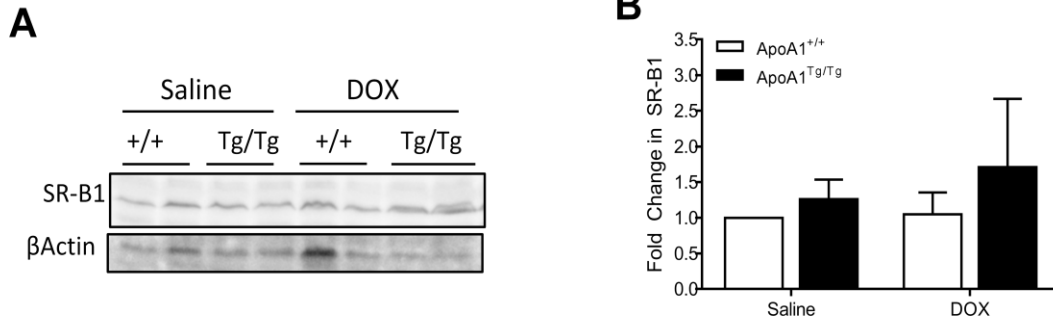
*p<0.001. All data represents mean±S.E.M.



Supplementary Figure 3.2 Plasma ApoA1 and HDL-C levels.

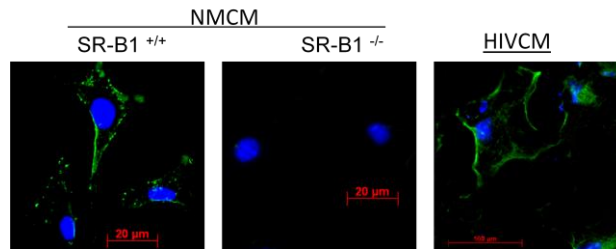
A) Immunoblotting of ApoA1 in plasma from SR-B1^{-/-} ApoA1^{+/+} and SR-B1^{-/-} ApoA1^{Tg/Tg} mice. N=3/group. B) Lipoprotein profile of plasma from SR-B1^{-/-} ApoA1^{+/+} and SR-B1^{-/-} ApoA1^{Tg/Tg} mice treated with saline. Curve represents averages of 3-4 animals/group. C) Quantification of area under the curve of lipoprotein profiles in fractions 18-42.

*p<0.001. All data represents mean±S.E.M.



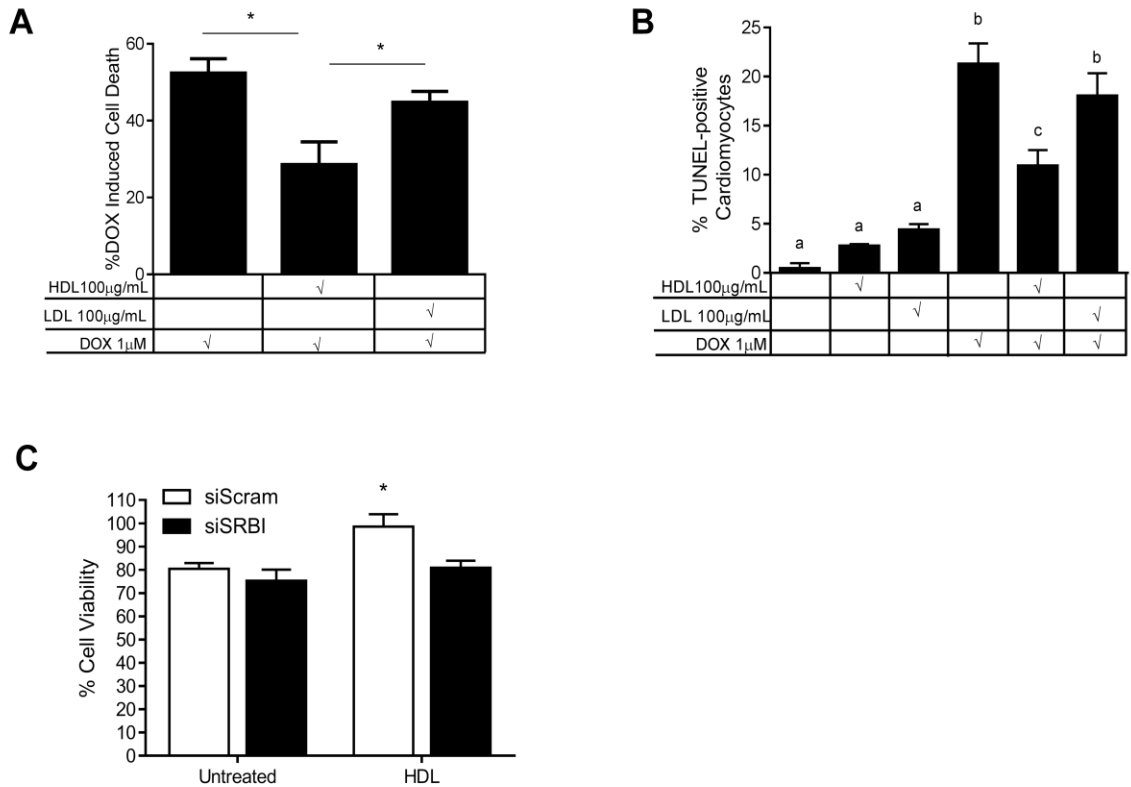
Supplementary Figure 3.3 SR-B1 expression levels do not differ in ApoA1^{+/+} and ApoA1^{Tg/Tg} heart homogenates following 5 weekly injections of saline or DOX.

A) Representative immunoblot. B) Quantification. N= 4/group. Data represents mean±S.E.M.



Supplementary Figure 3.4 Immunofluorescent staining of SR-B1 in isolated SR-B1^{+/+} or SR-B1^{-/-} NMCM or HIVCM.

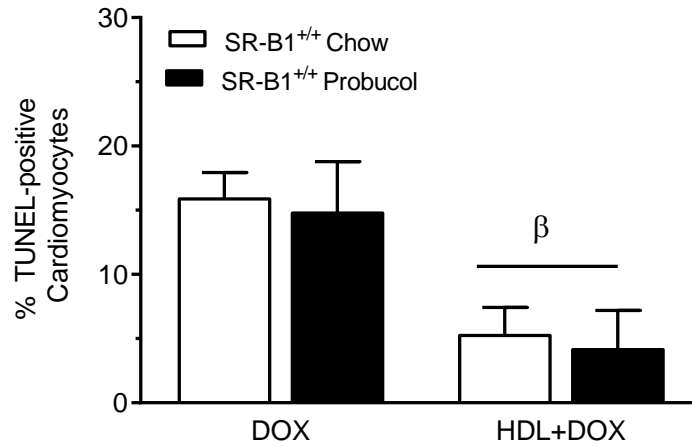
Blue=DAPI, Green=SR-B1. Scale bar= 20µm (NMCM), and 100µm (HIVCM).



Supplementary Figure 3.5 HDL but not LDL protects HIVCM against DOX-induced cell death.

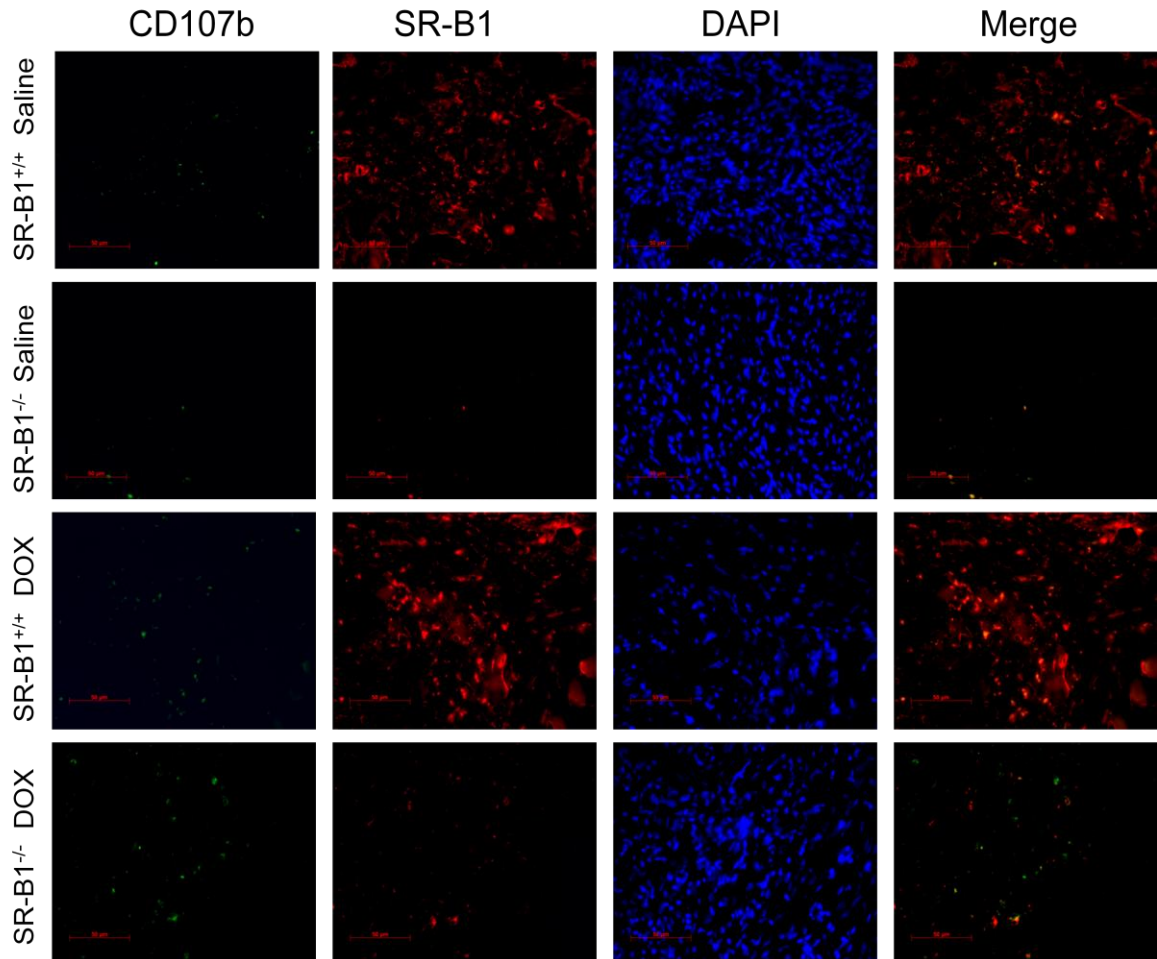
Protection against DOX induced apoptosis (A) or cell death (B) in HIVCM is specific to HDL, and not LDL, and protection by HDL requires SR-B1. HIVCM were starved of lipoproteins, and treated ±100µg/mL human HDL or LDL for 24h and subsequently stressed with 1µM DOX for 6h. A) HIVCM were assessed for viability using a resazurin assay (AlamarBlue, Thermo Fisher Scientific Inc., Waltham, MA) as per manufacturers' instructions. Briefly, following treatment, fresh media containing 1:20 AlamarBlue was added to wells. Cells were incubated for 18h and absorbance was recorded using a spectrophotometer. N=10 wells/group. B) HIVCM were stained for apoptosis using TUNEL staining. N=3 wells/group. C) Cell viability in HIVCM transfected with

siScram or siSR-B1. N=10 wells/group. Data represents means \pm S.E.M. Dissimilar letters and * are significantly different to $p<0.05$ and **= $p<0.001$.



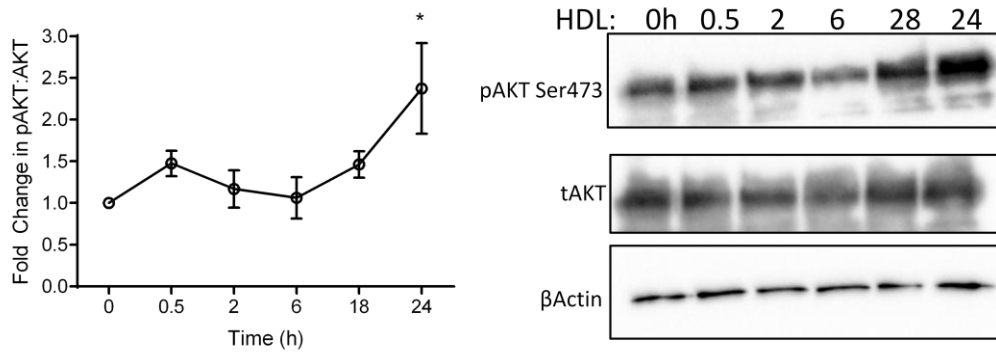
Supplementary Figure 3.6 NMCM isolated from litters born to parents on chow diet and probucol diet respond to DOX and HDL similarly.

NMCM were starved of lipoproteins, and treated $\pm 100\mu\text{g/mL}$ human HDL for 24h and subsequently stressed with $1\mu\text{M}$ DOX for 6h, and stained for apoptosis using TUNEL staining. N=3 wells/group. Data represents means \pm S.E.M. B= treatment effect = $p < 0.01$.



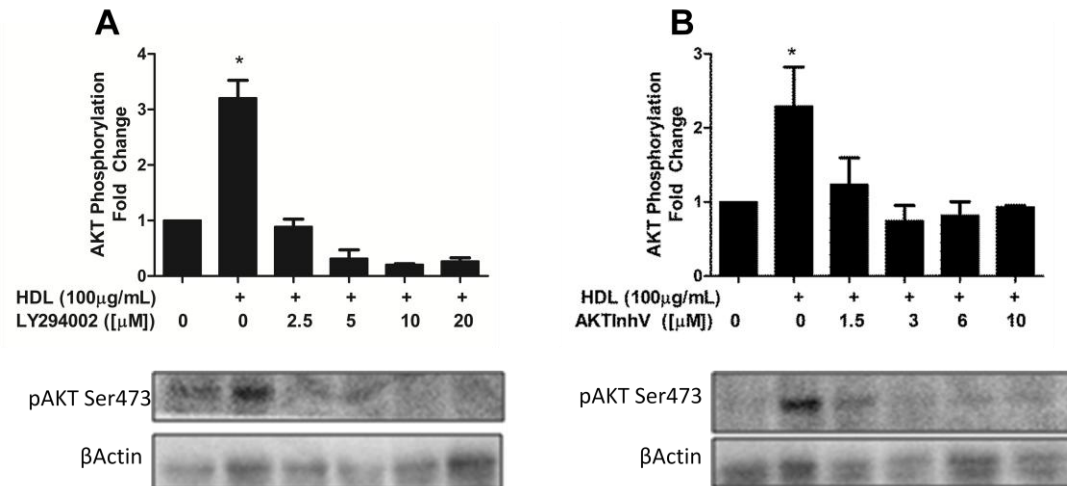
Supplementary Figure 3.7 Host macrophages (SR-BI^{+/+}) are present in both SR-B1^{+/+} and ^{-/-} transplanted hearts.

Representative images of transplanted heart sections stained for the macrophage marker CD107b (green) and SR-B1 (red). White arrows identify cells that co-stain for SR-B1 and CD107b.



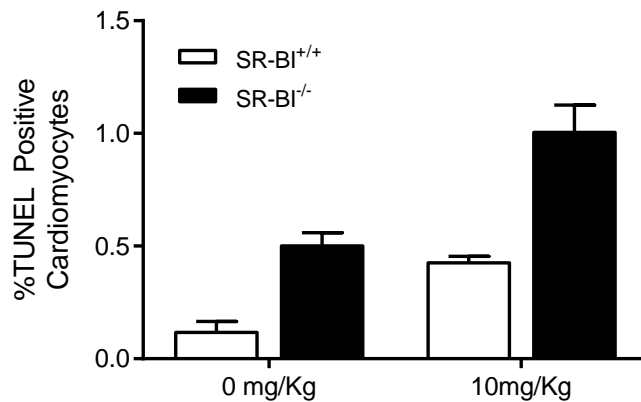
Supplementary Figure 3.8 Activation of AKT by HDL.

AKT phosphorylation at Ser473 in HIVCM following 0-24h incubations ±HDL. N=3 experiments/group. Data represents means±S.E.M. *=p<0.05.



Supplementary Figure 3.9 AKT inhibition by LY294002 and AKT Inh V.

Inhibition of AKT phosphorylation in HIVCM following 24h incubation ±HDL and A) LY294002 and B) AKT Inhibitor V at varying concentrations. N=3 experiments/group. Data represents means±S.E.M. *=p<0.05.



Supplementary Figure 3.10 Female mice lacking SR-B1 have exacerbated cardiomyocyte apoptosis following a single injection of DOX.

Animals were injected with a single injection of 10mg/Kg DOX or vehicle, and hearts were harvested for analysis of cardiomyocyte apoptosis 7 days later. N=4/group. Data represents means±S.E.M. *=p<0.05.

Supplementary Table 3.1 Physical Characteristics of Mice.

	Saline		DOX	
	ApoA1 ^{+/+}	ApoA1 ^{Tg/Tg}	ApoA1 ^{+/+}	ApoA1 ^{Tg/Tg}
Initial BW (g)	25.2 ± 0.7	23.5 ± 0.9	24.3 ± 0.6	23.5 ± 1.1
Final BW (g) *	26.7 ± 0.4	27.2 ± 0.8	23.8 ± 0.6	24.5 ± 0.8
HW (mg) *	138.9 ± 3.2	139.8 ± 4.8	116.2 ± 4.0	117.0 ± 3.4
TL (mm)	20.0 ± 0.4	20.0 ± 0.3	19.3 ± 0.2	18.5 ± 0.6
HW:TL (mg/mm) *	6.9 ± 0.2	7.0 ± 0.2	6.0 ± 0.2	6.4 ± 0.1

* drug effect p<0.05. BW: body weight, HW: heart weight, TL: tibial length. n=7-8 mice/group

Supplementary Table 3.2 Physical Characteristics of Mice

	Saline		DOX	
	SRB1 ^{-/-} ApoA1 ^{+/+}	SRB1 ^{-/-} ApoA1 ^{Tg/Tg}	SRB1 ^{-/-} ApoA1 ^{+/+}	SRB1 ^{-/-} ApoA1 ^{Tg/Tg}
Initial BW (g)	24.1±1.0	26.8±1.4	23.7±0.3	25.4±1.5
Final BW (g) *	28.0±0.8	31.0±1.4	23.2±0.4	25.1±1.4
HW (mg) *	164.1±3.5	165.7±1.5	132.5±6.6	131.1±7.3
TL (mm)	18.4±0.3	18.4±0.5	18.1±0.2	18.4±0.6
HW:TL (mg/mm) *	8.9±0.2	9.0±0.7	7.3±0.4	7.1±0.3

* drug effect $p < 0.05$. BW: body weight, HW: heart weight, TL: tibial length. n=6-8 mice/group

Supplementary Table 3.3 Physical Characteristics of Mice

	Saline		DOX	
	SR-B1 ^{+/+}	SR-B1 ^{-/-}	SR-B1 ^{+/+}	SR-B1 ^{-/-}
Initial BW (g)	25.8±0.3	25.0±1.0	26.2±0.9	24.3±0.7
Final BW (g) *	27.4±0.6	26.8±1.3	23.2±1.2	21.9±0.7
HW (mg) *	149.4±5.1	150.4±1.1	122.4±5.5	129.4±5.1
TL (mm)	22.7±0.5	23.0±0.5	23.2±0.4	22.1±0.2
HW:TL (mg/mm) *	6.6±0.3	6.5±0.4	5.3±0.2	5.8±0.2

* drug effect $p < 0.05$. BW: body weight, HW: heart weight, TL: tibial length. n=7-8 mice/group

Supplementary Table 3.4 List of siRNAs

siRNA Name	Supplier	Targeted Gene	Target Sequence
AllStars Negative Control siRNA	Qiagen	N/A	Proprietary
Hs_AKT1_10	Qiagen	AKT1	5'-CACGCTTGGTCCCGAGGCCAA-3'
Hs_AKT2_7	Qiagen	AKT2	5'-ACGGGCTAAAAGTGACCATGAA-3'
Hs_SCARB1_6	Qiagen	SCARB1	5'-CCGATCCATGAAGCTAATGTA-3'
Mm_Akt1_3	Qiagen	Akt1	5'-AACAATTAGATTCATGTAGAA-3'
Mm_Akt2_1	Qiagen	Akt2	5'-ACGGGCCAAAAGTGACCATGAA-3'

Supplementary Table 3.5 List of Primary Antibodies

Antibody Target	Supplier	Cat. Number	Species
β -Actin	Cell Signaling Technology	12620	Rabbit mAb
Akt	Cell Signaling Technology	9272	Rabbit pAb
Akt1	Cell Signaling Technology	2938	Rabbit mAb
Akt2	Cell Signaling Technology	3063	Rabbit mAb
Phospho Akt (Ser 473)	Cell Signaling Technology	4060	Rabbit mAb
Phospho Akt (Thr 308)	Cell Signaling Technology	13038	Rabbit mAb
CD107b	BD Pharmingen	553322	Rat mAb
Apolipoprotein A1	Midlands BioProducts Corp	71107	Goat pAb
Troponin T Cardiac Isoform	Thermo Scientific	MA5-12960	Mouse mAb
SR-B1	Novus Biologicals	NB400-104	Rabbit pAb

Supplementary Table 3.6 List of Secondary Antibodies

Target	Label/Dye	Supplier	Cat. Number	Species
Rabbit IgG (H+L)	488	Invitrogen	A11008	Goat
Mouse IgG (H+L)	488	Invitrogen	A11059	Rabbit
Streptavidin Conjugate	594	Invitrogen	532356	
Goat IgG (H+L)	HRP	Jackson ImmunoResearch	305-035-003	Rabbit
Rabbit IgG (H+L)	HRP	Jackson ImmunoResearch	711-035-152	Donkey
Mouse IgG (H+L)	HRP	Jackson ImmunoResearch	715-035-150	Donkey

3.8. References

1. Singal, P.K., Iliskovic, N., Li, T., and Kumar, D. 1997. Adriamycin cardiomyopathy: pathophysiology and prevention. *FASEB J* 11:931-936.
2. Hahn, V.S., Lenihan, D.J., and Ky, B. 2014. Cancer therapy-induced cardiotoxicity: basic mechanisms and potential cardioprotective therapies. *J Am Heart Assoc* 3:e000665.
3. Frias, M.A., Lang, U., Gerber-Wicht, C., and James, R.W. 2010. Native and reconstituted HDL protect cardiomyocytes from doxorubicin-induced apoptosis. *Cardiovasc Res* 85:118-126.
4. Calabresi, L., Rossoni, G., Gomaschi, M., Sisto, F., Berti, F., and Franceschini, G. 2003. High-density lipoproteins protect isolated rat hearts from ischemia-reperfusion injury by reducing cardiac tumor necrosis factor-alpha content and enhancing prostaglandin release. *Circ Res* 92:330-337.
5. Rossoni, G., Gomaschi, M., Berti, F., Sirtori, C.R., Franceschini, G., and Calabresi, L. 2004. Synthetic high-density lipoproteins exert cardioprotective effects in myocardial ischemia/reperfusion injury. *J Pharmacol Exp Ther* 308:79-84.
6. Gordts, S.C., Muthuramu, I., Nefyodova, E., Jacobs, F., Van Craeyveld, E., and De Geest, B. 2013. Beneficial effects of selective HDL-raising gene transfer on survival, cardiac remodelling and cardiac function after myocardial infarction in mice. *Gene Ther* 20:1053-1061.
7. Gao, M., Zhao, D., Schouteden, S., Sorci-Thomas, M.G., Van Veldhoven, P.P., Eggermont, K., Liu, G., Verfaillie, C.M., and Feng, Y. 2014. Regulation of high-

- density lipoprotein on hematopoietic stem/progenitor cells in atherosclerosis requires scavenger receptor type BI expression. *Arterioscler Thromb Vasc Biol* 34:1900-1909.
8. Xu, J., Qian, J., Xie, X., Lin, L., Ma, J., Huang, Z., Fu, M., Zou, Y., and Ge, J. 2012. High density lipoprotein cholesterol promotes the proliferation of bone-derived mesenchymal stem cells via binding scavenger receptor-B type I and activation of PI3K/Akt, MAPK/ERK1/2 pathways. *Mol Cell Biochem* 371:55-64.
 9. Li, X.A., Titlow, W.B., Jackson, B.A., Giltiay, N., Nikolova-Karakashian, M., Uittenbogaard, A., and Smart, E.J. 2002. High density lipoprotein binding to scavenger receptor, Class B, type I activates endothelial nitric-oxide synthase in a ceramide-dependent manner. *J Biol Chem* 277:11058-11063.
 10. Kimura, T., Tomura, H., Mogi, C., Kuwabara, A., Damirin, A., Ishizuka, T., Sekiguchi, A., Ishiwara, M., Im, D.S., Sato, K., et al. 2006. Role of scavenger receptor class B type I and sphingosine 1-phosphate receptors in high density lipoprotein-induced inhibition of adhesion molecule expression in endothelial cells. *J Biol Chem* 281:37457-37467.
 11. Mineo, C., Yuhanna, I.S., Quon, M.J., and Shaul, P.W. 2003. High density lipoprotein-induced endothelial nitric-oxide synthase activation is mediated by Akt and MAP kinases. *J Biol Chem* 278:9142-9149.
 12. Grewal, T., de Diego, I., Kirchhoff, M.F., Tebar, F., Heeren, J., Rinninger, F., and Enrich, C. 2003. High density lipoprotein-induced signaling of the MAPK pathway involves scavenger receptor type BI-mediated activation of Ras. *J Biol Chem* 278:16478-16481.

13. Al-Jarallah, A., Chen, X., Gonzalez, L., and Trigatti, B.L. 2014. High density lipoprotein stimulated migration of macrophages depends on the scavenger receptor class B, type I, PDZK1 and Akt1 and is blocked by sphingosine 1 phosphate receptor antagonists. *PLoS One* 9:e106487.
14. Zhang, Y., Ahmed, A.M., McFarlane, N., Capone, C., Boreham, D.R., Truant, R., Igdoura, S.A., and Trigatti, B.L. 2007. Regulation of SR-BI-mediated selective lipid uptake in Chinese hamster ovary-derived cells by protein kinase signaling pathways. *J Lipid Res* 48:405-416.
15. Wu, B.J., Chen, K., Shrestha, S., Ong, K.L., Barter, P.J., and Rye, K.A. 2013. High-density lipoproteins inhibit vascular endothelial inflammation by increasing 3beta-hydroxysteroid-Delta24 reductase expression and inducing heme oxygenase-1. *Circ Res* 112:278-288.
16. Matsui, T., and Rosenzweig, A. 2005. Convergent signal transduction pathways controlling cardiomyocyte survival and function: the role of PI 3-kinase and Akt. *J Mol Cell Cardiol* 38:63-71.
17. Rubin, E.M., Ishida, B.Y., Clift, S.M., and Krauss, R.M. 1991. Expression of human apolipoprotein A-I in transgenic mice results in reduced plasma levels of murine apolipoprotein A-I and the appearance of two new high density lipoprotein size subclasses. *Proceedings of the National Academy of Sciences of the United States of America* 88:434-438.
18. Rigotti, A., Trigatti, B.L., Penman, M., Rayburn, H., Herz, J., and Krieger, M. 1997. A targeted mutation in the murine gene encoding the high density

- lipoprotein (HDL) receptor scavenger receptor class B type I reveals its key role in HDL metabolism. *Proc Natl Acad Sci U S A* 94:12610-12615.
19. Fey, T.A., Krause, R.A., Hsieh, G.C., Andrews, J.M., Bretheim, P.T., Morgan, S.J., Luly, J.R., and Mollison, K.W. 1998. Improved methods for transplanting split-heart neonatal cardiac grafts into the ear pinna of mice and rats. *J Pharmacol Toxicol Methods* 39:9-17.
 20. Tardif, J.C., Gregoire, J., L'Allier, P.L., Ibrahim, R., Lesperance, J., Heinonen, T.M., Kouz, S., Berry, C., Bassar, R., Lavoie, M.A., et al. 2007. Effects of reconstituted high-density lipoprotein infusions on coronary atherosclerosis: a randomized controlled trial. *JAMA* 297:1675-1682.
 21. Tao, H., Yancey, P.G., Babaev, V.R., Blakemore, J.L., Zhang, Y., Ding, L., Fazio, S., and Linton, M.F. 2015. Macrophage SR-BI Mediates Efferocytosis via Src/PI3K/Rac1 Signaling and Reduces Atherosclerotic Lesion Necrosis. *Journal of Lipid Research*.
 22. Song, X., Fischer, P., Chen, X., Burton, C., and Wang, J. 2009. An apoA-I mimetic peptide facilitates off-loading cholesterol from HDL to liver cells through scavenger receptor BI. *Int J Biol Sci* 5:637-646.
 23. Nissen, S.E., Tsunoda, T., Tuzcu, E.M., Schoenhagen, P., Cooper, C.J., Yasin, M., Eaton, G.M., Lauer, M.A., Sheldon, W.S., Grines, C.L., et al. 2003. Effect of recombinant ApoA-I Milano on coronary atherosclerosis in patients with acute coronary syndromes: a randomized controlled trial. *JAMA* 290:2292-2300.
 24. Zamanian-Daryoush, M., Lindner, D., Tallant, T.C., Wang, Z., Buffa, J., Klipfell, E., Parker, Y., Hatala, D., Parsons-Wingerter, P., Rayman, P., et al. 2013. The

- cardioprotective protein apolipoprotein A1 promotes potent anti-tumorigenic effects. *J Biol Chem* 288:21237-21252.
25. Yuan, Y., Wang, W., Wang, B., Zhu, H., Zhang, B., and Feng, M. 2013. Delivery of hydrophilic drug doxorubicin hydrochloride-targeted liver using apoAI as carrier. *J Drug Target* 21:367-374.
 26. Berge, K.G., Canner, P.L., and Hainline, A., Jr. 1982. High-density lipoprotein cholesterol and prognosis after myocardial infarction. *Circulation* 66:1176-1178.
 27. Argraves, K.M., and Argraves, W.S. 2007. HDL serves as a S1P signaling platform mediating a multitude of cardiovascular effects. *Journal of Lipid Research* 48:2325-2333.
 28. Frias, M.A., Lecour, S., James, R.W., and Pedretti, S. 2012. High density lipoprotein/sphingosine-1-phosphate-induced cardioprotection: Role of STAT3 as part of the SAFE pathway. *JAKSTAT* 1:92-100.
 29. Tao, R., Hoover, H.E., Honbo, N., Kalinowski, M., Alano, C.C., Karliner, J.S., and Raffai, R. 2010. High-density lipoprotein determines adult mouse cardiomyocyte fate after hypoxia-reoxygenation through lipoprotein-associated sphingosine 1-phosphate. *Am J Physiol Heart Circ Physiol* 298:H1022-1028.
 30. Li, F.C., Gasser, R.B., Lok, J.B., Korhonen, P.K., He, L., Di, W.D., Yin, F.Y., Zhou, R., Zhou, Y.Q., Zhao, J.L., et al. 2016. Molecular characterization of the *Haemonchus contortus* phosphoinositide-dependent protein kinase-1 gene (Hc-pdk-1). *Parasit Vectors* 9:65.
 31. Chan, K.Y., Xiang, P., Zhou, L., Li, K., Ng, P.C., Wang, C.C., Zhang, L., Deng, H.Y., Pong, N.H., Zhao, H., et al. 2011. Thrombopoietin protects against

- doxorubicin-induced cardiomyopathy, improves cardiac function, and reversely alters specific signalling networks. *Eur J Heart Fail* 13:366-376.
32. Maruyama, S., Shibata, R., Ohashi, K., Ohashi, T., Daida, H., Walsh, K., Murohara, T., and Ouchi, N. 2011. Adiponectin ameliorates doxorubicin-induced cardiotoxicity through Akt protein-dependent mechanism. *J Biol Chem* 286:32790-32800.
33. Kim, K.H., Oudit, G.Y., and Backx, P.H. 2008. Erythropoietin protects against doxorubicin-induced cardiomyopathy via a phosphatidylinositol 3-kinase-dependent pathway. *J Pharmacol Exp Ther* 324:160-169.
34. An, T., Zhang, Y., Huang, Y., Zhang, R., Yin, S., Guo, X., Wang, Y., Zou, C., Wei, B., Lv, R., et al. 2013. Neuregulin-1 protects against doxorubicin-induced apoptosis in cardiomyocytes through an Akt-dependent pathway. *Physiol Res* 62:379-385.
35. Taniyama, Y., and Walsh, K. 2002. Elevated myocardial Akt signaling ameliorates doxorubicin-induced congestive heart failure and promotes heart growth. *J Mol Cell Cardiol* 34:1241-1247.
36. Kunuthur, S.P., Mocanu, M.M., Hemmings, B.A., Hausenloy, D.J., and Yellon, D.M. 2012. The Akt1 isoform is an essential mediator of ischaemic preconditioning. *J Cell Mol Med* 16:1739-1749.

Chapter 4. Therapeutic Administration of ApoA1 Protects Against Doxorubicin Induced Cardiomyocyte Apoptosis

Author List: Kristina Durham, Christy Mak, Melissa MacDonald, Bernardo Trigatti

4.1. Preface

In this manuscript we aimed to determine whether raising plasma HDL by a therapeutic injection of human ApoA1 would protect against the deleterious cardiotoxic side effects of DOX including cardiomyocyte apoptosis and atrophy. This project was initiated by Kristina Durham and Dr. Bernardo Trigatti. Experiments were designed by Kristina Durham with guidance from Dr. Bernardo Trigatti. Kristina Durham conducted all experiments involving animals, and data collected from analysis of tissues was produced and analyzed by both Kristina Durham and Christy Mak under the supervision of Kristina Durham. All data were interpreted by Kristina Durham with guidance from Dr. Bernardo Trigatti. This manuscript was written by Kristina Durham with guidance and editing from Dr. Bernardo Trigatti. Melissa MacDonald assisted with animal breeding. This manuscript will be submitted for publication in 2017, and is an ongoing study.

4.2. Abstract

The deleterious cardiotoxic side effects of doxorubicin, a clinically used chemotherapeutic, severely limits its use. To date there are no widely accepted therapies used to protect against the cardiotoxic side effects of DOX. Most importantly, a therapeutic aimed at cardioprotection must not lessen the anti-tumorigenic activity of doxorubicin. In 2010, researchers reported the ability of HDL to protect isolated rat cardiomyocytes against DOX-induced apoptosis (1). Our previous work has

demonstrated that raising plasma high density lipoprotein by overexpression of apolipoprotein A1 protects against doxorubicin -induced cardiotoxicity by inhibiting the pro-apoptotic and pro-atrophic effects. Other research has reported that overexpression or injection of apolipoprotein A1 into tumor bearing mice reduces tumor metastasis and improves survival. Here, we assess whether a therapeutic increase in plasma high density lipoprotein by injection of apolipoprotein A1 protects against the cardiotoxic side effects of doxorubicin. Secondly, we attempt to delineate whether increasing plasma high density lipoprotein leads to changes in the activation of the cardioprotective protein kinase B within the heart. Briefly, mice that were injected with apolipoprotein A1 were protected against doxorubicin-induced apoptosis, but not atrophy. Immunoblot analyses of the hearts revealed an increase in protein kinase B activation in hearts from mice treated with doxorubicin and apolipoprotein A1. We conclude that providing a therapeutic injection of apolipoprotein A1 prior to and following a single injection of doxorubicin protects against doxorubicin-induced cardiomyocyte apoptosis, and may be a result of protective signaling through the protein kinase B pathway, however; future research is required to delineate the role of protein kinase B.

4.3. Introduction

Doxorubicin (DOX) is an effective anthracycline used to treat both solid and hematologic cancers (2). Despite its therapeutic benefits, long term use of DOX is limited by its dose-dependent and deleterious side effects of cardiotoxicity and congestive heart failure (2). Others have reported the protective effect of high density lipoprotein (HDL) against DOX-induced cardiomyocyte apoptosis *in vitro* (1). Our previous work has demonstrated that increasing plasma HDL by overexpressing

apolipoprotein A1 (ApoA1) negates the cardiotoxic side effects of DOX as evidenced by maintained cardiomyocyte cross sectional area, and lack of induction of cardiomyocyte apoptosis, as well as maintenance of cardiac function following chronic DOX exposure (see Chapter 3, Unpublished data, Durham K. and Trigatti B. *et al*, 2016). This protection afforded by increased HDL was dependent on the expression of the scavenger receptor class B type I (SR-B1), and the intracellular targets phosphoinositide 3-kinase (PI3K), and protein kinase B (AKT) (see Chapter 3, Unpublished data, Durham K. and Trigatti B. *et al.*, 2016). Research has demonstrated that both transgenic expression of ApoA1 and injection of ApoA1 reduces tumor growth and metastasis, and increases survival of tumor bearing mice (3). The anti-tumor effects of ApoA1 were attributed to a transition of macrophages associated with the tumor from a pro-tumor M2 to anti-tumor M1 type (3). Additionally, encapsulating DOX in reconstituted HDL particles enhances the cytotoxic effects of DOX on tumors *in vivo*, and cancer cells *in vitro* (4, 5). Given the paradoxical cardioprotective and anti-tumor nature of ApoA1- the backbone of HDL, and the enhanced anti-tumorigenic activity of DOX when encapsulated in HDL, we postulate that ApoA1, and therefore HDL, may be a notable therapeutic target for generating protection against the deleterious side effect of DOX.

As proof of principle, we used transgenic overexpression of human ApoA1 to dramatically raise HDL in experimental mice and showed that overexpression of ApoA1 attenuated DOX-induced cardiomyocyte apoptosis, atrophy, and dysfunction. To test the effects of a more pharmacologically relevant intervention, here we evaluate whether intraperitoneal (IP) injection of ApoA1 leads to a moderate and clinically relevant increase in plasma ApoA1, and whether this therapeutic increase in ApoA1 will protect

against DOX-induced cardiomyocyte apoptosis and atrophy. Secondly, we have assessed the hearts for activation of the cardioprotective kinase AKT, in order to evaluate whether (in line with our previous chronic DOX studies, see Chapter 3), AKT activation may play a role in mediating protection of the heart against cardiotoxic stress.

4.4. Results

A therapeutic IP injection of human ApoA1 increases plasma ApoA1. Plasma ApoA1 was increased by ~2.2 times following a single injection of 14mg/Kg human ApoA1 (Fig. 4.2A). When a second injection of 14mg/Kg of human ApoA1 was administered 8h following the first, plasma ApoA1 was increased ~3.4 times (Fig. 4.2A). One week following the start of treatment, plasma ApoA1 levels did not differ between Control, ApoA1, DOX, or ApoA1+DOX treated animals (Fig. 4.2B). This suggests that ApoA1 is being catabolized over the course of a week which is expected given that ApoA1 clearance is approximately 4.5 days (6). Plasma from mice harvested at 11h following initiation of treatment was fractionated by fast protein liquid chromatography (FPLC) and assayed for cholesterol in order to determine whether the increase in plasma ApoA1 (and therefore HDL particle number) corresponded to an increase in cholesterol contained in HDL sized particles. No detectable differences in cholesterol contained in HDL sized fractions were observed suggesting at this time point the increase in HDL number (due to increased ApoA1) does not correspond to an increase in HDL associated cholesterol (HDL-C) (Fig. 4.2E).

Animal Characteristics. Animal characteristics including initial body weight (BW), heart weight (HW), and HW:tibial length (TL) did not differ between any groups regardless of treatment (Table 4.1). Some non-significant reductions were observed such as a DOX-

induced reduction in HW:TL, however; greater numbers of animals per group would be required to achieve greater statistical power. Of note is the higher final BW of Control and DOX treated animals in comparison to ApoA1 animals and is likely related to the lower initial BW of these animals (Table 4.1).

Injection of ApoA1 protects against DOX-induced cardiomyocyte apoptosis but not atrophy. Injection of ApoA1 alone did not affect apoptosis of cardiomyocytes as evidenced by similar and low levels of apoptosis compared to Control animals (1.14 ± 0.47 vs. $1.31 \pm 0.5\%$ TUNEL-positive cardiomyocytes, Fig. 4.3A, B). A single injection of 10mg/Kg DOX resulted in a 5.1 fold increase in apoptotic cardiomyocytes compared to Control animals (6.65 ± 0.47 vs. $1.31 \pm 0.5\%$ TUNEL-positive cardiomyocytes, Fig. 4.3A, B). In contrast, hearts from ApoA1 injected mice treated with either saline or DOX exhibited similar and low levels of cardiomyocyte apoptosis (1.14 ± 0.47 vs. 0.47 ± 0.48 TUNEL-positive cardiomyocytes, Fig. 4.3A, B), indicating ApoA1 injection protects against DOX-induced cardiomyocyte apoptosis *in vivo*. Injection of ApoA1 alone did not affect cardiomyocyte CSA as evidenced by similar CSA compared to control animals (136.4 ± 0.7 vs. $122.7 \pm 5.1 \mu\text{m}^2$, Fig. 4.3C, D). Cardiomyocyte CSA was reduced by 35% in mice treated with DOX (136.4 ± 0.7 vs. $88.8 \pm 7.6 \mu\text{m}^2$, Fig. 4.3C, D). Injection of ApoA1 did not entirely protect against DOX-induced cardiomyocyte atrophy as evidenced by a DOX-induced 20% reduction in CSA compared to ApoA1 treated hearts (122.7 ± 5.1 vs. $98.7 \pm 4.2 \mu\text{m}^2$, Fig. 4.3C, D).

AKT is activated in an ApoA1/stress-dependent manner. Hearts collected 7 days following the start of treatment were homogenized and assessed by immunoblotting for activation of AKT. One week following the initiation of treatment, phosphorylation of

AKT at ser473 was increased 4.5 times in hearts from ApoA1+DOX treated mice compared to Control hearts (Fig. 4.4B), suggesting ApoA1 promotes activation of AKT in a stress-dependent manner. It should be noted that there was a non-statistically significant trend towards increased phosphorylation of AKT at ser473 in hearts treated with ApoA1 alone.

4.5. Discussion

Our previous work (see Chapter 3) identified the cardioprotective role of HDL in attenuation of the deleterious cardiotoxic side effects of DOX. Previously we raised HDL levels in a murine model by overexpressing the HDL backbone ApoA1. As genetic manipulation is currently not a clinically relevant means to increase HDL, and also results in a chronically sustained and large magnitude of increase in HDL levels, we identified the need to evaluate whether a moderate increase in HDL by therapeutic delivery of ApoA1 would provide protection against the deleterious cardiotoxic side effects of DOX. Here we evaluated whether raising plasma ApoA1 by IP injection of human ApoA1 led to protection against DOX-induced cardiomyocyte apoptosis and atrophy. Firstly, we validated a method to increase plasma ApoA1 that resulted in a ~2.2 fold increase in plasma ApoA1 after a single IP injection of 14mg/Kg of human ApoA1 into a wild-type mouse. Following a second injection of ApoA1, spaced 8h from the first, plasma ApoA1 was increased 3.4 fold. Next, administration of a single injection of 10mg/Kg DOX led to increased cardiomyocyte apoptosis compared to Control mice, however; when ApoA1 was administered in combination with DOX, animals did not show elevated cardiomyocyte apoptosis in response to DOX treatment, suggesting a 2.2-

3.4 fold increase in plasma ApoA1 is sufficient for protection against DOX-induced apoptosis.

We have previously demonstrated that overexpression of ApoA1 protects against chronic DOX-induced cardiomyocyte atrophy. In the current study a single injection of DOX reduced cardiomyocyte CSA as compared to control animals, indicating DOX-induced atrophy. Raising plasma ApoA1 by injection did not protect against DOX-induced cardiomyocyte atrophy. Interestingly, the increase in ApoA1 was not enough to overcome the atrophic effects of DOX but was sufficient to protect against DOX-induced apoptosis. Perhaps protective effects of ApoA1 against DOX-induced atrophy require greater or sustained increases in plasma ApoA1.

Analysis of hearts from mice harvested 7 days following initiation of experiments revealed a greater level of AKT activation in hearts from mice treated with both ApoA1 and DOX. This is in line with our previous results in ApoA1^{Tg/Tg} mice which found AKT was activated by overexpression of ApoA1 in a DOX-dependent manner, and that ApoA1 overexpression alone did not affect AKT phosphorylation (See Chapter 3). This stress-dependency of ApoA1-induced activation of AKT may be due to control mechanisms in non-stressed hearts which control the dynamic activation of AKT, such as phosphatase and tensin homolog or phospholipase 2A- both negative regulators of AKT activation (7, 8).

Overall our data reflects the protective effects of a small increase in ApoA1 against the apoptotic effect of DOX on cardiomyocytes. Future studies should aim to delineate the dose-dependent effects of ApoA1 to identify a therapeutically relevant dose of ApoA1 that leads to protection against both DOX-induced apoptosis and atrophy. This

work is ongoing, and currently mice lacking SR-B1 specifically in cardiomyocytes are being generated in order to test whether the protection afforded by ApoA1 injection against DOX-induced cardiomyocyte apoptosis is dependent on SR-B1. See Chapter 6: Limitations and Future Directions for a detailed description of the future directions of this project.

4.6. Methods

Treatment of Mice

Male C57Bl/6 mice were group housed and allowed free access to normal chow diet and water. A timeline of the experimental protocol can be found in Figure 4.1. At 7-8 weeks of age, mice received two injections, 8h apart, of 14mg/Kg human ApoA1 or 0.9% sterile saline IP (as a vehicle control, Alfa Aesar, Ward Hill, MA). Animals were injected IP with 10mg/Kg DOX (Toronto Research Chemicals, Toronto, ON, Canada) or 0.9% sterile saline 3h following the first injection of ApoA1. Blood was collected by saphenous bleed 3h following each injection of ApoA1 for assessment of plasma ApoA1, and at time of euthanasia by cardiac puncture for assessment of plasma lipoprotein cholesterol. Animals were anesthetized and organs were collected at either 1 week following the start of experiments for analysis of cardiomyocyte apoptosis and atrophy, or 3h following the second ApoA1 injection for assessment of plasma lipoprotein cholesterol. Groups labels are: Control- all vehicle treated, DOX- vehicle for ApoA1 and DOX treated, ApoA1- ApoA1 treated and vehicle for DOX, ApoA1+DOX- ApoA1 and DOX treated.

Collection of Hearts for Analyses

At the time of euthanasia, blood was collected by cardiac puncture, and mice were perfused with heparinized saline to flush blood from tissues. The hearts were excised and cut into two- a piece was snap frozen for immunoblotting, and the other half was fixed in 10% formalin for paraffin embedding.

Cardiomyocyte CSA Analysis

Fixed hearts were paraffin embedded and sectioned at 4 μ m. Sections were deparaffinised, stained with hematoxylin and eosin, and imaged using light microscopy. Cardiomyocyte CSA was determined using ImageJ software by measuring a minimum of 130 cardiomyocytes/heart from three different heart sections which represented the base, midline, and apex of the heart. Only round or cuboidal and nucleated cardiomyocytes were included in analyses.

Quantification of Apoptosis

Heart sections were subjected to antigen retrieval by boiling the samples for 5 min in a commercially available microwave pressurizer in Antigen Unmasking Solution (Vector Laboratories, Burlington, ON, Canada) for Immunofluorescent staining. Apoptotic nuclei were immunofluorescently labeled using the terminal deoxynucleotidyl transferase-mediated dUTP nick end-labeling (TUNEL) assay according to manufacturer's instructions (Millipore Canada Ltd., Etobicoke, ON, Canada). To distinguish cardiomyocytes from other cardiac cells, sections were co-stained with a mouse monoclonal anti cardiac troponin T antibody (cTnT, Thermo Fisher Scientific Inc., Waltham, MA) using a Mouse on Mouse Kit and biotinylated secondary (Vector Laboratories, Burlington, ON, Canada) and tertiary labeling with a streptavidin conjugated AlexaFluor 568 antibody (Life Technologies, Burlington, ON, Canada).

Nuclei were stained with DAPI. Apoptotic cardiomyocytes were identified as having a TUNEL-positive nucleus that was surrounded by cTnT staining. TUNEL positive nuclei were counted in 3 sections per heart representing the base, midline, and apex of the heart, from 4 randomly selected fields per section. Apoptosis was expressed as a ratio of TUNEL positive cardiomyocyte nuclei to total cardiomyocyte nuclei.

Microscopy

Bright field and fluorescent images were captured using a Zeiss Axiovert 200M inverted microscope (Carl Zeiss Canada Ltd. Toronto, ON, Canada), or an Olympus BX41TF microscope (Olympus Canada Inc., Richmond Hill, ON, Canada).

Immunoblotting

Hearts were homogenized in a lysis buffer containing 20mM Tris-HCl pH 7.5, 150mM NaCl, 1mM Na₂EDTA, 1mM EGTA, 1% Triton, 2.5mM Na₄P₂O₇, 1mM β-glycerophosphate, 1mM Na₃VO₃, with 1μg/mL Pepstatin A, 1mg/mL leupeptin 2μg/mL aprotinin, 50μM p-Amidinophenylmethylsulfonylfluoride (all from Sigma-Aldrich Canada Co., Oakville, ON, Canada). Heart homogenates (25μg total protein), or plasma (1.5μL) were denatured and separated by SDS-polyacrylamide gel electrophoresis and transferred onto a PVDF membrane. Antibodies were applied following manufacturer's instructions, and visualized using enhanced chemiluminescence (Thermo Fisher Scientific Inc., Waltham, MA). Antibodies were purchased from Cell Signaling Technologies Inc. (Danvers, MA) with the exception of anti-ApoA1 (Midlands BioProducts Corp, Boone, IA). See Supplementary Table 3.5 for source, catalogue number, and species of primary antibodies, and Supplementary Table 3.6 for secondary antibodies used.

Statistical Analyses

All data are expressed as mean \pm standard error of the mean (S.E.M.).

Differences are considered statistically significant at $p < 0.05$. Data was analyzed for statistical significance using GraphPad software (GraphPad Software, Inc., La Jolla, CA). Normality was assessed using the Shapiro-Wilk or D'Agostino-Pearson omnibus test and equal variance by F test. Data that was normally distributed and showed equal variance were analyzed by one way ANOVA to compare more than two groups. Post hoc analysis of statistically relevant comparisons were tested using the Tukey test for groups with equal N groups, or the Tukey-Kramer test for groups with unequal N.

4.7. Figures

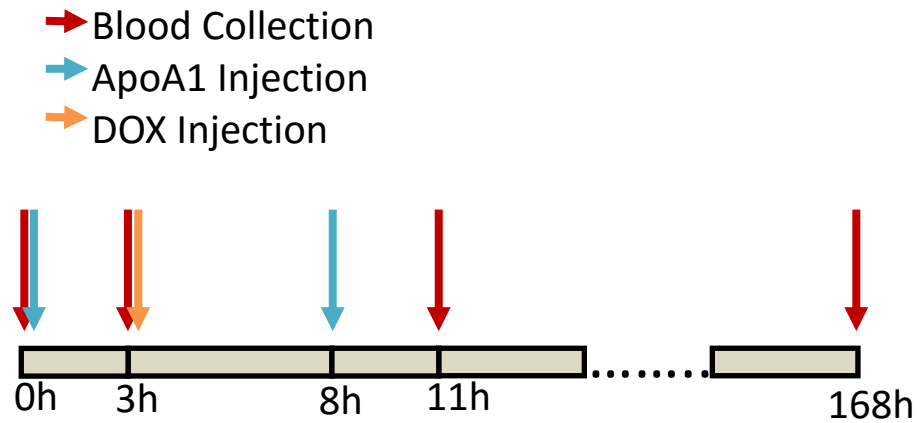


Figure 4.1 Experimental timeline.

Red arrows represent collection of blood by saphenous bleed or cardiac puncture (at time of euthanasia), blue arrows represent injection of ApoA1 or vehicle, and orange arrows represent injection of DOX or vehicle.

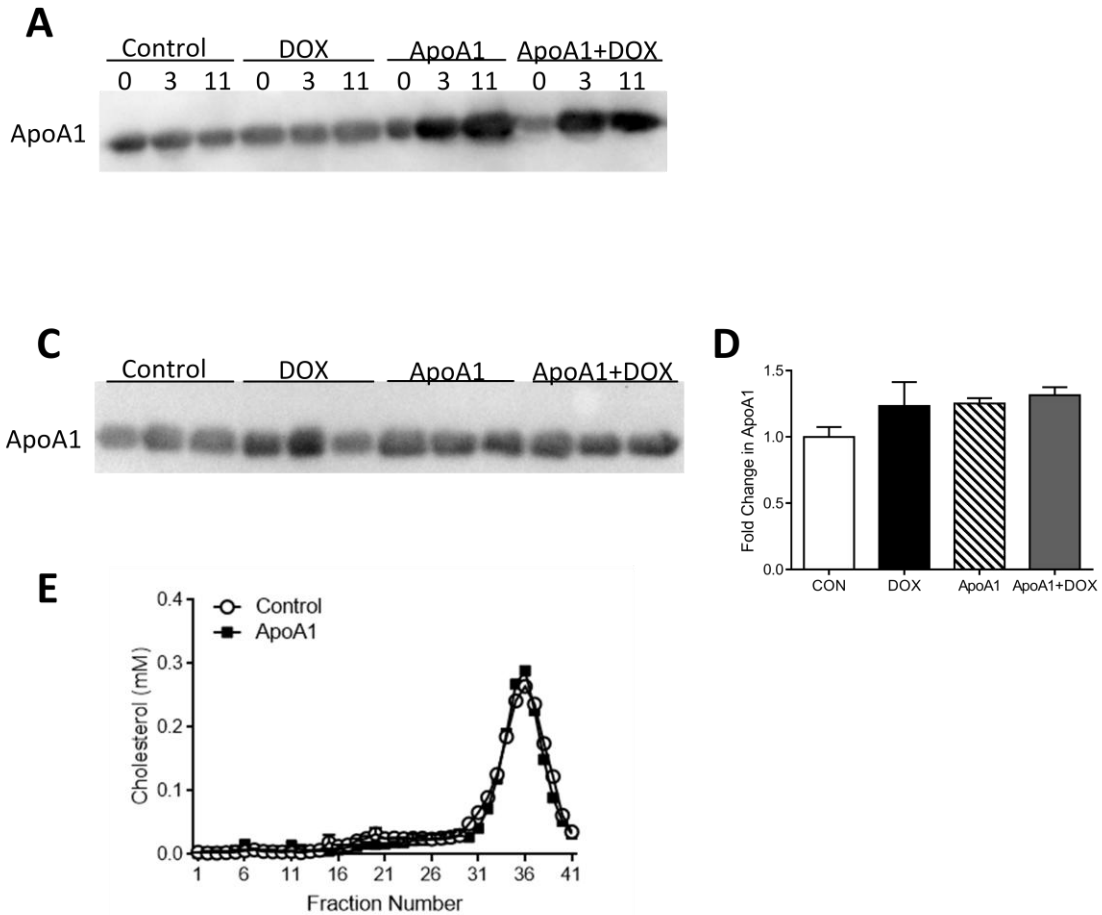


Figure 4.2 IP injection of ApoA1 increases plasma ApoA1 levels.

A) Representative immunoblot of ApoA1 from plasma collected at the 0, 3, and 11h time points, and B) quantification. C) Representative immunoblot of ApoA1 from plasma collected at day 7 and D) quantification. E) Representative lipoprotein profiles of plasma from Control or ApoA1 treated mice collected 11h following initiation of treatment. N=3 animals/group for all experiments except E) where a representative curve from a single animal in each group is shown. *p<0.0001. Data represent means±S.E.M.

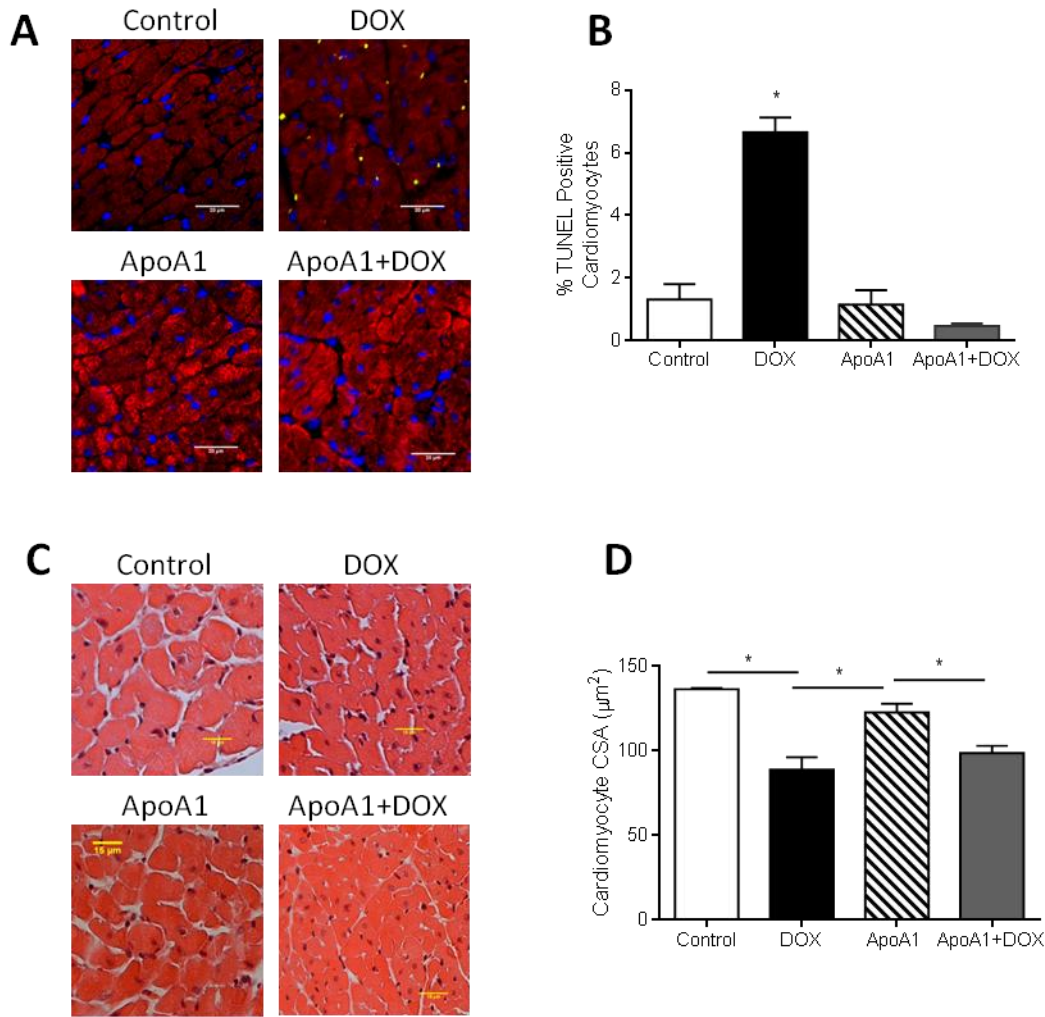


Figure 4.3 Increasing ApoA1 by injection protects against the apoptotic effect of a single DOX injection.

A) Representative images of heart sections stained for apoptosis with TUNEL (green), cardiomyocytes with cTnT (red), and nuclei with DAPI (blue). B) Quantification of apoptotic cardiomyocytes. C) Representative images of heart sections stained with H&E to assess cardiomyocyte CSA. D) Quantification of CSA. N=3 animals/group. Data represent means±S.E.M.. *p<0.01

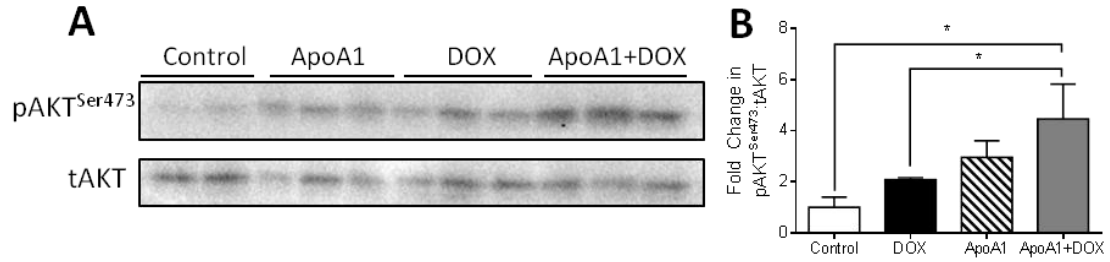


Figure 4.4 AKT is activated in an ApoA1 and stress dependent manner at Ser473.

A) Representative immunoblots and B) quantification of pAKT^{Ser473}:tAKT from hearts collected 7 days following the initiation of treatment. N=3animals/group. Data represent means±S.E.M.. *p<0.01

Table 4.1 Animal Characteristics

	Control	ApoA1	DOX	ApoA1+DOX
Initial Body Weight (g)	24.8±2.6	29.7±0.3	23.7±0.2	28.4±0.8
Final Body Weight (g)	24.2±1.7*	28.8±0.3	21.9±0.3*	26.1±0.9
Heart Weight (mg)	127.7±4.8	147.4±4.2	110.7±3.2	138.6±14.5
TL, mm	18.7±1.2	19.8±0.4	17.3±0.3	20.5±0.3
HW:TL (mg/mm)	6.9±0.5	7.4±0.2	6.4±0.3	6.8±0.7

*p<0.05 versus ApoA1

4.8. References

1. Frias, M.A., Lang, U., Gerber-Wicht, C., and James, R.W. 2010. Native and reconstituted HDL protect cardiomyocytes from doxorubicin-induced apoptosis. *Cardiovasc Res* 85:118-126.
2. Singal, P.K., Iliskovic, N., Li, T., and Kumar, D. 1997. Adriamycin cardiomyopathy: pathophysiology and prevention. *FASEB J* 11:931-936.
3. Zamanian-Daryoush, M., Lindner, D., Tallant, T.C., Wang, Z., Buffa, J., Klipfell, E., Parker, Y., Hatala, D., Parsons-Wingerter, P., Rayman, P., et al. 2013. The cardioprotective protein apolipoprotein A1 promotes potent anti-tumorigenic effects. *J Biol Chem* 288:21237-21252.
4. Kader, A., and Pater, A. 2002. Loading anticancer drugs into HDL as well as LDL has little affect on properties of complexes and enhances cytotoxicity to human carcinoma cells. *J Control Release* 80:29-44.
5. Yuan, Y., Wang, W., Wang, B., Zhu, H., Zhang, B., and Feng, M. 2013. Delivery of hydrophilic drug doxorubicin hydrochloride-targeted liver using apoAI as carrier. *J Drug Target* 21:367-374.
6. Schaefer, E.J., Zech, L.A., Jenkins, L.L., Bronzert, T.J., Rubalcaba, E.A., Lindgren, F.T., Aamodt, R.L., and Brewer, H.B., Jr. 1982. Human apolipoprotein A-I and A-II metabolism. *J Lipid Res* 23:850-862.
7. Kishimoto, H., Hamada, K., Saunders, M., Backman, S., Sasaki, T., Nakano, T., Mak, T.W., and Suzuki, A. 2003. Physiological functions of Pten in mouse tissues. *Cell Struct Funct* 28:11-21.

8. Oudit, G.Y., and Penninger, J.M. 2009. Cardiac regulation by phosphoinositide 3-kinases and PTEN. *Cardiovasc Res* 82:250-260.

Chapter 5. HDL protects cardiomyocytes against necrosis induced by simulated ischemia, through SR-B1, PI3K, and AKT1/2

Author List: Kristina Durham, Bernardo Trigatti

5.1. Preface

The aim of this manuscript was to evaluate whether the SR-B1/PI3K/AKT pathway is involved in HDL mediated protection against other forms of cardiac stress. Here we assessed the mechanistic involvement of this pathway in HDL mediated protection against oxygen glucose deprivation -induced necrosis, a form of simulated ischemia. This project was initiated and designed by Kristina Durham and Dr. Bernardo Trigatti. Kristina Durham conducted all experiments. All data were analyzed and interpreted by Kristina Durham with guidance from Dr. Bernardo Trigatti. This manuscript was written by Kristina Durham with guidance and editing from Dr. Bernardo Trigatti. This manuscript will be submitted to AJP-Heart and Circulation.

5.2. Abstract

The cardioprotective lipoprotein HDL aids in preventing myocardial infarction, and cardiomyocyte death due to ischemia/reperfusion injury. The scavenger receptor class B, type 1 (SR-B1) acts as a high affinity HDL receptor and has been shown to mediate HDL dependent lipid transport as well as signaling in a variety of different cell types. The contribution of SR-B1 in cardiomyocytes to the protective effects of HDL on cardiomyocyte survival following ischemia have not yet been studied. Here we use a model of simulated ischemia (oxygen glucose deprivation; OGD), to assess the mechanistic involvement of SR-B1, PI3K, and AKT in HDL mediated cardiomyocyte protection. Neonatal mouse cardiomyocytes and immortalized human ventricular

cardiomyocytes were treated with HDL and then subjected to OGD. HDL, but not LDL, protected against OGD-induced necrosis. Inhibition of PI3K or inhibition of AKT abolished HDL mediated protection against OGD-induced necrosis in both HIVCM and NMCM. Knockout or silencing of SR-B1, AKT1, and AKT2 resulted in loss of the protection afforded by HDL. Similarly, activation of AKT in HIVCM by HDL was abolished following silencing of SR-B1, suggesting SR-B1 is required for HDL mediated activation of AKT. These results are the first to identify a role of SR-B1 in mediating the protective effects of HDL against necrosis in cardiomyocytes, and the first to identify AKT activation downstream of SR-B1 in cardiomyocytes.

5.3. Introduction

Cardiovascular disease is a leading cause of death, and a major burden to the health care systems of developed societies (1). Three quarters all cardiovascular related deaths are due to ischemic heart disease and heart attack (1). Partial or complete occlusion in one or more areas of the coronary arteries renders an ischemic myocardial environment, which if left un-perfused, results in infarction due to irreversible cardiomyocyte death and myocardial infarction. Over time the increased demand on the non infarcted tissue may lead to detrimental functional changes and heart failure; therefore it is of utmost importance to prevent or limit the amount of infarcted tissue.

Clinical and experimental research has described the protection HDL affords in response to myocardial ischemia. Low plasma HDL cholesterol (HDL-C) is associated with increased risk of mortality in patients recovering from myocardial infarction (2), and HDL-C levels are inversely correlated with CVD risk (3). The clinical data is supported by *ex vivo* experimental evidence, where administration of HDL provides protection

against ischemia-reperfusion injury in rodent hearts (4, 5), and *in vivo* experimental evidence that demonstrates following coronary artery ligation, adenovirus mediated gene transfer of ApoA1 (the major apolipoprotein (Apo) component of HDL) in a low density lipoprotein receptor knockout mouse (LDLR^{-/-}) significantly protects against a decline in cardiac function, reduces infarct size, and improves survival (6). Lack of ApoA1, by genetic knockout, and a resultant reduction in HDL impairs cardiomyocyte mitochondrial function and generates larger infarctions following LAD ligation (7).

Although the physiological effects of HDL against myocardial ischemia are well documented in both humans and rodents, the receptor(s) and pathways through which HDL induces protection at the cardiomyocyte are not completely defined. The scavenger receptor class B type I (SR-B1) is a high affinity HDL receptor that is present in heart tissue, and has been implicated in mediating cytoprotective intracellular signaling by HDL in a number of cell types (8-14), though its role in mediating HDL-induced protection of cardiomyocytes against myocardial ischemic injury has yet to be assessed.

In murine models, typically atherosclerosis does not develop spontaneously in the coronary arteries. Therefore, genetic modification or high fat diet feeding is required to initiate myocardial ischemia as a manifestation of coronary artery atherosclerosis. Coronary artery atherosclerosis and non-lethal myocardial infarcts can be induced in LDLR/Apo E double knockout (dKO) mice by feeding a high fat diet for prolonged times (15). On the other hand, coronary artery atherosclerosis and lethal myocardial infarcts develop spontaneously in mice lacking SR-B1 and ApoE (SR-B1/ApoE dKO) (16) and in a high fat/high cholesterol diet dependent manner in SR-B1/LDLR dKO mice (17) or SR-B1^{-/-} mice with a hypomorphic mutation in apoE (18). In SR-B1-deficient models,

spontaneous or diet-induced coronary artery atherosclerosis and myocardial infarction are accompanied by cardiac conductance abnormalities, reduced heart function, and rapid death (16-18). The striking phenotype of extensive myocardial infarction when SR-B1 is knocked out in atherosclerosis susceptible strains of mice led us to hypothesize that the effects of SR-B1 extend beyond its role in atherosclerosis, such as to facilitate protection against clinical manifestations including myocardial infarction.

Protection afforded by HDL to cardiomyocytes undergoing hypoxia/reoxygenation involves activation of phosphoinositide 3-kinase (PI3K), and protein kinase B (AKT) (19, 20). PI3K and AKT are well characterized in their cytoprotective role against cardiomyocyte death (21, 22). The binding of HDL to SR-B1 triggers activation of PI3K and AKT in a variety of cell types including endothelial cells, macrophages and Chinese hamster ovary cells (12-14, 23). Whether SR-B1 is required for HDL mediated induction of PI3K/AKT signaling in cardiomyocytes has not been tested.

Given the striking phenotype of CAD in SR-B1 ApoE dKO mice, and the protective signaling initiated by HDL through SR-B1 in various cell types, we hypothesize that SR-B1 mediates the cardioprotective effects of HDL against ischemia-induced cardiomyocyte death. Thus, we have evaluated the role of SR-B1 and downstream mediators PI3K and AKT in the protective signaling by HDL against oxygen glucose deprivation (OGD)-induced cardiomyocyte death.

5.4. Results

HDL protects against OGD-induced necrosis. HIVCM viability was reduced by $75 \pm 2.6\%$ following 4h of OGD. The reduction in cell viability was attenuated, however,

when cells were pre-treated with HDL prior to OGD ($60 \pm 2.7\%$, Fig. 5.1A). Cells subjected to OGD exhibited only very low levels of apoptosis, as measured by AxV and TUNEL staining, and these very low levels were unaffected HDL treatment (Fig. 5.1B-D, F). The lack of cardiomyocyte apoptosis following 4h of OGD in our experiment is mirrored in recent research that demonstrates a time dependant induction of apoptosis in H9c2 cells exposed to 6 or more hours of hypoxia (24). Despite the low levels of apoptosis, OGD caused membrane permeabilization of HIVCM (a marker of necrotic or necroptotic cell death) as evidenced by increased nuclear staining with propidium iodide (PI) compared to corresponding normoxic controls (82.6 ± 1.7 vs. $0 \pm 0\%$ PI-positive cardiomyocytes, Fig. 5.1E, G), and treatment with HDL attenuated PI uptake (82.6 ± 1.7 vs. $49.2 \pm 12.1\%$ PI-positive cardiomyocytes, Fig. 5.1E, G). Conversely, treatment with low density lipoprotein (LDL) was unable to protect HIVCM against OGD-induced PI uptake (58.4 ± 2.5 vs. $52.8 \pm 1.8\%$ PI-positive cardiomyocytes, Fig. 5.1F). Cellular uptake due to permeabilized membranes, and nuclear accumulation of PI could represent necrosis or necroptosis (a form of programmed necrotic cell death), as membrane permeabilization is a feature of both (25). To distinguish between these two types of cell death, cells were treated with the necroptosis inhibitor Nec-1s. Nec-1s did not reduce PI uptake following OGD (62.5 ± 1.4 vs. $63.6 \pm 13.6\%$ PI-positive cardiomyocytes, Fig. 5.2C), however it did substantially reduce PI uptake following exposure to TNF- α (Fig 5.2A), a known inducer of necroptosis (25). This suggested that the PI uptake following OGD is a consequence of unprogrammed necrotic cell death, and not necroptosis.

HDL requires SR-B1 to protect against OGD-induced cell death. Neonatal mouse cardiomyocytes (NMCs) were isolated from SR-B1^{+/+} and SR-B1^{-/-} mice to test the role

of SR-B1 in facilitating HDL mediated protection against OGD-induced necrosis. OGD led to similar levels of necrosis in SR-B1^{+/+} and SR-B1^{-/-} NMCMs (60.6±7.7 vs. 55.1±2.1% PI-positive cardiomyocytes, Fig. 5.3). HDL pretreatment reduced the extent of OGD-induced necrosis in SR-B1^{+/+} NMCMs compared to SR-B1^{+/+} treated with DOX alone (28.5±8.3 vs. 60.6±7.7 % PI-positive cardiomyocytes, Fig 5.3), but failed to protect SR-B1^{-/-} NMCMs against OGD-induced necrosis (59.1±8.4 vs. 55.1±2.9% PI-positive cardiomyocytes, Fig. 5.3). This suggests that SR-B1 in murine cardiomyocytes is required for HDL mediated protection against OGD-induced necrosis. Similarly, siRNA mediated knockdown of SR-B1, which resulted in a reduction in SR-B1 protein levels by ~87% (Fig. 5.4A), prevented HDL-dependent protection of HIVCM against OGD-induced necrosis (Fig. 5.4B). These data demonstrate that cardiomyocyte SR-B1 is required for HDL-mediated protection against OGD-induced necrosis.

HDL activates AKT in an SR-B1 dependent manner. To test whether AKT activation in HIVCM by HDL is downstream of SR-B1, we incubated HIVCM that were transfected with siScram or siSR-B1 with HDL for 30min. HDL-treatment led to increased AKT phosphorylation at Ser 473 in HIVCM treated with siScram (1.7 fold induction in pAKT:tAKT, Fig. 5.4C), and conversely, when SR-B1 was silenced, HDL-treatment did not increase AKT Ser 473 phosphorylation, suggesting AKT is activated by HDL in an SR-B1 dependant manner (Fig. 5.4C).

Inhibition of PI3K or AKT abolishes HDL mediated protection. As AKT is activated in an SR-B1 dependent manner, we sought to assess whether inhibition of AKT, or inhibition of PI3K (an upstream activator of AKT) impaired the ability of HDL to protect against OGD-induced necrosis. Treatment of cells with the PI3K inhibitor

LY294002, or with the pan-AKT Inhibitor V (AKTInhV) abolished HDL mediated protection against OGD-induced necrosis in HIVCM (Fig. 5.5A).

Silencing AKT1 or 2 abolishes HDL mediated protection. AKT1 and AKT2 are the major isoforms of AKT expressed in the heart (26). HIVCM were transfected with siScram or siRNA for AKT1, AKT2 or a mixture of siRNA's targeting each of AKT1 and AKT2. Transfection with siAKT1 or siAKT2 resulted in reduction of AKT1 and 2 levels by 85 and 95% respectively (Fig. 5.5B). Protection by HDL against OGD-induced necrosis was abolished when AKT1 or AKT2 alone, or the combination of AKT1 and 2 together were knocked down, suggesting both major isoforms of AKT in the heart mediate HDL protection against necrosis.

5.5. Discussion

As a cardioprotective lipoprotein, we sought to assess whether HDL protects against OGD-induced cell death of HIVCM, and NMCM, and evaluate whether SR-B1, PI3K, and AKT are involved in the protective signaling elicited by HDL. Others have shown that following 4h of hypoxic stress, neonatal rat ventricular cardiomyocyte cell death was a result of necrosis, though reoxygenating cells for increasing lengths of time resulted in a shift of cell death from necrosis to apoptosis (24). Similarly, we found that in HIVCM and NMCM deprived of oxygen and glucose for 4h, necrosis was the primary driver of cell death, and little to no induction of apoptosis, or necroptosis. We have provided evidence that HDL against cardiomyocyte necrosis via a pathway requiring SR-B1, AKT1, and AKT2. These results are in line with our previous research using doxorubicin as a cardiomyocyte stress. Interestingly, HDL provided protection against cardiomyocyte apoptosis in the setting of doxorubicin, yet against necrosis in the setting

of OGD. This highlights the pleiotropic effects of HDL, and the ability to generate protection against various forms of cardiomyocyte death.

Sphingosine 1-phosphate (S1P) is a bioactive sphingolipid that is primarily carried by HDL (27), and when applied to cardiomyocytes alone, or as part of reconstituted HDL, can protect cardiomyocytes against various stresses (20, 28, 29). Sphingosine-1-phosphate receptors (S1PRs) have been implicated in facilitating cardiomyocyte viability by following hypoxia and reoxygenation by the S1P cargo of HDL (19, 30). S1PR₃ is required for HDL mediated protection against MI in mice *in vivo* (30), and mouse cardiomyocytes subjected to hypoxia reoxygenation required both S1PR₁ and S1PR₃ for protection by HDL (19). Here we conclude that SR-B1 is also a critical receptor for HDL mediated protection of cardiomyocytes. It is conceivable that SR-B1 could function to anchor HDL in close proximity to S1PRs or alternatively, as SR-B1 is known to mediate the cellular uptake of HDL bound lipids such as S1P, SR-B1 may mediate the uptake of HDL bound S1P, making it accessible to S1PRs. Regardless, our data indicates a role of SR-B1 in facilitating HDL mediated protection against OGD-induced cardiomyocyte necrosis. Future research should determine whether SR-B1 acts alone or in combination with the S1PRs.

OGD can be applied to cardiomyocytes *in vitro* in order to mimic the *in vivo* ischemic environment, and assists in defining mechanistic and direct effects of cardioprotective agents specifically on the cardiomyocyte. A limitation of this study is that we employed an *in vitro* model of ischemia, and that the primary form of cell death was necrosis. In an ischemic/reperfused heart, various cells other than cardiomyocytes are present in or enter the heart and contribute to the generation of infarction (30, 31),

therefore; further studies will employ an *in vivo* model of myocardial ischemia/reperfusion to confirm the role of HDL/SR-B1/AKT1/2 in protection against myocardial infarction. Additionally, our model of OGD led to cell death by way of necrosis and not apoptosis or necroptosis. As apoptosis is a major contributor to cell death in the infarct border zone (32), and emerging research is connecting the role of necroptosis to infarct generation and remodeling (33), it would be important to assess the role of HDL and the signaling mechanism against ischemia induced apoptosis and necroptosis both *in vitro* and *in vivo*.

Given the extensive and lethal myocardial infarctions occurring at a young age in SR-B1/ApoE dKO mice on a normal chow diet (16), and in a high fat/high cholesterol diet dependent manner in SR-B1/LDLR dKO mice (17) or SR-B1^{-/-} mice with a hypomorphic mutation in apoE (18), we hypothesized that the lethal myocardial infarction may be a consequence of both the coronary artery atherosclerosis, but also a consequence of increased susceptibility of cardiomyocytes lacking SR-B1 to cell death. Here we have demonstrated that cardiomyocytes (human and mouse) depend on SR-B1 to facilitate the activation of AKT and protective effects elicited by HDL in order to attenuate cardiomyocyte necrosis.

This research will have important implications both for our understanding of how the protective properties of HDL extend beyond the atherosclerotic plaque to affect clinical manifestations of CAD such as cardiomyocyte death. With the knowledge of the importance of SR-B1 in facilitating HDL-mediated protection of cardiomyocytes, our research may also lead to new insights into therapeutic interventions for HDL.

5.6. Methods

Culture of Neonatal Mouse Cardiomyocytes and Human Immortalized Ventricular Cardiomyocytes

NMCM were isolated from hearts of 1-3 day old mice. Briefly, neonatal mice were euthanized by decapitation and hearts were excised and washed with Hank's balanced saline solution (HBSS, Life Technologies, Burlington, ON, Canada). The ventricles were serially digested at 37 °C using 0.2mg/mL collagenase type II (Worthington Biochemical Corp., Lakewood, NJ), and 0.6mg/mL pancreatin (Sigma-Aldrich Canada Co., Oakville, ON, Canada) in HBSS. The cell suspension was centrifuged at 300 × g for 10 min at 4°C, the supernatant was removed, and the cell pellet was re-suspended in 37°C DMEM/M199 (4:1) medium supplemented with 10% horse serum, 5% fetal bovine serum (FBS), 100µM bromo-deoxyuridine, 100U/mL penicillin, 100µg/L streptomycin, and 0.5mM L-glutamine (Life Technologies, Burlington, ON, Canada). Non-cardiomyocytes were removed by plating on an uncoated plate for 1hr. The myocyte-enriched suspension was then plated at 1×10^5 cells/cm² on collagen type I (Life Technologies, Burlington, ON, Canada) coated dishes and incubated in a humid 5% CO₂ incubator at 37°C for 48 hrs at which point they were used for experiments. SV40 large T antigen immortalized human ventricular CMs (HIVCM) were obtained from Applied Biological Materials Inc. (Richmond, BC, Canada). HIVCMs were cultured in Prigrow I media (Applied Biological Materials Inc., Richmond, BC, Canada) supplemented with 10% FBS, and 100U/mL penicillin (Life Technologies, Burlington, ON, Canada).

OGD of Human and Mouse Cardiomyocytes

Forty-eight hrs after plating, cell culture media was replaced with media containing 3 % newborn calf lipoprotein deficient serum and cells were cultured for a further 24 hrs; all experiments were carried out in media supplemented with serum depleted of lipoproteins. Cells were incubated with or without 100µg(protein)/mL human HDL or LDL (Alfa Aesar, Ward Hill, MA) for 30min, then media was changed to OGD media (DMEM with no glucose and 1% lipoprotein deficient serum), and cells were incubated in a humidified chamber with 100% N₂ at 37°C for 4 hrs. Alternatively, normoxic control cells received DMEM containing glucose, and 1% lipoprotein deficient serum, and were incubated in 95% air, 5% CO₂ at 37°C. In some experiments, HIVCMs were transfected with 30nM siRNAs in the presence of Lipofectamine RNAi Max (Life Technologies, Burlington, ON, Canada), 24 hrs prior to lipoprotein starvation. See Supplementary Table 3.4 for a list of siRNA used. In other experiments, cells were treated with 10µM LY294002 (PI3K inhibitor; Cell Signaling Technologies Inc., Danvers, MA), 3µM AKT Inhibitor V (pan-AKT inhibitor; Millipore Canada Ltd., Etobicoke, ON, Canada), 10µM Nec-1s (necroptosis inhibitor; BioVision Inc., Milpitas, CA) or vehicle (DMSO, Sigma-Aldrich Canada Co., Oakville, ON, Canada) 30 min prior to, and during HDL treatment. All inhibitors were applied to cells 10min prior to and during HDL incubation and for the duration of OGD treatment.

Measurement of Cell Viability

Cells were cultured and treated in a 96 well plate. Following OGD, cells were incubated with the Cell Titer Blue (Promega Corp., Madison, WI) assay reagent (a resazurin dye) according to manufacturer's instructions to assess cell viability using a spectrophotometer. Cell viability was expressed as a percentage of OGD-induced cell

death compared to normoxic controls (OGD-induced cell death (%)=(1.0- (OGD cell viability with /normoxic cell viability)X100)).

Measurement of Necrosis

Following OGD, cells were stained with PI, washed extensively, fixed with 4% paraformaldehyde, and counterstained with DAPI to identify nuclei. Necrotic cells were identified as cells with co-staining of DAPI and PI. Additionally, NMCM were co-stained with a mouse monoclonal anti-cardiac troponin T antibody (cTnT, MA5-12960, Fisher Scientific Inc., Waltham, MA) using a Mouse on Mouse Kit (Vector Laboratories, Burlington, ON, Canada), biotinylated secondary, and tertiary labeling with streptavidin conjugated with AlexaFluor 568 (Life Technologies, Burlington, ON, Canada) to identify cardiomyocytes from other cardiac cells.

Measurement of Apoptosis

Following treatment, apoptosis was assessed using the terminal deoxynucleotidyl transferase-mediated dUTP nick end-labeling (TUNEL) assay (Millipore Canada Ltd., Etobicoke, ON, Canada), or by staining with FITC conjugated Annexin V (AxV, Life Technologies, Burlington, ON, Canada) according to manufacturer's instructions. All cells were counterstained with DAPI to identify nuclei.

Microscopy and Quantification of Necrotic and Apoptotic Cells

Fluorescent images were captured using a Zeiss Axiovert 200M inverted microscope (Carl Zeiss Canada Ltd. Toronto, ON, Canada), or an Olympus BX41TF microscope (Olympus Canada Inc., Richmond Hill, ON, Canada). A minimum of 4, and maximum of 10 fields of view were imaged per well. Necrotic nuclei were identified as having PI and DAPI co-staining, and apoptotic cells were identified as having DAPI and

AxV staining. Necrotic and apoptotic cell numbers/field of view were summed within a well, and averaged across triplicates.

Statistics

All data are expressed as means \pm S.E.M. Data was graphed and statistically analyzed using GraphPad Prism (GraphPad Software, Inc., La Jolla, CA). Data comparing two groups was tested for significance by Student's t test, data comparing more than two groups with one independent variable was tested using one-way ANOVA and Tukey's post-hoc, and data comparing two or more independent variables was tested using Two-way ANOVA with Tukey's post hoc. $P < 0.05$ was considered statistically significant.

5.7. Figures

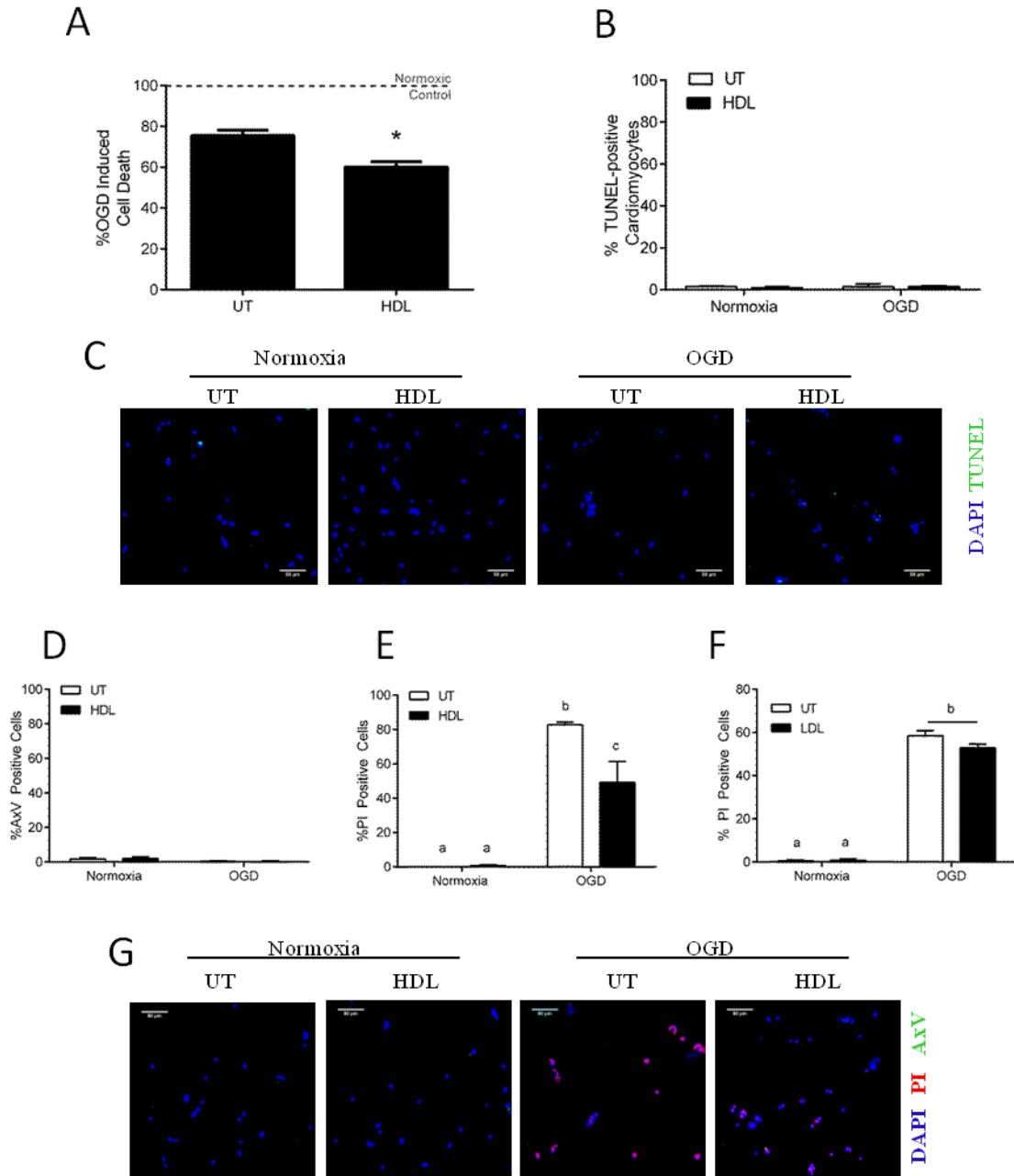


Figure 5. 1 HDL protects against OGD-induced necrosis of HIVCM

A) OGD-induced cell death of HIVCM treated \pm HDL, was measured by the Cell Titer Blue viability assay. $n=10$ wells/group. $*p<0.001$. B) Quantification and C) representative images of TUNEL stained HIVCM (green) and nuclei in blue.

n=3wells/group. Quantification of OGD-induced cell death by FITC-AxV staining (D) or PI staining (E) in HIVCM treated \pm HDL, and representative images (G). F)

Quantification of OGD-induced cell death by PI staining in HIVCM treated \pm LDL.

n=3wells/group. All scale bars=50 μ m. Data represents means \pm S.E.M. *p<0.05, and different lower case letters indicate statistically significant differences to p<0.05.

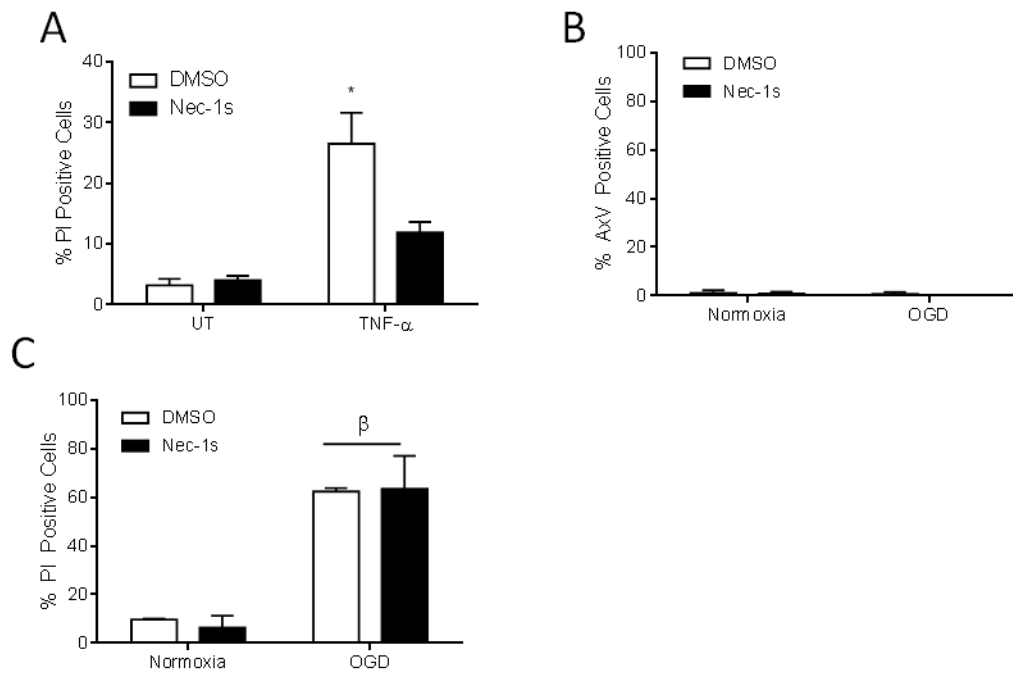


Figure 5.2 4 hrs of OGD induced necrosis of cardiomyocytes.

A) Quantification of TNF- α induced PI staining of HIVCM, and effect of Nec-1s.

n=3wells/group. B) Quantification of FITC-AxV staining of HIVCM exposed to OGD

and treated \pm Nec-1s. n=3wells/group. C) Quantification of OGD-induced PI uptake in

HIVCM treated \pm Nec-1s. n=3wells/group. Data represents means \pm S.E.M. *p<0.01.

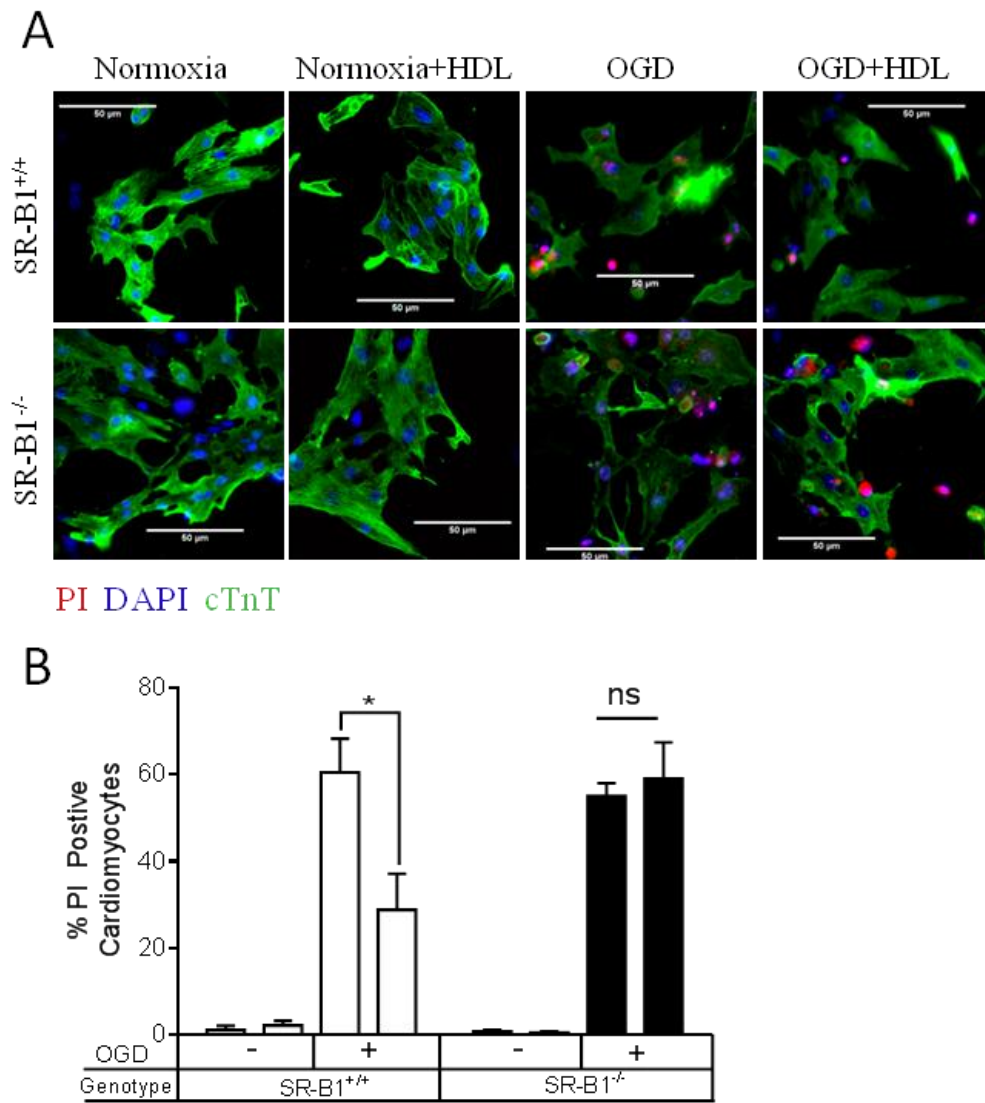


Figure 5.3 SR-B1 is required for HDL mediated protection of NMCM against OGD-induced necrosis.

A) Representative images and B) quantification of PI staining in SR-B1^{+/+} and SR-B1^{-/-} NMCM exposed to OGD and treatment \pm HDL. In panel A, cells were stained prior to fixation with PI (red) or, after fixation with DAPI (blue) and cTnT (green). Data represents means \pm S.E.M. * p <0.05, n=3wells/group.

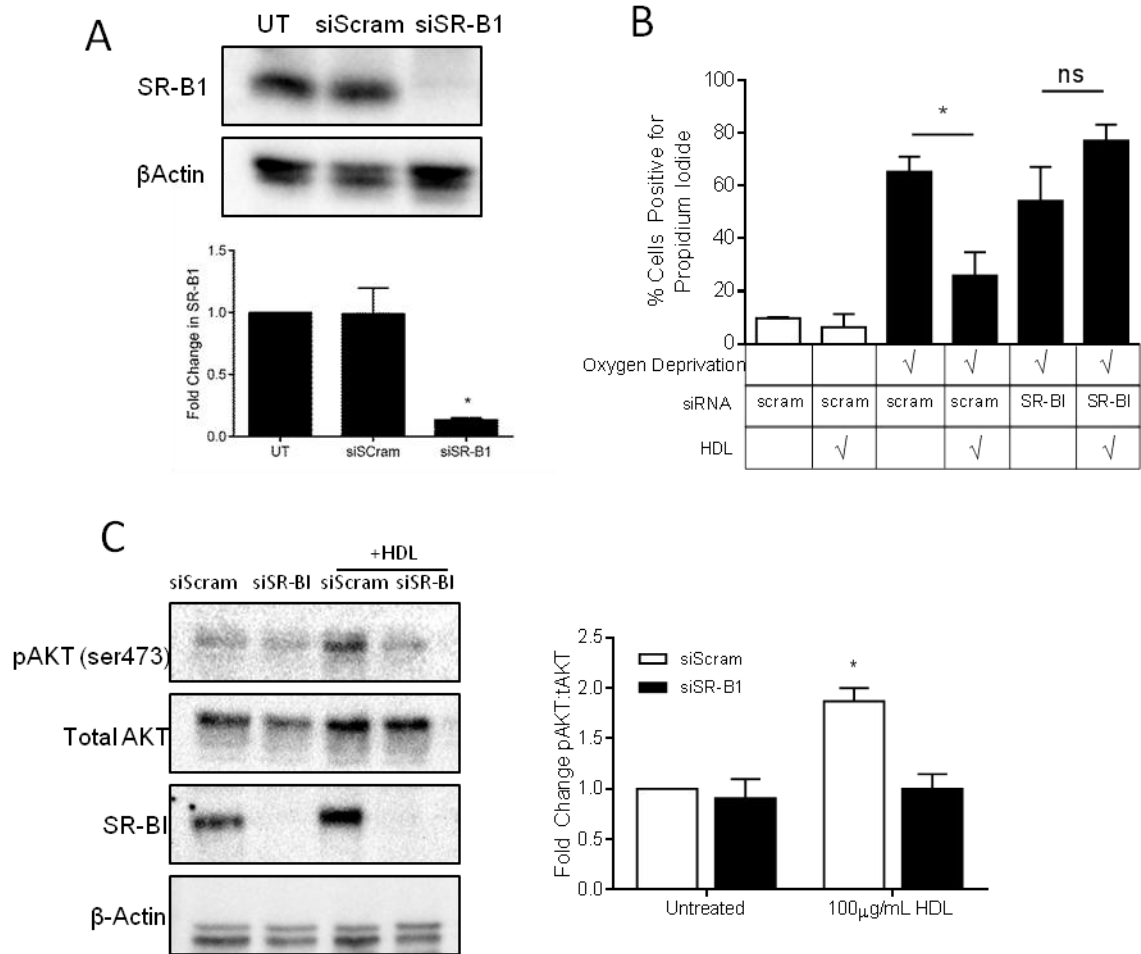


Figure 5.4 SR-B1 is required for HDL-mediated protection of HIVCM against OGD-induced necrosis, and activation of AKT.

A) Representative immunoblot and quantification of SR-B1 knockdown by siRNA in HIVCM. * $p < 0.001$. B) Quantification of OGD-induced necrosis in HIVCM treated with siScram or siSR-B1. Silencing of SR-B1 by siRNA abolished HDL mediated protection against OGD-induced necrosis, $n = 3$ wells/group. * $p < 0.05$. C) Representative immunoblots (left) and quantification of pAKT^{Ser473}:tAKT in bar graph (right) for HIVCM transfected with scrambled or SR-B1 siRNA, and treated for 30min \pm 100 μ g/ml HDL. * $p < 0.001$. Data represents means \pm S.E.M.

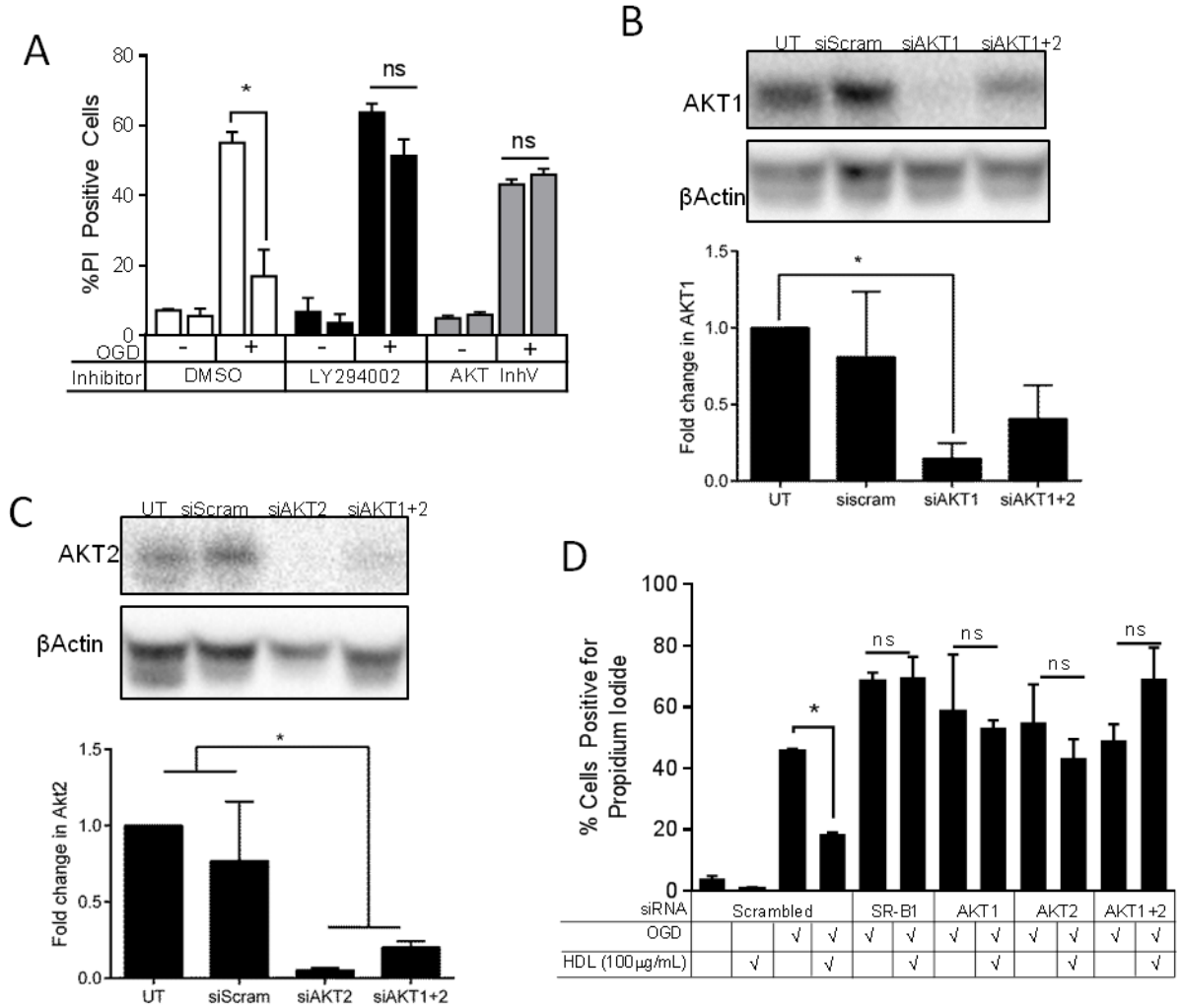


Figure 5.5 PI3K, AKT1, and AKT2 are required for HDL mediated protection of HIVCM against OGD-induced necrosis.

A) Quantification of OGD-induced necrosis in HIVCM treated ±HDL and inhibitors of PI3K (10 µM LY294002) or AKT (3µM AKT InhV). B) Representative immunoblot and quantification of AKT1 knockdown by siRNA in HIVCM. C) Representative immunoblot and quantification of AKT2 knockdown by siRNA in HIVCM. D) Quantification of OGD-induced necrosis in HIVCM treated ±HDL where AKT1, AKT2, or AKT1+2 were silenced by siRNA. $p < 0.05$, $n = 3$ wells/group. Data represents means ± S.E.M. * indicates $p < 0.05$. N.S. indicates not statistically significant.

5.8. References

1. Roger, V.L., Go, A.S., Lloyd-Jones, D.M., Benjamin, E.J., Berry, J.D., Borden, W.B., Bravata, D.M., Dai, S., Ford, E.S., Fox, C.S., et al. 2012. Heart disease and stroke statistics--2012 update: a report from the American Heart Association. *Circulation* 125:e2-e220.
2. Berge, K.G., Canner, P.L., and Hainline, A., Jr. 1982. High-density lipoprotein cholesterol and prognosis after myocardial infarction. *Circulation* 66:1176-1178.
3. Castelli, W.P., Anderson, K., Wilson, P.W., and Levy, D. 1992. Lipids and risk of coronary heart disease. The Framingham Study. *Ann Epidemiol* 2:23-28.
4. Calabresi, L., Rossoni, G., Gomaschi, M., Sisto, F., Berti, F., and Franceschini, G. 2003. High-density lipoproteins protect isolated rat hearts from ischemia-reperfusion injury by reducing cardiac tumor necrosis factor-alpha content and enhancing prostaglandin release. *Circ Res* 92:330-337.
5. Rossoni, G., Gomaschi, M., Berti, F., Sirtori, C.R., Franceschini, G., and Calabresi, L. 2004. Synthetic high-density lipoproteins exert cardioprotective effects in myocardial ischemia/reperfusion injury. *J Pharmacol Exp Ther* 308:79-84.
6. Gordts, S.C., Muthuramu, I., Nefyodova, E., Jacobs, F., Van Craeyveld, E., and De Geest, B. 2013. Beneficial effects of selective HDL-raising gene transfer on survival, cardiac remodelling and cardiac function after myocardial infarction in mice. *Gene Ther* 20:1053-1061.
7. Dadabayev, A.R., Yin, G., Latchoumycandane, C., McIntyre, T.M., Lesnefsky, E.J., and Penn, M.S. 2014. Apolipoprotein A1 regulates coenzyme Q10

- absorption, mitochondrial function, and infarct size in a mouse model of myocardial infarction. *J Nutr* 144:1030-1036.
8. Gao, M., Zhao, D., Schouteden, S., Sorci-Thomas, M.G., Van Veldhoven, P.P., Eggermont, K., Liu, G., Verfaillie, C.M., and Feng, Y. 2014. Regulation of high-density lipoprotein on hematopoietic stem/progenitor cells in atherosclerosis requires scavenger receptor type BI expression. *Arterioscler Thromb Vasc Biol* 34:1900-1909.
 9. Xu, J., Qian, J., Xie, X., Lin, L., Ma, J., Huang, Z., Fu, M., Zou, Y., and Ge, J. 2012. High density lipoprotein cholesterol promotes the proliferation of bone-derived mesenchymal stem cells via binding scavenger receptor-B type I and activation of PI3K/Akt, MAPK/ERK1/2 pathways. *Mol Cell Biochem* 371:55-64.
 10. Li, X.A., Titlow, W.B., Jackson, B.A., Giltiay, N., Nikolova-Karakashian, M., Uittenbogaard, A., and Smart, E.J. 2002. High density lipoprotein binding to scavenger receptor, Class B, type I activates endothelial nitric-oxide synthase in a ceramide-dependent manner. *J Biol Chem* 277:11058-11063.
 11. Kimura, T., Tomura, H., Mogi, C., Kuwabara, A., Damirin, A., Ishizuka, T., Sekiguchi, A., Ishiwara, M., Im, D.S., Sato, K., et al. 2006. Role of scavenger receptor class B type I and sphingosine 1-phosphate receptors in high density lipoprotein-induced inhibition of adhesion molecule expression in endothelial cells. *J Biol Chem* 281:37457-37467.
 12. Mineo, C., Yuhanna, I.S., Quon, M.J., and Shaul, P.W. 2003. High density lipoprotein-induced endothelial nitric-oxide synthase activation is mediated by Akt and MAP kinases. *J Biol Chem* 278:9142-9149.

13. Grewal, T., de Diego, I., Kirchhoff, M.F., Tebar, F., Heeren, J., Rinninger, F., and Enrich, C. 2003. High density lipoprotein-induced signaling of the MAPK pathway involves scavenger receptor type BI-mediated activation of Ras. *J Biol Chem* 278:16478-16481.
14. Al-Jarallah, A., Chen, X., Gonzalez, L., and Trigatti, B.L. 2014. High density lipoprotein stimulated migration of macrophages depends on the scavenger receptor class B, type I, PDZK1 and Akt1 and is blocked by sphingosine 1 phosphate receptor antagonists. *PLoS One* 9:e106487.
15. Caligiuri, G., Levy, B., Pernow, J., Thoren, P., and Hansson, G.K. 1999. Myocardial infarction mediated by endothelin receptor signaling in hypercholesterolemic mice. *Proc Natl Acad Sci U S A* 96:6920-6924.
16. Braun, A., Trigatti, B.L., Post, M.J., Sato, K., Simons, M., Edelberg, J.M., Rosenberg, R.D., Schrenzel, M., and Krieger, M. 2002. Loss of SR-BI expression leads to the early onset of occlusive atherosclerotic coronary artery disease, spontaneous myocardial infarctions, severe cardiac dysfunction, and premature death in apolipoprotein E-deficient mice. *Circ Res* 90:270-276.
17. Fuller, M., Dadoo, O., Serkis, V., Abutouk, D., MacDonald, M., Dhingani, N., Macri, J., Igdoura, S.A., and Trigatti, B.L. 2014. The effects of diet on occlusive coronary artery atherosclerosis and myocardial infarction in scavenger receptor class B, type 1/low-density lipoprotein receptor double knockout mice. *Arterioscler Thromb Vasc Biol* 34:2394-2403.
18. Zhang, S., Picard, M.H., Vasile, E., Zhu, Y., Raffai, R.L., Weisgraber, K.H., and Krieger, M. 2005. Diet-induced occlusive coronary atherosclerosis, myocardial

- infarction, cardiac dysfunction, and premature death in scavenger receptor class B type I-deficient, hypomorphic apolipoprotein ER61 mice. *Circulation* 111:3457-3464.
19. Tao, R., Hoover, H.E., Honbo, N., Kalinowski, M., Alano, C.C., Karliner, J.S., and Raffai, R. 2010. *High-density lipoprotein determines adult mouse cardiomyocyte fate after hypoxia-reoxygenation through lipoprotein-associated sphingosine 1-phosphate*. H1022-H1028 pp.
 20. Frias, M.A., Lecour, S., James, R.W., and Pedretti, S. 2012. High density lipoprotein/sphingosine-1-phosphate-induced cardioprotection: Role of STAT3 as part of the SAFE pathway. *JAKSTAT* 1:92-100.
 21. Juhaszova, M., Zorov, D.B., Kim, S.H., Pepe, S., Fu, Q., Fishbein, K.W., Ziman, B.D., Wang, S., Ytrehus, K., Antos, C.L., et al. 2004. Glycogen synthase kinase-3beta mediates convergence of protection signaling to inhibit the mitochondrial permeability transition pore. *J Clin Invest* 113:1535-1549.
 22. Matsui, T., and Rosenzweig, A. 2005. Convergent signal transduction pathways controlling cardiomyocyte survival and function: the role of PI 3-kinase and Akt. *J Mol Cell Cardiol* 38:63-71.
 23. Zhang, Y., Ahmed, A.M., McFarlane, N., Capone, C., Boreham, D.R., Truant, R., Igdoura, S.A., and Trigatti, B.L. 2007. Regulation of SR-BI-mediated selective lipid uptake in Chinese hamster ovary-derived cells by protein kinase signaling pathways. *J Lipid Res* 48:405-416.
 24. Budhram-Mahadeo, V., Fujita, R., Bitsi, S., Sicard, P., and Heads, R. 2014. Co-expression of POU4F2/Brn-3b with p53 may be important for controlling

- expression of pro-apoptotic genes in cardiomyocytes following ischaemic/hypoxic insults. *Cell Death Dis* 5:e1503.
25. Vanden Berghe, T., Linkermann, A., Jouan-Lanhouet, S., Walczak, H., and Vandenabeele, P. 2014. Regulated necrosis: the expanding network of non-apoptotic cell death pathways. *Nat Rev Mol Cell Biol* 15:135-147.
 26. Song, X., Fischer, P., Chen, X., Burton, C., and Wang, J. 2009. An apoA-I mimetic peptide facilitates off-loading cholesterol from HDL to liver cells through scavenger receptor BI. *Int J Biol Sci* 5:637-646.
 27. Argraves, K.M., and Argraves, W.S. 2007. HDL serves as a S1P signaling platform mediating a multitude of cardiovascular effects. *Journal of Lipid Research* 48:2325-2333.
 28. Tao, R., Hoover, H.E., Honbo, N., Kalinowski, M., Alano, C.C., Karliner, J.S., and Raffai, R. 2010. High-density lipoprotein determines adult mouse cardiomyocyte fate after hypoxia-reoxygenation through lipoprotein-associated sphingosine 1-phosphate. *Am J Physiol Heart Circ Physiol* 298:H1022-1028.
 29. Frias, M.A., Lang, U., Gerber-Wicht, C., and James, R.W. 2010. Native and reconstituted HDL protect cardiomyocytes from doxorubicin-induced apoptosis. *Cardiovasc Res* 85:118-126.
 30. Theilmeyer, G., Schmidt, C., Herrmann, J., Keul, P., Schafers, M., Herrgott, I., Mersmann, J., Larmann, J., Hermann, S., Stypmann, J., et al. 2006. High-density lipoproteins and their constituent, sphingosine-1-phosphate, directly protect the heart against ischemia/reperfusion injury in vivo via the S1P3 lysophospholipid receptor. *Circulation* 114:1403-1409.

31. Yan, B., A, J., Hao, H., Wang, G., Zhu, X., Zha, W., Liu, L., Guan, E., Zhang, Y., Gu, S., et al. 2009. Metabonomic phenotype and identification of "heart blood stasis obstruction pattern" and "qi and yin deficiency pattern" of myocardial ischemia rat models. *Sci China C Life Sci* 52:1081-1090.
32. Navab, M., Anantharamaiah, G.M., Hama, S., Garber, D.W., Chaddha, M., Hough, G., Lallone, R., and Fogelman, A.M. 2002. Oral administration of an Apo A-I mimetic Peptide synthesized from D-amino acids dramatically reduces atherosclerosis in mice independent of plasma cholesterol. *Circulation* 105:290-292.
33. Luedde, M., Lutz, M., Carter, N., Sosna, J., Jacoby, C., Vucur, M., Gautheron, J., Roderburg, C., Borg, N., Reisinger, F., et al. 2014. *RIP3, a kinase promoting necroptotic cell death, mediates adverse remodelling after myocardial infarction.* 206-216 pp.

Chapter 6. Limitations, and Future Directions

Effect of Increased HDL on DOX Chemotherapy and Tumor Size

A recent study consisting of 12 adult females undergoing chemotherapy treatment for breast cancer (7 of which were treated with DOX) reported a reduction in plasma ApoA1 and a corresponding decrease in plasma HDL-C (173). There is also evidence that HDL-C levels are inversely correlated to the risk and prognosis of cancer (174, 175). Experimentally increasing HDL by overexpression or therapeutic injection of ApoA1 protects mice against DOX induced cardiotoxicity and tumor regression (176), and DOX encapsulated in HDL particles provides greater tumor regression than DOX alone (177). Taken together with our data suggesting that raising HDL-C by modulating ApoA1 protects against the cardiotoxic side effects of DOX, HDL-raising therapies may be of importance for improving the anti-tumor effects of anthracycline based chemotherapeutics, while protecting against the deleterious side effect of cardiotoxicity. Whether increased HDL, either by genetic modification or therapeutics, will provide both chemotherapeutic and cardioprotective effects in the context of DOX therapy remains to be evaluated. Therefore; future work should employ a tumor bearing mouse model, and test whether raising HDL affects the use of DOX as a chemotherapeutic while providing protection against the cardiotoxic side effects.

Increasing HDL-C Versus Improving HDL Composition and Function

Classical epidemiological studies reported the association and inverse relationship of HDL-C and CVD risk and this relationship exists regardless of sex, and across many populations and ethnicities (75). In light of this, HDL was regarded as a cardioprotective molecule, hence its common name “good cholesterol” (75), and the hypothesis that

increasing HDL-C would translate to improved protection against CVD and manifestations of CVD (178). This led to the development of HDL-C raising drugs, such as niacin, statins, and CETP inhibitors though paradoxically, these HDL-C raising drugs did not correlate with a lower risk of heart disease, in fact, HDL-targeting drugs have been unsuccessful in the prevention or treatment of CVD (178).

Elevated HDL-C levels could indicate an increase in HDL particle number, or simply an increase in the cholesterol associated with a given number of HDL particles, or both. In addition, measurement of HDL-C does not allow for evaluation the HDL population composition or function, both of which are crucial to understanding HDL function. Research has reported differences in HDL particle composition and function between diseased patients and healthy humans, therefore increasing HDL-C in diseased populations may actually result in a rise in pathological HDL particles. This is evident in a recent population study which has identified a loss-of-function variant in the gene encoding SR-BI (SCARB1) that results in the inability of SR-B1 to uptake cholesterol from HDL (179). Homo- and heterozygous carriers of this variant have increased HDL-C, yet despite this increase, were at higher risk for coronary heart disease (179).

Similarly, in our animal studies, SR-B1^{-/-} mice were more sensitive to chronic DOX-induced cardiotoxicity despite the ~2-fold higher HDL-C levels compared to SR-B1^{+/+} mice. We interpret this to reflect that HDL signaling via SR-B1 in cardiomyocytes is the important parameter that confers cardioprotection, rather than merely an increase in HDL-C (which appears not to be sufficient for cardioprotection). As HDL composition appears to be a main determinant of HDL function, newer research is shifting away from

finding ways to increase HDL-C, and towards identifying particle subspecies and particle compositions associated with specific functions of HDL.

In diseased states such as inflammatory or metabolic disorders, HDL particles can undergo modifications such as oxidation, nitration, or glycation, or compositional changes (180). These alterations can render the HDL particle dysfunctional due to loss of their cyto-protective effects, and gain of pathological effects (181). For example, HDL particles isolated from CVD, or metabolic syndrome patients are no longer anti-oxidative, anti-apoptotic, or anti-adhesive, and in some cases are pro-inflammatory (182-185). These particles have altered composition and carry less of the antioxidant paroxonase 1 (182). HDL particles isolated from patients with diabetes mellitus are glycated and less effective in protection of cardiomyocytes against DOX-induced death (87). In type 2 diabetics, HDL composition is abnormal and these particles have decreased capacity for cholesterol efflux (186-188). Interestingly, the HDL-associated S1P levels are inversely correlated with the occurrence of ischemic heart disease (189), and protection of cardiomyocytes against DOX-induced apoptosis (87). Lastly, a diet high in saturated fat negates the anti-inflammatory properties of HDL, conversely, a diet high in polyunsaturated fat improves the anti-inflammatory activity of HDL (190). This evidence of disease related dysfunction of HDL leads to the question of whether HDL particle composition and function are affected by cancer or DOX treatment. In light of this, future research should characterize 1) HDL composition and function from healthy, and tumor bearing mice (or humans should the samples be available), as well as 2) HDL from mice (or humans) treated with and without DOX or other chemotherapeutics.

Therapeutically increasing HDL

Clinically, raising HDL-C has not provided the protection expected, and therefore newer research is focusing on increasing the number of HDL particles. The most physiologically relevant approach for raising HDL particle number is by the infusion of HDL, or mimetics such as reconstituted HDL (rHDL), native or lipidated ApoA1, ApoA1 mimetic peptides, or genetic variants of ApoA1 (ApoA1 milano) (178). The small amphipathic ApoA1 mimetic peptides structurally and functionally resemble ApoA1 (191). To date, clinical research evaluating these therapeutics encompass small numbers of participants. Despite this, clinical trials have demonstrated a regression in coronary atheroma following 4-5 weekly infusions of rHDL containing recombinant ApoA1 milano (a genetic variant of ApoA1) complexed with phospholipids or lecithin (77, 192, 193). Infusion of HDL therapeutics rapidly increase plasma ApoA1 and discoidal HDL particles, and promote the efflux of cholesterol from peripheral tissues (194, 195). In animal models, orally administered ApoA1 mimetic peptides activate RCT and reduce atherosclerosis (196-199). Two mimetic peptides- 5A and 6F are in clinical development (178).

The ease of administration of rHDL or ApoA1 (protein or mimetic peptides) is limited by transient effect on HDL levels, short half life, and need for multiple infusions for chronic treatment (178). Alternatively, one could assess whether raising HDL levels through lifestyle modification could reverse or prevent disease induced HDL dysfunction. Modification of diet and exercise has been reported to revert disease-induced pro-oxidative HDL back to anti-oxidative HDL (200, 201). Future research should continue to delineate whether increased ApoA1, through therapeutic manipulations such as ApoA1

mimetic peptides, or lifestyle modification (ex. exercise, diet) could provide an increase in levels of or cardioprotective function of HDL to promote protection against both DOX-induced cardiotoxicity, and ischemia reperfusion-induced myocardial infarction.

The Role of SR-B1; Peripheral Versus Systemic Effects of HDL

A limiting factor to our DOX studies is that to assess the mechanistic role of SR-B1, we tested mice with whole-body deletion of SR-B1 due to (at the time) lack of availability of floxed SR-B1 mice. Use of a total body SR-B1 knockout left us with the inability to comprehensively test whether protection against cardiotoxicity by genetic overexpression of ApoA1 was due to a lack of SR-B1-induced cardioprotective signaling in cardiomyocytes, or peripheral effects such as increased HDL-C. Because of the increase in cholesterol carried by HDL sized particles in SR-B1^{-/-} mice, and due to the role of SR-B1 in mediating macrophage efferocytosis, we were unable to separate the influence of SR-B1 on the liver or macrophages from SR-B1 in the heart. To test this we used an ear pinna transplant model, and found that SR-B1^{-/-} neonatal heart transplants were sensitized to DOX-induced cardiomyocyte apoptosis compared to SR-B1^{+/+} transplant in the same adult recipient SR-B1^{+/+} mouse. Still, confounding factors exist such as stress of ischemia during implantation, and endogenous SR-B1^{-/-} macrophages carried over with the cardiac tissue. In light of these issues and in order to test the role of cardiomyocyte SR-B1, one could test whether ApoA1 overexpression or injection of ApoA1 protects against DOX-induced cardiotoxicity of mice lacking SR-B1 specifically in cardiomyocytes. Briefly, to generate cardiomyocyte specific knockout of SR-B1, mice expressing cre recombinase under the cardiac specific murine α myosin heavy chain 6 promoter (Myh6Cre^{+/+}, [B6.FVBTg(Myh6-cre)2182Mds], Jackson Labs) could be

crossed with SR-B1 floxed mice (202) to generate cardiac specific deletion of SR-B1. Liver SR-B1 governs the increase in HDL particle size, therefore by selectively deleting SR-B1 in cardiomyocytes, HDL particles should be unaffected. This model will allow us to test whether SR-B1, specifically on the cardiomyocyte is responsible the cardioprotective effects of HDL. Finally, crossing the conditional SR-B1 knockout mice with ApoA1^{Tg/Tg} mice, or increasing plasma ApoA1 by injection of ApoA1 will allow for the assessment of whether lack of SR-B1 on the cardiomyocyte, or peripheral effects mediate the protective effect of increasing ApoA1 on DOX induced cardiotoxicity. There are two conceivable outcomes from these analyses: 1) cardiomyocyte SR-B1 specifically is required for ApoA1 mediated protection where cardiomyocyte specific SR-B1 null mice will not be protected against DOX-induced cardiotoxicity or 2) peripheral effects account for the protection afforded by increased HDL, where overexpression of ApoA1 in cardiomyocyte specific SR-B1 null mice will still protect against DOX-induced cardiotoxicity.

Translation of OGD Studies to a Clinically Relevant Model of Myocardial Ischemia and Reperfusion

Our OGD studies were useful for obtaining mechanistic data on HDL-mediated protection. Although *in vitro* studies allow for precise control of experiments, *in vivo* studies are crucial for understanding the contribution of a single cell type to an outcome that involves many cell types and systems. It is therefore of importance to assess the role of HDL/SR-B1/PI3K/AKT *in vivo* during ischemia/reperfusion by probing the contribution of this pathway to protection of the ischemic/reperfused cardiomyocyte. Evaluating the effect of HDL on cardiomyocytes *in vivo* is complicated because of the

nature of HDL; it is present in plasma and therefore has widespread effects throughout the body, and the components of the signaling pathway (SR-B1/PI3K/AKT) are also expressed by numerous cell types. Thus, use of whole body knockout or transgenic models could confound interpretation. Briefly, to generate cardiomyocyte specific knockout of individual AKT isoforms, mice expressing cre recombinase under the cardiac specific murine α myosin heavy chain 6 promoter (Myh6Cre^{+/+}, [B6.FVBTg(Myh6-cre)2182Mds], Jackson Labs) will be crossed with the AKT1 floxed mice (B6.129S4(FVB)-*Akt1*^{tm2.2Mbb}/J; Jackson Labs) or AKT2 floxed mice (B6.129-*Akt2*^{tm1.2Mbb}/J; Jackson Labs). For clinical relevance, myocardial ischemia/reperfusion could be induced *in vivo* using a model of LAD coronary artery ligation and release which allows for timed control of the ischemic period and subsequent reperfusion.

Removing the Antagonistic Activity on PI3K Signaling

At the cellular level a dynamic control system exists where balance between antagonistic and agonistic signaling is maintained. In our studies, we identified PI3K and AKT as being major mediators of the protective effects initiated by HDL/SR-B1 in cardiomyocytes. An initial step in the activation of AKT is the conversion of PIP2 to PIP3 by PI3K (102). PTEN is a lipid phosphatase and functions as an antagonist of PI3K activity by converting PIP3 back to PIP2 and thereby reducing the cellular pool of PIP3 (110). It would be of interest to determine whether removing this ‘break’ on PI3K activity would allow for increased protective signaling through the HDL/SR-B1 pathway. The PI3K/AKT pathway is not only a cardioprotective pathway, but is also important in the growth of tumors, and currently PTEN is a heavily studied as a tumor suppressor. Tissue specific deletion of PTEN promotes tumor genesis (203), and loss of PTEN

activity and promotion of cancer cell growth and proliferation is common across many tumor types (204). Yet on the other hand, inducible deletion, or downregulation of cardiac PTEN protects against cardiac injury from ischemia (205, 206). In light of PTENs role in inhibiting cancer cell growth, targeting PTEN for prevention of the cardiotoxic side effects of DOX would not be suitable. It may, however, be a notable short-term target to improve HDL therapies in protection against myocardial ischemia, by enhancing cardioprotective signaling through PI3K/AKT. Unfortunately at the current time, PTEN inhibitors are not highly selective in their target (207) and often affect other protein tyrosine phosphatases, making it difficult to use as a therapeutic. Should a highly specific inhibitor be discovered in the future, it would be interesting to test whether the PTEN inhibitor given in combination with an HDL-raising therapy would provide substantially more protection against myocardial ischemia. In the mean time, one could delete cardiac PTEN by crossing the mice expressing tamoxifen-inducible cre recombinase under the cardiac specific murine α myosin heavy chain 6 promoter (B6.FVB(129)-Tg(Myh6-cre/Esr1*)1Jmk/J) to mice expressing floxed PTEN (C;129S4-*Pten*^{tm1Hwu}/J, Jackson Labs) and test whether transient deletion of PTEN reduces sensitivity to DOX-induced cardiotoxicity under conditions of normal levels of HDL, as well as whether there is further protection afforded by increasing ApoA1 when PTEN is deleted by crossing with an ApoA1^{Tg/Tg} mouse or by injecting with ApoA1.

We have shown that activation of AKT is required for the anti-apoptotic and anti-necrotic effects of HDL in cardiomyocytes. It is possible that by inhibiting the dephosphorylation of AKT, one might increase downstream activation of AKT targets. Unfortunately, PP2A, the protein phosphatase that regulates AKT dephosphorylation, is

ubiquitously expressed and together with PP1 account for 90% of protein dephosphorylation in the heart (208). Others have reported that hearts from cardiac-deficient PP2A mice undergo dysfunctional cardiac hypertrophic remodeling (209). Reducing the dephosphorylation of AKT by targeting PP2A would likely result in a number of off target effects due to the dephosphorylation of proteins other than AKT.

Chapter 7. Conclusions

This thesis centers around the role of SR-B1 and downstream targets PI3K and AKT in facilitating cardioprotective signaling against various cardiac stresses including drug induced cardiotoxicity and myocardial ischemia. Chapters 3 and 4 evaluate whether increasing plasma HDL by 1) overexpression of ApoA1, or 2) therapeutic injection of ApoA1 can protect against the deleterious side effects of the cardiotoxic drug DOX. Chapter 3 employed *in vivo* methods to determine the role of SR-B1 in facilitating the protective effects elicited by raising HDL. Chapter 5 assesses the role of SR-B1 and downstream targets PI3K and AKT in protection of cardiomyocytes against simulated ischemia (OGD)-induced cardiomyocyte necrosis. Overall our work demonstrates that increasing HDL through genetic manipulation of ApoA1 and therapeutic injection of ApoA1 lead to protection against the cardiotoxic drug DOX, and that HDL requires SR-B1, PI3K and AKT for protection. Secondly, our work highlights the importance of HDL and SR-B1 not only in facilitating protection against drug induced cardiotoxicity, but also in protection against cardiomyocyte necrosis. This research suggests HDL raising therapies may be of benefit during chemotherapy, and is the first to identify a cardioprotective role of SR-B1 beyond plaque development.

Chapter 8. References

1. Uygur, A., and Lee, R.T. 2016. Mechanisms of Cardiac Regeneration. *Dev Cell* 36:362-374.
2. Bergmann, O., Bhardwaj, R.D., Bernard, S., Zdunek, S., Barnabe-Heider, F., Walsh, S., Zupicich, J., Alkass, K., Buchholz, B.A., Druid, H., et al. 2009. Evidence for cardiomyocyte renewal in humans. *Science* 324:98-102.
3. Bergmann, O., Zdunek, S., Felker, A., Salehpour, M., Alkass, K., Bernard, S., Sjostrom, S.L., Szewczykowska, M., Jackowska, T., Dos Remedios, C., et al. 2015. Dynamics of Cell Generation and Turnover in the Human Heart. *Cell* 161:1566-1575.
4. Porrello, E.R., and Olson, E.N. 2014. A neonatal blueprint for cardiac regeneration. *Stem Cell Res* 13:556-570.
5. Global Burden of Disease Cancer, C., Fitzmaurice, C., Dicker, D., Pain, A., Hamavid, H., Moradi-Lakeh, M., MacIntyre, M.F., Allen, C., Hansen, G., Woodbrook, R., et al. 2015. The Global Burden of Cancer 2013. *JAMA Oncol* 1:505-527.
6. Camaggi, C.M., Comparsi, R., Strocchi, E., Testoni, F., Angelelli, B., and Pannuti, F. 1988. Epirubicin and doxorubicin comparative metabolism and pharmacokinetics. A cross-over study. *Cancer Chemother Pharmacol* 21:221-228.
7. Robert, J., Vrignaud, P., Nguyen-Ngoc, T., Iliadis, A., Mauriac, L., and Hurteloup, P. 1985. Comparative pharmacokinetics and metabolism of

- doxorubicin and epirubicin in patients with metastatic breast cancer. *Cancer Treat Rep* 69:633-640.
8. Shakir, D.K., and Rasul, K.I. 2009. Chemotherapy induced cardiomyopathy: pathogenesis, monitoring and management. *J Clin Med Res* 1:8-12.
 9. Swain, S.M., Whaley, F.S., and Ewer, M.S. 2003. Congestive heart failure in patients treated with doxorubicin: a retrospective analysis of three trials. *Cancer* 97:2869-2879.
 10. Li, J., Xuan, W., Yan, R., Tropak, M.B., Jean-St-Michel, E., Liang, W., Gladstone, R., Backx, P.H., Kharbanda, R.K., and Redington, A.N. 2011. Remote preconditioning provides potent cardioprotection via PI3K/Akt activation and is associated with nuclear accumulation of beta-catenin. *Clin Sci (Lond)* 120:451-462.
 11. Steinherz, L.J., Steinherz, P.G., Tan, C.T., Heller, G., and Murphy, M.L. 1991. Cardiac toxicity 4 to 20 years after completing anthracycline therapy. *JAMA* 266:1672-1677.
 12. Rugbjerg, K., Mellekjaer, L., Boice, J.D., Kober, L., Ewertz, M., and Olsen, J.H. 2014. Cardiovascular disease in survivors of adolescent and young adult cancer: a Danish cohort study, 1943-2009. *J Natl Cancer Inst* 106:dju110.
 13. Doroshov, J.H. 1983. Effect of anthracycline antibiotics on oxygen radical formation in rat heart. *Cancer Res* 43:460-472.
 14. Kiyomiya, K., Matsuo, S., and Kurebe, M. 2001. Mechanism of specific nuclear transport of adriamycin: the mode of nuclear translocation of adriamycin-proteasome complex. *Cancer Res* 61:2467-2471.

15. Sobek, S., and Boege, F. 2014. DNA topoisomerases in mtDNA maintenance and ageing. *Exp Gerontol* 56:135-141.
16. Zheng, J., Koh, X., Hua, F., Li, G., Larrick, J.W., and Bian, J.S. 2011. Cardioprotection induced by Na(+)/K(+)-ATPase activation involves extracellular signal-regulated kinase 1/2 and phosphoinositide 3-kinase/Akt pathway. *Cardiovasc Res* 89:51-59.
17. Houtkooper, R.H., and Vaz, F.M. 2008. Cardiolipin, the heart of mitochondrial metabolism. *Cell Mol Life Sci* 65:2493-2506.
18. Hahn, V.S., Lenihan, D.J., and Ky, B. 2014. Cancer therapy-induced cardiotoxicity: basic mechanisms and potential cardioprotective therapies. *J Am Heart Assoc* 3:e000665.
19. Arola, O.J., Saraste, A., Pulkki, K., Kallajoki, M., Parvinen, M., and Voipio-Pulkki, L.M. 2000. Acute doxorubicin cardiotoxicity involves cardiomyocyte apoptosis. *Cancer Res* 60:1789-1792.
20. Zhang, Y.W., Shi, J., Li, Y.J., and Wei, L. 2009. Cardiomyocyte death in doxorubicin-induced cardiotoxicity. *Arch Immunol Ther Exp (Warsz)* 57:435-445.
21. Kutateladze, T.G. 2010. Translation of the phosphoinositide code by PI effectors. *Nat Chem Biol* 6:507-513.
22. Deng, S., Yan, T., Jendry, C., Nemecek, A., Vincetic, M., Godtel-Armbrust, U., and Wojnowski, L. 2014. Dexrazoxane may prevent doxorubicin-induced DNA damage via depleting both topoisomerase II isoforms. *BMC Cancer* 14:842.

23. Seifert, C.F., Nesser, M.E., and Thompson, D.F. 1994. Dexrazoxane in the prevention of doxorubicin-induced cardiotoxicity. *Ann Pharmacother* 28:1063-1072.
24. Hasinoff, B.B., Kuschak, T.I., Yalowich, J.C., and Creighton, A.M. 1995. A QSAR study comparing the cytotoxicity and DNA topoisomerase II inhibitory effects of bisdioxopiperazine analogs of ICRF-187 (dexrazoxane). *Biochem Pharmacol* 50:953-958.
25. Shaikh, F., Dupuis, L.L., Alexander, S., Gupta, A., Mertens, L., and Nathan, P.C. 2016. Cardioprotection and Second Malignant Neoplasms Associated With Dexrazoxane in Children Receiving Anthracycline Chemotherapy: A Systematic Review and Meta-Analysis. *J Natl Cancer Inst* 108.
26. Zhang, S., Liu, X., Bawa-Khalife, T., Lu, L.-S., Lyu, Y.L., Liu, L.F., and Yeh, E.T.H. 2012. Identification of the molecular basis of doxorubicin-induced cardiotoxicity. *Nat Med* 18:1639-1642.
27. Minotti, G., Menna, P., Salvatorelli, E., Cairo, G., and Gianni, L. 2004. Anthracyclines: molecular advances and pharmacologic developments in antitumor activity and cardiotoxicity. *Pharmacol Rev* 56:185-229.
28. Zhuo, C., Wang, Y., Wang, X., Wang, Y., and Chen, Y. 2011. Cardioprotection by ischemic postconditioning is abolished in depressed rats: role of Akt and signal transducer and activator of transcription-3. *Mol Cell Biochem* 346:39-47.
29. Burchfield, J.S., Xie, M., and Hill, J.A. 2013. Pathological ventricular remodeling: mechanisms: part 1 of 2. *Circulation* 128:388-400.

30. Willis, M.S., Bevilacqua, A., Pulinilkunnil, T., Kienesberger, P., Tannu, M., and Patterson, C. 2014. The role of ubiquitin ligases in cardiac disease. *J Mol Cell Cardiol* 71:43-53.
31. Yamamoto, Y., Hoshino, Y., Ito, T., Nariai, T., Mohri, T., Obana, M., Hayata, N., Uozumi, Y., Maeda, M., Fujio, Y., et al. 2008. Atrogin-1 ubiquitin ligase is upregulated by doxorubicin via p38-MAP kinase in cardiac myocytes. *Cardiovasc Res* 79:89-96.
32. Roger, V.L., Go, A.S., Lloyd-Jones, D.M., Benjamin, E.J., Berry, J.D., Borden, W.B., Bravata, D.M., Dai, S., Ford, E.S., Fox, C.S., et al. 2012. Heart disease and stroke statistics--2012 update: a report from the American Heart Association. *Circulation* 125:e2-e220.
33. Eltzschig, H.K., and Eckle, T. 2011. Ischemia and reperfusion--from mechanism to translation. *Nat Med* 17:1391-1401.
34. Cokkinos, D.V. 2006. *Myocardial ischemia : from mechanisms to therapeutic potentials*. New York: Springer. viii, 204 p. pp.
35. Luedde, M., Lutz, M., Carter, N., Sosna, J., Jacoby, C., Vucur, M., Gautheron, J., Roderburg, C., Borg, N., Reisinger, F., et al. 2014. RIP3, a kinase promoting necroptotic cell death, mediates adverse remodelling after myocardial infarction. *Cardiovasc Res* 103:206-216.
36. Kalogeris, T., Baines, C.P., Krenz, M., and Korthuis, R.J. 2012. Cell biology of ischemia/reperfusion injury. *Int Rev Cell Mol Biol* 298:229-317.
37. Konstantinidis, K., Whelan, R.S., and Kitsis, R.N. 2012. Mechanisms of cell death in heart disease. *Arterioscler Thromb Vasc Biol* 32:1552-1562.

38. Lopaschuk, G.D., Ussher, J.R., Folmes, C.D., Jaswal, J.S., and Stanley, W.C. 2010. Myocardial fatty acid metabolism in health and disease. *Physiol Rev* 90:207-258.
39. Bolukoglu, H., Goodwin, G.W., Guthrie, P.H., Carmical, S.G., Chen, T.M., and Taegtmeyer, H. 1996. Metabolic fate of glucose in reversible low-flow ischemia of the isolated working rat heart. *Am J Physiol* 270:H817-826.
40. Kubler, W., and Spieckermann, P.G. 1970. Regulation of glycolysis in the ischemic and the anoxic myocardium. *J Mol Cell Cardiol* 1:351-377.
41. Frank, A., Bonney, M., Bonney, S., Weitzel, L., Koeppen, M., and Eckle, T. 2012. Myocardial ischemia reperfusion injury: from basic science to clinical bedside. *Semin Cardiothorac Vasc Anesth* 16:123-132.
42. Marks, A.R. 2003. Calcium and the heart: a question of life and death. *J Clin Invest* 111:597-600.
43. Hanna, A.D., Lam, A., Tham, S., Dulhunty, A.F., and Beard, N.A. 2014. Adverse effects of doxorubicin and its metabolic product on cardiac RyR2 and SERCA2A. *Mol Pharmacol* 86:438-449.
44. Saeki, K., Obi, I., Ogiku, N., Shigekawa, M., Imagawa, T., and Matsumoto, T. 2002. Doxorubicin directly binds to the cardiac-type ryanodine receptor. *Life Sci* 70:2377-2389.
45. Dhalla, N.S., Elmoselhi, A.B., Hata, T., and Makino, N. 2000. Status of myocardial antioxidants in ischemia-reperfusion injury. *Cardiovasc Res* 47:446-456.

46. Santos, C.X., Anilkumar, N., Zhang, M., Brewer, A.C., and Shah, A.M. 2011. Redox signaling in cardiac myocytes. *Free Radic Biol Med* 50:777-793.
47. Makazan, Z., Saini, H.K., and Dhalla, N.S. 2007. Role of oxidative stress in alterations of mitochondrial function in ischemic-reperfused hearts. *Am J Physiol Heart Circ Physiol* 292:H1986-1994.
48. Netticadan, T., Temsah, R., Osada, M., and Dhalla, N.S. 1999. Status of Ca²⁺/calmodulin protein kinase phosphorylation of cardiac SR proteins in ischemia-reperfusion. *Am J Physiol* 277:C384-391.
49. Kuster, G.M., Lancel, S., Zhang, J., Communal, C., Trucillo, M.P., Lim, C.C., Pfister, O., Weinberg, E.O., Cohen, R.A., Liao, R., et al. 2010. Redox-mediated reciprocal regulation of SERCA and Na⁺-Ca²⁺ exchanger contributes to sarcoplasmic reticulum Ca²⁺ depletion in cardiac myocytes. *Free Radic Biol Med* 48:1182-1187.
50. Ichikawa, Y., Ghanefar, M., Bayeva, M., Wu, R., Khechaduri, A., Naga Prasad, S.V., Mutharasan, R.K., Naik, T.J., and Ardehali, H. 2014. Cardiotoxicity of doxorubicin is mediated through mitochondrial iron accumulation. *J Clin Invest* 124:617-630.
51. Li, T., and Singal, P.K. 2000. Adriamycin-induced early changes in myocardial antioxidant enzymes and their modulation by probucol. *Circulation* 102:2105-2110.
52. Van Vleet, J.F., Ferrans, V.J., and Weirich, W.E. 1980. Cardiac disease induced by chronic adriamycin administration in dogs and an evaluation of vitamin E and selenium as cardioprotectants. *Am J Pathol* 99:13-42.

53. Herman, E.H., Ferrans, V.J., Myers, C.E., and Van Vleet, J.F. 1985. Comparison of the effectiveness of (+/-)-1,2-bis(3,5-dioxopiperazinyl-1-yl)propane (ICRF-187) and N-acetylcysteine in preventing chronic doxorubicin cardiotoxicity in beagles. *Cancer Res* 45:276-281.
54. Dresdale, A.R., Barr, L.H., Bonow, R.O., Mathisen, D.J., Myers, C.E., Schwartz, D.E., d'Angelo, T., and Rosenberg, S.A. 1982. Prospective randomized study of the role of N-acetyl cysteine in reversing doxorubicin-induced cardiomyopathy. *Am J Clin Oncol* 5:657-663.
55. Mahley, R.W., Innerarity, T.L., Rall, S.C., Jr., and Weisgraber, K.H. 1984. Plasma lipoproteins: apolipoprotein structure and function. *J Lipid Res* 25:1277-1294.
56. Shah, A.S., Tan, L., Long, J.L., and Davidson, W.S. 2013. Proteomic diversity of high density lipoproteins: our emerging understanding of its importance in lipid transport and beyond. *J Lipid Res* 54:2575-2585.
57. Silverman, D.I., Ginsburg, G.S., and Pasternak, R.C. 1993. High-density lipoprotein subfractions. *Am J Med* 94:636-645.
58. De Lalla, O.F., and Gofman, J.W. 1954. Ultracentrifugal analysis of serum lipoproteins. *Methods Biochem Anal* 1:459-478.
59. Schaefer, E.J., Foster, D.M., Jenkins, L.L., Lindgren, F.T., Berman, M., Levy, R.I., and Brewer, H.B., Jr. 1979. The composition and metabolism of high density lipoprotein subfractions. *Lipids* 14:511-522.
60. Nichols, A.V., Krauss, R.M., and Musliner, T.A. 1986. Nondenaturing polyacrylamide gradient gel electrophoresis. *Methods Enzymol* 128:417-431.

61. Davidson, W.S., Sparks, D.L., Lund-Katz, S., and Phillips, M.C. 1994. The molecular basis for the difference in charge between pre-beta- and alpha-migrating high density lipoproteins. *J Biol Chem* 269:8959-8965.
62. Zannis, V.I., Cole, F.S., Jackson, C.L., Kurnit, D.M., and Karathanasis, S.K. 1985. Distribution of apolipoprotein A-I, C-II, C-III, and E mRNA in fetal human tissues. Time-dependent induction of apolipoprotein E mRNA by cultures of human monocyte-macrophages. *Biochemistry* 24:4450-4455.
63. Klein, I., Sarkadi, B., and Varadi, A. 1999. An inventory of the human ABC proteins. *Biochim Biophys Acta* 1461:237-262.
64. Wang, N., Silver, D.L., Costet, P., and Tall, A.R. 2000. Specific binding of ApoA-I, enhanced cholesterol efflux, and altered plasma membrane morphology in cells expressing ABC1. *J Biol Chem* 275:33053-33058.
65. Langmann, T., Klucken, J., Reil, M., Liebisch, G., Luciani, M.F., Chimini, G., Kaminski, W.E., and Schmitz, G. 1999. Molecular cloning of the human ATP-binding cassette transporter 1 (hABC1): evidence for sterol-dependent regulation in macrophages. *Biochem Biophys Res Commun* 257:29-33.
66. Zannis, V.I., Chroni, A., and Krieger, M. 2006. Role of apoA-I, ABCA1, LCAT, and SR-BI in the biogenesis of HDL. *J Mol Med (Berl)* 84:276-294.
67. Wang, N., Lan, D., Chen, W., Matsuura, F., and Tall, A.R. 2004. ATP-binding cassette transporters G1 and G4 mediate cellular cholesterol efflux to high-density lipoproteins. *Proc Natl Acad Sci U S A* 101:9774-9779.

68. Rigotti, A., Trigatti, B., Babitt, J., Penman, M., Xu, S., and Krieger, M. 1997. Scavenger receptor BI--a cell surface receptor for high density lipoprotein. *Curr Opin Lipidol* 8:181-188.
69. Krieger, M. 1999. Charting the fate of the "good cholesterol": identification and characterization of the high-density lipoprotein receptor SR-BI. *Annu Rev Biochem* 68:523-558.
70. Acton, S., Rigotti, A., Landschulz, K.T., Xu, S., Hobbs, H.H., and Krieger, M. 1996. Identification of scavenger receptor SR-BI as a high density lipoprotein receptor. *Science* 271:518-520.
71. Phillips, M.C. 2014. Molecular mechanisms of cellular cholesterol efflux. *J Biol Chem* 289:24020-24029.
72. Chajek, T., and Fielding, C.J. 1978. Isolation and characterization of a human serum cholesteryl ester transfer protein. *Proc Natl Acad Sci U S A* 75:3445-3449.
73. Jaye, M., Lynch, K.J., Krawiec, J., Marchadier, D., Maugeais, C., Doan, K., South, V., Amin, D., Perrone, M., and Rader, D.J. 1999. A novel endothelial-derived lipase that modulates HDL metabolism. *Nat Genet* 21:424-428.
74. Clay, M.A., Newnham, H.H., Forte, T.M., and Barter, P.I. 1992. Cholesteryl ester transfer protein and hepatic lipase activity promote shedding of apo A-I from HDL and subsequent formation of discoidal HDL. *Biochim Biophys Acta* 1124:52-58.
75. Castelli, W.P., Anderson, K., Wilson, P.W., and Levy, D. 1992. Lipids and risk of coronary heart disease. The Framingham Study. *Ann Epidemiol* 2:23-28.

76. Gordon, D.J., and Rifkind, B.M. 1989. High-density lipoprotein--the clinical implications of recent studies. *N Engl J Med* 321:1311-1316.
77. Nissen, S.E., Tsunoda, T., Tuzcu, E.M., Schoenhagen, P., Cooper, C.J., Yasin, M., Eaton, G.M., Lauer, M.A., Sheldon, W.S., Grines, C.L., et al. 2003. Effect of recombinant ApoA-I Milano on coronary atherosclerosis in patients with acute coronary syndromes: a randomized controlled trial. *JAMA* 290:2292-2300.
78. Navab, M., Anantharamaiah, G.M., Reddy, S.T., Van Lenten, B.J., Datta, G., Garber, D., and Fogelman, A.M. 2004. Human apolipoprotein A-I and A-I mimetic peptides: potential for atherosclerosis reversal. *Curr Opin Lipidol* 15:645-649.
79. Calabresi, L., Rossoni, G., Gomaschi, M., Sisto, F., Berti, F., and Franceschini, G. 2003. High-density lipoproteins protect isolated rat hearts from ischemia-reperfusion injury by reducing cardiac tumor necrosis factor-alpha content and enhancing prostaglandin release. *Circ Res* 92:330-337.
80. Rossoni, G., Gomaschi, M., Berti, F., Sirtori, C.R., Franceschini, G., and Calabresi, L. 2004. Synthetic high-density lipoproteins exert cardioprotective effects in myocardial ischemia/reperfusion injury. *J Pharmacol Exp Ther* 308:79-84.
81. Gordts, S.C., Muthuramu, I., Nefyodova, E., Jacobs, F., Van Craeyveld, E., and De Geest, B. 2013. Beneficial effects of selective HDL-raising gene transfer on survival, cardiac remodelling and cardiac function after myocardial infarction in mice. *Gene Ther* 20:1053-1061.

82. Ballantyne, F.C., Clark, R.S., Simpson, H.S., and Ballantyne, D. 1982. High density and low density lipoprotein subfractions in survivors of myocardial infarction and in control subjects. *Metabolism* 31:433-437.
83. Marchesi, M., Booth, E.A., Davis, T., Bisgaier, C.L., and Lucchesi, B.R. 2004. Apolipoprotein A-IMilano and 1-palmitoyl-2-oleoyl phosphatidylcholine complex (ETC-216) protects the in vivo rabbit heart from regional ischemia-reperfusion injury. *J Pharmacol Exp Ther* 311:1023-1031.
84. Frias, M.A., Lang, U., Gerber-Wicht, C., and James, R.W. 2010. Native and reconstituted HDL protect cardiomyocytes from doxorubicin-induced apoptosis. *Cardiovasc Res* 85:118-126.
85. Parini, P., Johansson, L., Broijersen, A., Angelin, B., and Rudling, M. 2006. Lipoprotein profiles in plasma and interstitial fluid analyzed with an automated gel-filtration system. *Eur J Clin Invest* 36:98-104.
86. Cavelier, C., Ohnsorg, P.M., Rohrer, L., and von Eckardstein, A. 2012. The beta-chain of cell surface F(0)F(1) ATPase modulates apoA-I and HDL transcytosis through aortic endothelial cells. *Arterioscler Thromb Vasc Biol* 32:131-139.
87. Brinck, J.W., Thomas, A., Lauer, E., Jornayvaz, F.R., Brulhart-Meynet, M.C., Prost, J.C., Pataky, Z., Lofgren, P., Hoffstedt, J., Eriksson, M., et al. 2016. Diabetes Mellitus Is Associated With Reduced High-Density Lipoprotein Sphingosine-1-Phosphate Content and Impaired High-Density Lipoprotein Cardiac Cell Protection. *Arterioscler Thromb Vasc Biol* 36:817-824.
88. Shah, P.K., Nilsson, J., Kaul, S., Fishbein, M.C., Ageland, H., Hamsten, A., Johansson, J., Karpe, F., and Cercek, B. 1998. Effects of recombinant

- apolipoprotein A-I(Milano) on aortic atherosclerosis in apolipoprotein E-deficient mice. *Circulation* 97:780-785.
89. Miyazaki, A., Sakuma, S., Morikawa, W., Takiue, T., Miake, F., Terano, T., Sakai, M., Hakamata, H., Sakamoto, Y., Natio, M., et al. 1995. Intravenous injection of rabbit apolipoprotein A-I inhibits the progression of atherosclerosis in cholesterol-fed rabbits. *Arterioscler Thromb Vasc Biol* 15:1882-1888.
90. Dadabayev, A.R., Yin, G., Latchoumycandane, C., McIntyre, T.M., Lesnefsky, E.J., and Penn, M.S. 2014. Apolipoprotein A1 regulates coenzyme Q10 absorption, mitochondrial function, and infarct size in a mouse model of myocardial infarction. *J Nutr* 144:1030-1036.
91. Rohrbach, S., Troidl, C., Hamm, C., and Schulz, R. 2015. Ischemia and reperfusion related myocardial inflammation: A network of cells and mediators targeting the cardiomyocyte. *IUBMB Life* 67:110-119.
92. Theilmeyer, G., Schmidt, C., Herrmann, J., Keul, P., Schafers, M., Herrgott, I., Mersmann, J., Larmann, J., Hermann, S., Stypmann, J., et al. 2006. High-density lipoproteins and their constituent, sphingosine-1-phosphate, directly protect the heart against ischemia/reperfusion injury in vivo via the S1P3 lysophospholipid receptor. *Circulation* 114:1403-1409.
93. Gu, S.S., Shi, N., and Wu, M.P. 2007. The protective effect of ApolipoproteinA-I on myocardial ischemia-reperfusion injury in rats. *Life Sci* 81:702-709.
94. Kalakech, H., Hibert, P., Prunier-Mirebeau, D., Tamareille, S., Letournel, F., Macchi, L., Pinet, F., Furber, A., and Prunier, F. 2014. RISK and SAFE signaling

- pathway involvement in apolipoprotein A-I-induced cardioprotection. *PLoS One* 9:e107950.
95. Tao, R., Hoover, H.E., Honbo, N., Kalinowski, M., Alano, C.C., Karliner, J.S., and Raffai, R. 2010. *High-density lipoprotein determines adult mouse cardiomyocyte fate after hypoxia-reoxygenation through lipoprotein-associated sphingosine 1-phosphate*. H1022-H1028 pp.
96. Matsui, T., and Rosenzweig, A. 2005. Convergent signal transduction pathways controlling cardiomyocyte survival and function: the role of PI 3-kinase and Akt. *J Mol Cell Cardiol* 38:63-71.
97. Matsui, T., Li, L., del Monte, F., Fukui, Y., Franke, T.F., Hajjar, R.J., and Rosenzweig, A. 1999. Adenoviral gene transfer of activated phosphatidylinositol 3'-kinase and Akt inhibits apoptosis of hypoxic cardiomyocytes in vitro. *Circulation* 100:2373-2379.
98. Matsui, T., Tao, J., del Monte, F., Lee, K.H., Li, L., Picard, M., Force, T.L., Franke, T.F., Hajjar, R.J., and Rosenzweig, A. 2001. Akt activation preserves cardiac function and prevents injury after transient cardiac ischemia in vivo. *Circulation* 104:330-335.
99. Liu, P., Cheng, H., Roberts, T.M., and Zhao, J.J. 2009. Targeting the phosphoinositide 3-kinase pathway in cancer. *Nat Rev Drug Discov* 8:627-644.
100. Tao, H., Yancey, P.G., Babaev, V.R., Blakemore, J.L., Zhang, Y., Ding, L., Fazio, S., and Linton, M.F. 2015. Macrophage SR-BI Mediates Efferocytosis via Src/PI3K/Rac1 Signaling and Reduces Atherosclerotic Lesion Necrosis. *Journal of Lipid Research*.

101. Arcaro, A., Aubert, M., Espinosa del Hierro, M.E., Khanzada, U.K., Angelidou, S., Tetley, T.D., Bittermann, A.G., Frame, M.C., and Seckl, M.J. 2007. Critical role for lipid raft-associated Src kinases in activation of PI3K-Akt signalling. *Cell Signal* 19:1081-1092.
102. Currie, R.A., Walker, K.S., Gray, A., Deak, M., Casamayor, A., Downes, C.P., Cohen, P., Alessi, D.R., and Lucocq, J. 1999. Role of phosphatidylinositol 3,4,5-trisphosphate in regulating the activity and localization of 3-phosphoinositide-dependent protein kinase-1. *Biochem J* 337 (Pt 3):575-583.
103. Cohen, M.M., Jr. 2013. The AKT genes and their roles in various disorders. *Am J Med Genet A* 161A:2931-2937.
104. Cho, H., Thorvaldsen, J.L., Chu, Q., Feng, F., and Birnbaum, M.J. 2001. Akt1/PKBalpha is required for normal growth but dispensable for maintenance of glucose homeostasis in mice. *J Biol Chem* 276:38349-38352.
105. Chen, W.S., Xu, P.Z., Gottlob, K., Chen, M.L., Sokol, K., Shiyanova, T., Roninson, I., Weng, W., Suzuki, R., Tobe, K., et al. 2001. Growth retardation and increased apoptosis in mice with homozygous disruption of the Akt1 gene. *Genes Dev* 15:2203-2208.
106. Cho, H., Mu, J., Kim, J.K., Thorvaldsen, J.L., Chu, Q., Crenshaw, E.B., 3rd, Kaestner, K.H., Bartolomei, M.S., Shulman, G.I., and Birnbaum, M.J. 2001. Insulin resistance and a diabetes mellitus-like syndrome in mice lacking the protein kinase Akt2 (PKB beta). *Science* 292:1728-1731.
107. Easton, R.M., Cho, H., Roovers, K., Shineman, D.W., Mizrahi, M., Forman, M.S., Lee, V.M., Szabolcs, M., de Jong, R., Oltersdorf, T., et al. 2005. Role for

- Akt3/protein kinase Bgamma in attainment of normal brain size. *Mol Cell Biol* 25:1869-1878.
108. Alessi, D.R., James, S.R., Downes, C.P., Holmes, A.B., Gaffney, P.R., Reese, C.B., and Cohen, P. 1997. Characterization of a 3-phosphoinositide-dependent protein kinase which phosphorylates and activates protein kinase Balpha. *Curr Biol* 7:261-269.
109. Sarbassov, D.D., Guertin, D.A., Ali, S.M., and Sabatini, D.M. 2005. Phosphorylation and regulation of Akt/PKB by the rictor-mTOR complex. *Science* 307:1098-1101.
110. Worby, C.A., and Dixon, J.E. 2014. Pten. *Annu Rev Biochem* 83:641-669.
111. Resjo, S., Goransson, O., Harndahl, L., Zolnierowicz, S., Manganiello, V., and Degerman, E. 2002. Protein phosphatase 2A is the main phosphatase involved in the regulation of protein kinase B in rat adipocytes. *Cell Signal* 14:231-238.
112. Brunet, A., Bonni, A., Zigmond, M.J., Lin, M.Z., Juo, P., Hu, L.S., Anderson, M.J., Arden, K.C., Blenis, J., and Greenberg, M.E. 1999. Akt promotes cell survival by phosphorylating and inhibiting a Forkhead transcription factor. *Cell* 96:857-868.
113. Fulton, D., Gratton, J.P., McCabe, T.J., Fontana, J., Fujio, Y., Walsh, K., Franke, T.F., Papapetropoulos, A., and Sessa, W.C. 1999. Regulation of endothelium-derived nitric oxide production by the protein kinase Akt. *Nature* 399:597-601.
114. Gao, F., Gao, E., Yue, T.L., Ohlstein, E.H., Lopez, B.L., Christopher, T.A., and Ma, X.L. 2002. Nitric oxide mediates the antiapoptotic effect of insulin in

- myocardial ischemia-reperfusion: the roles of PI3-kinase, Akt, and endothelial nitric oxide synthase phosphorylation. *Circulation* 105:1497-1502.
115. Massion, P.B., Feron, O., Dessy, C., and Balligand, J.L. 2003. Nitric oxide and cardiac function: ten years after, and continuing. *Circ Res* 93:388-398.
116. Morisco, C., Zebrowski, D., Condorelli, G., Tschlis, P., Vatner, S.F., and Sadoshima, J. 2000. The Akt-glycogen synthase kinase 3beta pathway regulates transcription of atrial natriuretic factor induced by beta-adrenergic receptor stimulation in cardiac myocytes. *J Biol Chem* 275:14466-14475.
117. Haq, S., Choukroun, G., Kang, Z.B., Ranu, H., Matsui, T., Rosenzweig, A., Molkentin, J.D., Alessandrini, A., Woodgett, J., Hajjar, R., et al. 2000. Glycogen synthase kinase-3beta is a negative regulator of cardiomyocyte hypertrophy. *J Cell Biol* 151:117-130.
118. Potter, C.J., Pedraza, L.G., and Xu, T. 2002. Akt regulates growth by directly phosphorylating Tsc2. *Nat Cell Biol* 4:658-665.
119. Heineke, J., and Molkentin, J.D. 2006. Regulation of cardiac hypertrophy by intracellular signalling pathways. *Nat Rev Mol Cell Biol* 7:589-600.
120. Taniyama, Y., and Walsh, K. 2002. Elevated myocardial Akt signaling ameliorates doxorubicin-induced congestive heart failure and promotes heart growth. *J Mol Cell Cardiol* 34:1241-1247.
121. Kim, Y.K., Kim, S.J., Yatani, A., Huang, Y., Castelli, G., Vatner, D.E., Liu, J., Zhang, Q., Diaz, G., Zieba, R., et al. 2003. Mechanism of enhanced cardiac function in mice with hypertrophy induced by overexpressed Akt. *J Biol Chem* 278:47622-47628.

122. Hajjar, R.J., Kang, J.X., Gwathmey, J.K., and Rosenzweig, A. 1997. Physiological effects of adenoviral gene transfer of sarcoplasmic reticulum calcium ATPase in isolated rat myocytes. *Circulation* 95:423-429.
123. Cittadini, A., Monti, M.G., Iaccarino, G., Di Rella, F., Tsihchlis, P.N., Di Gianni, A., Stromer, H., Sorriento, D., Peschle, C., Trimarco, B., et al. 2006. Adenoviral gene transfer of Akt enhances myocardial contractility and intracellular calcium handling. *Gene Ther* 13:8-19.
124. Horie, T., Ono, K., Nagao, K., Nishi, H., Kinoshita, M., Kawamura, T., Wada, H., Shimatsu, A., Kita, T., and Hasegawa, K. 2008. Oxidative stress induces GLUT4 translocation by activation of PI3-K/Akt and dual AMPK kinase in cardiac myocytes. *J Cell Physiol* 215:733-742.
125. Markou, T., Cullingford, T.E., Giraldo, A., Weiss, S.C., Alsafi, A., Fuller, S.J., Clerk, A., and Sugden, P.H. 2008. Glycogen synthase kinases 3alpha and 3beta in cardiac myocytes: regulation and consequences of their inhibition. *Cell Signal* 20:206-218.
126. Tong, H., Imahashi, K., Steenbergen, C., and Murphy, E. 2002. Phosphorylation of glycogen synthase kinase-3beta during preconditioning through a phosphatidylinositol-3-kinase--dependent pathway is cardioprotective. *Circ Res* 90:377-379.
127. Canton, J., Neculai, D., and Grinstein, S. 2013. Scavenger receptors in homeostasis and immunity. *Nat Rev Immunol* 13:621-634.
128. Krieger, M. 1998. The "best" of cholesterol, the "worst" of cholesterol: a tale of two receptors. *Proc Natl Acad Sci U S A* 95:4077-4080.

129. Babitt, J., Trigatti, B., Rigotti, A., Smart, E.J., Anderson, R.G., Xu, S., and Krieger, M. 1997. Murine SR-BI, a high density lipoprotein receptor that mediates selective lipid uptake, is N-glycosylated and fatty acylated and colocalizes with plasma membrane caveolae. *J Biol Chem* 272:13242-13249.
130. Neculai, D., Schwake, M., Ravichandran, M., Zunke, F., Collins, R.F., Peters, J., Neculai, M., Plumb, J., Loppnau, P., Pizarro, J.C., et al. 2013. Structure of LIMP-2 provides functional insights with implications for SR-BI and CD36. *Nature* 504:172-176.
131. Yeh, Y.C., Hwang, G.Y., Liu, I.P., and Yang, V.C. 2002. Identification and expression of scavenger receptor SR-BI in endothelial cells and smooth muscle cells of rat aorta in vitro and in vivo. *Atherosclerosis* 161:95-103.
132. Acton, S.L., Scherer, P.E., Lodish, H.F., and Krieger, M. 1994. Expression cloning of SR-BI, a CD36-related class B scavenger receptor. *J Biol Chem* 269:21003-21009.
133. Catanese, M.T., Ansuini, H., Graziani, R., Huby, T., Moreau, M., Ball, J.K., Paonessa, G., Rice, C.M., Cortese, R., Vitelli, A., et al. 2010. Role of scavenger receptor class B type I in hepatitis C virus entry: kinetics and molecular determinants. *J Virol* 84:34-43.
134. Rigotti, A., Trigatti, B.L., Penman, M., Rayburn, H., Herz, J., and Krieger, M. 1997. A targeted mutation in the murine gene encoding the high density lipoprotein (HDL) receptor scavenger receptor class B type I reveals its key role in HDL metabolism. *Proc Natl Acad Sci U S A* 94:12610-12615.

135. Rye, K.A., and Barter, P.J. 2014. Cardioprotective functions of HDLs. *J Lipid Res* 55:168-179.
136. Williams, D.L., de La Llera-Moya, M., Thuahnai, S.T., Lund-Katz, S., Connelly, M.A., Azhar, S., Anantharamaiah, G.M., and Phillips, M.C. 2000. Binding and cross-linking studies show that scavenger receptor BI interacts with multiple sites in apolipoprotein A-I and identify the class A amphipathic alpha-helix as a recognition motif. *J Biol Chem* 275:18897-18904.
137. Gu, X., Kozarsky, K., and Krieger, M. 2000. Scavenger receptor class B, type I-mediated [3H]cholesterol efflux to high and low density lipoproteins is dependent on lipoprotein binding to the receptor. *J Biol Chem* 275:29993-30001.
138. Thuahnai, S.T., Lund-Katz, S., Williams, D.L., and Phillips, M.C. 2001. Scavenger receptor class B, type I-mediated uptake of various lipids into cells. Influence of the nature of the donor particle interaction with the receptor. *J Biol Chem* 276:43801-43808.
139. Gu, X., Trigatti, B., Xu, S., Acton, S., Babitt, J., and Krieger, M. 1998. The efficient cellular uptake of high density lipoprotein lipids via scavenger receptor class B type I requires not only receptor-mediated surface binding but also receptor-specific lipid transfer mediated by its extracellular domain. *J Biol Chem* 273:26338-26348.
140. Pagler, T.A., Rhode, S., Neuhofer, A., Laggner, H., Strobl, W., Hinterdorfer, C., Volf, I., Pavelka, M., Eckhardt, E.R., van der Westhuyzen, D.R., et al. 2006. SR-BI-mediated high density lipoprotein (HDL) endocytosis leads to HDL resecretion facilitating cholesterol efflux. *J Biol Chem* 281:11193-11204.

141. Zhang, Y., Ahmed, A.M., Tran, T.L., Lin, J., McFarlane, N., Boreham, D.R., Igdoura, S.A., Truant, R., and Trigatti, B.L. 2007. The inhibition of endocytosis affects HDL-lipid uptake mediated by the human scavenger receptor class B type I. *Mol Membr Biol* 24:442-454.
142. Li, X.A., Titlow, W.B., Jackson, B.A., Giltiay, N., Nikolova-Karakashian, M., Uittenbogaard, A., and Smart, E.J. 2002. High density lipoprotein binding to scavenger receptor, Class B, type I activates endothelial nitric-oxide synthase in a ceramide-dependent manner. *J Biol Chem* 277:11058-11063.
143. Kimura, T., Tomura, H., Mogi, C., Kuwabara, A., Damirin, A., Ishizuka, T., Sekiguchi, A., Ishiwara, M., Im, D.S., Sato, K., et al. 2006. Role of scavenger receptor class B type I and sphingosine 1-phosphate receptors in high density lipoprotein-induced inhibition of adhesion molecule expression in endothelial cells. *J Biol Chem* 281:37457-37467.
144. Nofer, J.R., Geigenmuller, S., Gopfert, C., Assmann, G., Buddecke, E., and Schmidt, A. 2003. High density lipoprotein-associated lysosphingolipids reduce E-selectin expression in human endothelial cells. *Biochem Biophys Res Commun* 310:98-103.
145. Gong, M., Wilson, M., Kelly, T., Su, W., Dressman, J., Kincer, J., Matveev, S.V., Guo, L., Guerin, T., Li, X.A., et al. 2003. HDL-associated estradiol stimulates endothelial NO synthase and vasodilation in an SR-BI-dependent manner. *J Clin Invest* 111:1579-1587.
146. Gao, M., Zhao, D., Schouteden, S., Sorci-Thomas, M.G., Van Veldhoven, P.P., Eggermont, K., Liu, G., Verfaillie, C.M., and Feng, Y. 2014. Regulation of high-

- density lipoprotein on hematopoietic stem/progenitor cells in atherosclerosis requires scavenger receptor type BI expression. *Arterioscler Thromb Vasc Biol* 34:1900-1909.
147. Xu, J., Qian, J., Xie, X., Lin, L., Ma, J., Huang, Z., Fu, M., Zou, Y., and Ge, J. 2012. High density lipoprotein cholesterol promotes the proliferation of bone-derived mesenchymal stem cells via binding scavenger receptor-B type I and activation of PI3K/Akt, MAPK/ERK1/2 pathways. *Mol Cell Biochem* 371:55-64.
148. Mineo, C., Yuhanna, I.S., Quon, M.J., and Shaul, P.W. 2003. High density lipoprotein-induced endothelial nitric-oxide synthase activation is mediated by Akt and MAP kinases. *J Biol Chem* 278:9142-9149.
149. Grewal, T., de Diego, I., Kirchhoff, M.F., Tebar, F., Heeren, J., Rinninger, F., and Enrich, C. 2003. High density lipoprotein-induced signaling of the MAPK pathway involves scavenger receptor type BI-mediated activation of Ras. *J Biol Chem* 278:16478-16481.
150. Al-Jarallah, A., Chen, X., Gonzalez, L., and Trigatti, B.L. 2014. High density lipoprotein stimulated migration of macrophages depends on the scavenger receptor class B, type I, PDZK1 and Akt1 and is blocked by sphingosine 1 phosphate receptor antagonists. *PLoS One* 9:e106487.
151. Zhang, Y., Ahmed, A.M., McFarlane, N., Capone, C., Boreham, D.R., Truant, R., Igdoura, S.A., and Trigatti, B.L. 2007. Regulation of SR-BI-mediated selective lipid uptake in Chinese hamster ovary-derived cells by protein kinase signaling pathways. *J Lipid Res* 48:405-416.

152. Wu, B.J., Chen, K., Shrestha, S., Ong, K.L., Barter, P.J., and Rye, K.A. 2013. High-density lipoproteins inhibit vascular endothelial inflammation by increasing 3beta-hydroxysteroid-Delta24 reductase expression and inducing heme oxygenase-1. *Circ Res* 112:278-288.
153. Al-Jarallah, A. 2011. Insights into the development of atherosclerosis and coronary artery disease: studies from gene targeted mice lacking the high density lipoprotein receptor, SR-B1 In *Biochemistry and Biomedical Sciences*: McMaster University. 311.
154. P., Y. 2016. The high density lipoprotein and atherosclerosis. In *Biochemistry and Biomedical Sciences*: McMaster University.
155. Bhuiyan, M.S., and Fukunaga, K. 2009. Cardioprotection by vanadium compounds targeting Akt-mediated signaling. *J Pharmacol Sci* 110:1-13.
156. Yet, S.F., Tian, R., Layne, M.D., Wang, Z.Y., Maemura, K., Solovyeva, M., Ith, B., Melo, L.G., Zhang, L., Ingwall, J.S., et al. 2001. Cardiac-specific expression of heme oxygenase-1 protects against ischemia and reperfusion injury in transgenic mice. *Circ Res* 89:168-173.
157. Hangaishi, M., Ishizaka, N., Aizawa, T., Kurihara, Y., Taguchi, J., Nagai, R., Kimura, S., and Ohno, M. 2000. Induction of heme oxygenase-1 can act protectively against cardiac ischemia/reperfusion in vivo. *Biochem Biophys Res Commun* 279:582-588.
158. Yan, B., A, J., Hao, H., Wang, G., Zhu, X., Zha, W., Liu, L., Guan, E., Zhang, Y., Gu, S., et al. 2009. Metabonomic phenotype and identification of "heart blood

- stasis obstruction pattern" and "qi and yin deficiency pattern" of myocardial ischemia rat models. *Sci China C Life Sci* 52:1081-1090.
159. Yuhanna, I.S., Zhu, Y., Cox, B.E., Hahner, L.D., Osborne-Lawrence, S., Lu, P., Marcel, Y.L., Anderson, R.G., Mendelsohn, M.E., Hobbs, H.H., et al. 2001. High-density lipoprotein binding to scavenger receptor-BI activates endothelial nitric oxide synthase. *Nat Med* 7:853-857.
160. Ryu, S.M., Kim, H.J., Cho, K.R., and Jo, W.M. 2009. Myocardial protective effect of tezosentan, an endothelin receptor antagonist, for ischemia-reperfusion injury in experimental heart failure models. *J Korean Med Sci* 24:782-788.
161. Mitsos, S., Katsanos, K., Dougeni, E., Koletsis, E.N., and Dougenis, D. 2009. A critical appraisal of open- and closed-chest models of experimental myocardial ischemia. *Lab Anim (NY)* 38:167-177.
162. Fu, X.C., Wang, X., Zheng, H., and Ma, L.P. 2007. [Protective effects of orientin on myocardial ischemia and hypoxia in animal models]. *Nan Fang Yi Ke Da Xue Xue Bao* 27:1173-1175.
163. Seetharam, D., Mineo, C., Gormley, A.K., Gibson, L.L., Vongpatanasin, W., Chambliss, K.L., Hahner, L.D., Cummings, M.L., Kitchens, R.L., Marcel, Y.L., et al. 2006. High-density lipoprotein promotes endothelial cell migration and reendothelialization via scavenger receptor-B type I. *Circ Res* 98:63-72.
164. Caligiuri, G., Levy, B., Pernow, J., Thoren, P., and Hansson, G.K. 1999. Myocardial infarction mediated by endothelin receptor signaling in hypercholesterolemic mice. *Proc Natl Acad Sci U S A* 96:6920-6924.

165. Braun, A., Trigatti, B.L., Post, M.J., Sato, K., Simons, M., Edelberg, J.M., Rosenberg, R.D., Schrenzel, M., and Krieger, M. 2002. Loss of SR-BI expression leads to the early onset of occlusive atherosclerotic coronary artery disease, spontaneous myocardial infarctions, severe cardiac dysfunction, and premature death in apolipoprotein E-deficient mice. *Circ Res* 90:270-276.
166. Fuller, M., Dadoo, O., Serkis, V., Abutouk, D., MacDonald, M., Dhingani, N., Macri, J., Igdoura, S.A., and Trigatti, B.L. 2014. The effects of diet on occlusive coronary artery atherosclerosis and myocardial infarction in scavenger receptor class B, type 1/low-density lipoprotein receptor double knockout mice. *Arterioscler Thromb Vasc Biol* 34:2394-2403.
167. Zhang, S., Picard, M.H., Vasile, E., Zhu, Y., Raffai, R.L., Weisgraber, K.H., and Krieger, M. 2005. Diet-induced occlusive coronary atherosclerosis, myocardial infarction, cardiac dysfunction, and premature death in scavenger receptor class B type I-deficient, hypomorphic apolipoprotein ER61 mice. *Circulation* 111:3457-3464.
168. Tao, R., Hoover, H.E., Honbo, N., Kalinowski, M., Alano, C.C., Karliner, J.S., and Raffai, R. 2010. High-density lipoprotein determines adult mouse cardiomyocyte fate after hypoxia-reoxygenation through lipoprotein-associated sphingosine 1-phosphate. *Am J Physiol Heart Circ Physiol* 298:H1022-1028.
169. Black, S.C. 2000. In vivo models of myocardial ischemia and reperfusion injury: application to drug discovery and evaluation. *J Pharmacol Toxicol Methods* 43:153-167.

170. Zhu, H.M., and Deng, L. 2012. Evaluation of cardiomyocyte hypoxia injury models for the pharmacological study in vitro. *Pharm Biol* 50:167-174.
171. Miettinen, H.E., Rayburn, H., and Krieger, M. 2001. Abnormal lipoprotein metabolism and reversible female infertility in HDL receptor (SR-BI)-deficient mice. *J Clin Invest* 108:1717-1722.
172. Rubin, E.M., Ishida, B.Y., Clift, S.M., and Krauss, R.M. 1991. Expression of human apolipoprotein A-I in transgenic mice results in reduced plasma levels of murine apolipoprotein A-I and the appearance of two new high density lipoprotein size subclasses. *Proceedings of the National Academy of Sciences of the United States of America* 88:434-438.
173. Sharma, M., Tuaine, J., McLaren, B., Waters, D.L., Black, K., Jones, L.M., and McCormick, S.P. 2016. Chemotherapy Agents Alter Plasma Lipids in Breast Cancer Patients and Show Differential Effects on Lipid Metabolism Genes in Liver Cells. *PLoS One* 11:e0148049.
174. Kotani, K., Sekine, Y., Ishikawa, S., Ikpot, I.Z., Suzuki, K., and Remaley, A.T. 2013. High-density lipoprotein and prostate cancer: an overview. *J Epidemiol* 23:313-319.
175. Jafri, H., Alsheikh-Ali, A.A., and Karas, R.H. 2010. Baseline and on-treatment high-density lipoprotein cholesterol and the risk of cancer in randomized controlled trials of lipid-altering therapy. *J Am Coll Cardiol* 55:2846-2854.
176. Zamanian-Daryoush, M., Lindner, D., Tallant, T.C., Wang, Z., Buffa, J., Klipfell, E., Parker, Y., Hatala, D., Parsons-Wingerter, P., Rayman, P., et al. 2013. The

- cardioprotective protein apolipoprotein A1 promotes potent anti-tumorigenic effects. *J Biol Chem* 288:21237-21252.
177. Yuan, Y., Wang, W., Wang, B., Zhu, H., Zhang, B., and Feng, M. 2013. Delivery of hydrophilic drug doxorubicin hydrochloride-targeted liver using apoAI as carrier. *J Drug Target* 21:367-374.
178. Kingwell, B.A., Chapman, M.J., Kontush, A., and Miller, N.E. 2014. HDL-targeted therapies: progress, failures and future. *Nat Rev Drug Discov* 13:445-464.
179. Goldbourt, U., Cohen, L., and Neufeld, H.N. 1986. High density lipoprotein cholesterol: prognosis after myocardial infarction. The Israeli Ischemic Heart Disease Study. *Int J Epidemiol* 15:51-55.
180. Smith, J.D. 2010. Dysfunctional HDL as a diagnostic and therapeutic target. *Arterioscler Thromb Vasc Biol* 30:151-155.
181. Annema, W., and von Eckardstein, A. 2016. Dysfunctional high-density lipoproteins in coronary heart disease: implications for diagnostics and therapy. *Transl Res*.
182. Besler, C., Heinrich, K., Rohrer, L., Doerries, C., Riwanto, M., Shih, D.M., Chroni, A., Yonekawa, K., Stein, S., Schaefer, N., et al. 2011. Mechanisms underlying adverse effects of HDL on eNOS-activating pathways in patients with coronary artery disease. *J Clin Invest* 121:2693-2708.
183. Riwanto, M., Rohrer, L., Roschitzki, B., Besler, C., Mocharla, P., Mueller, M., Perisa, D., Heinrich, K., Altwegg, L., von Eckardstein, A., et al. 2013. Altered activation of endothelial anti- and proapoptotic pathways by high-density

- lipoprotein from patients with coronary artery disease: role of high-density lipoprotein-proteome remodeling. *Circulation* 127:891-904.
184. Navab, M., Hama, S.Y., Anantharamaiah, G.M., Hassan, K., Hough, G.P., Watson, A.D., Reddy, S.T., Sevanian, A., Fonarow, G.C., and Fogelman, A.M. 2000. Normal high density lipoprotein inhibits three steps in the formation of mildly oxidized low density lipoprotein: steps 2 and 3. *J Lipid Res* 41:1495-1508.
185. Hansel, B., Giral, P., Nobecourt, E., Chantepie, S., Bruckert, E., Chapman, M.J., and Kontush, A. 2004. Metabolic syndrome is associated with elevated oxidative stress and dysfunctional dense high-density lipoprotein particles displaying impaired antioxidative activity. *J Clin Endocrinol Metab* 89:4963-4971.
186. Cavallero, E., Dachet, C., Neufcour, D., Wirquin, E., Mathe, D., and Jacotot, B. 1994. Postprandial amplification of lipoprotein abnormalities in controlled type II diabetic subjects: relationship to postprandial lipemia and C-peptide/glucagon levels. *Metabolism* 43:270-278.
187. Biesbroeck, R.C., Albers, J.J., Wahl, P.W., Weinberg, C.R., Bassett, M.L., and Bierman, E.L. 1982. Abnormal composition of high density lipoproteins in non-insulin-dependent diabetics. *Diabetes* 31:126-131.
188. Gowri, M.S., Van der Westhuyzen, D.R., Bridges, S.R., and Anderson, J.W. 1999. Decreased protection by HDL from poorly controlled type 2 diabetic subjects against LDL oxidation may be due to the abnormal composition of HDL. *Arterioscler Thromb Vasc Biol* 19:2226-2233.
189. Argraves, K.M., Sethi, A.A., Gazzolo, P.J., Wilkerson, B.A., Remaley, A.T., Tybjaerg-Hansen, A., Nordestgaard, B.G., Yeatts, S.D., Nicholas, K.S., Barth,

- J.L., et al. 2011. S1P, dihydro-S1P and C24:1-ceramide levels in the HDL-containing fraction of serum inversely correlate with occurrence of ischemic heart disease. *Lipids Health Dis* 10:70.
190. Nicholls, S.J., Lundman, P., Harmer, J.A., Cutri, B., Griffiths, K.A., Rye, K.A., Barter, P.J., and Celermajer, D.S. 2006. Consumption of saturated fat impairs the anti-inflammatory properties of high-density lipoproteins and endothelial function. *J Am Coll Cardiol* 48:715-720.
191. Navab, M., Anantharamaiah, G.M., Reddy, S.T., Hama, S., Hough, G., Grijalva, V.R., Yu, N., Ansell, B.J., Datta, G., Garber, D.W., et al. 2005. Apolipoprotein A-I mimetic peptides. *Arterioscler Thromb Vasc Biol* 25:1325-1331.
192. Tardif, J.C., Gregoire, J., L'Allier, P.L., Ibrahim, R., Lesperance, J., Heinonen, T.M., Kouz, S., Berry, C., Basser, R., Lavoie, M.A., et al. 2007. Effects of reconstituted high-density lipoprotein infusions on coronary atherosclerosis: a randomized controlled trial. *JAMA* 297:1675-1682.
193. Nicholls, S.J., Tuzcu, E.M., Sipahi, I., Schoenhagen, P., Crowe, T., Kapadia, S., and Nissen, S.E. 2006. Relationship between atheroma regression and change in lumen size after infusion of apolipoprotein A-I Milano. *J Am Coll Cardiol* 47:992-997.
194. Patel, S., Drew, B.G., Nakhla, S., Duffy, S.J., Murphy, A.J., Barter, P.J., Rye, K.A., Chin-Dusting, J., Hoang, A., Sviridov, D., et al. 2009. Reconstituted high-density lipoprotein increases plasma high-density lipoprotein anti-inflammatory properties and cholesterol efflux capacity in patients with type 2 diabetes. *J Am Coll Cardiol* 53:962-971.

195. Nanjee, M.N., Doran, J.E., Lerch, P.G., and Miller, N.E. 1999. Acute effects of intravenous infusion of ApoA1/phosphatidylcholine discs on plasma lipoproteins in humans. *Arterioscler Thromb Vasc Biol* 19:979-989.
196. Carballo-Jane, E., Chen, Z., O'Neill, E., Wang, J., Burton, C., Chang, C.H., Chen, X., Eveland, S., Frantz-Wattley, B., Gagen, K., et al. 2010. ApoA-I mimetic peptides promote pre-beta HDL formation in vivo causing remodeling of HDL and triglyceride accumulation at higher dose. *Bioorg Med Chem* 18:8669-8678.
197. Song, X., Fischer, P., Chen, X., Burton, C., and Wang, J. 2009. An apoA-I mimetic peptide facilitates off-loading cholesterol from HDL to liver cells through scavenger receptor BI. *Int J Biol Sci* 5:637-646.
198. Garber, D.W., Datta, G., Chaddha, M., Palgunachari, M.N., Hama, S.Y., Navab, M., Fogelman, A.M., Segrest, J.P., and Anantharamaiah, G.M. 2001. A new synthetic class A amphipathic peptide analogue protects mice from diet-induced atherosclerosis. *J Lipid Res* 42:545-552.
199. Navab, M., Anantharamaiah, G.M., Hama, S., Garber, D.W., Chaddha, M., Hough, G., Lallone, R., and Fogelman, A.M. 2002. Oral administration of an Apo A-I mimetic Peptide synthesized from D-amino acids dramatically reduces atherosclerosis in mice independent of plasma cholesterol. *Circulation* 105:290-292.
200. Roberts, C.K., Ng, C., Hama, S., Eliseo, A.J., and Barnard, R.J. 2006. Effect of a short-term diet and exercise intervention on inflammatory/anti-inflammatory properties of HDL in overweight/obese men with cardiovascular risk factors. *J Appl Physiol (1985)* 101:1727-1732.

201. Casella-Filho, A., Chagas, A.C., Maranhao, R.C., Trombetta, I.C., Cesena, F.H., Silva, V.M., Tanus-Santos, J.E., Negrao, C.E., and da Luz, P.L. 2011. Effect of exercise training on plasma levels and functional properties of high-density lipoprotein cholesterol in the metabolic syndrome. *Am J Cardiol* 107:1168-1172.
202. Huby, T., Doucet, C., Dachet, C., Ouzilleau, B., Ueda, Y., Afzal, V., Rubin, E., Chapman, M.J., and Lesnik, P. 2006. Knockdown expression and hepatic deficiency reveal an atheroprotective role for SR-BI in liver and peripheral tissues. *J Clin Invest* 116:2767-2776.
203. Suzuki, A., Nakano, T., Mak, T.W., and Sasaki, T. 2008. Portrait of PTEN: messages from mutant mice. *Cancer Sci* 99:209-213.
204. Dillon, L.M., and Miller, T.W. 2014. Therapeutic targeting of cancers with loss of PTEN function. *Curr Drug Targets* 15:65-79.
205. Ruan, H., Li, J., Ren, S., Gao, J., Li, G., Kim, R., Wu, H., and Wang, Y. 2009. Inducible and cardiac specific PTEN inactivation protects ischemia/reperfusion injury. *J Mol Cell Cardiol* 46:193-200.
206. Wang, J., Chen, H., Su, Q., Zhou, Y., Liu, T., and Li, L. 2016. The PTEN/Akt Signaling Pathway Mediates Myocardial Apoptosis in Swine After Coronary Microembolization. *J Cardiovasc Pharmacol Ther.*
207. Spinelli, L., Lindsay, Y.E., and Leslie, N.R. 2015. PTEN inhibitors: an evaluation of current compounds. *Adv Biol Regul* 57:102-111.
208. Luss, H., Klein-Wiele, O., Boknik, P., Herzig, S., Knapp, J., Linck, B., Muller, F.U., Scheld, H.H., Schmid, C., Schmitz, W., et al. 2000. Regional expression of

protein phosphatase type 1 and 2A catalytic subunit isoforms in the human heart.

J Mol Cell Cardiol 32:2349-2359.

209. Li, L., Fang, C., Xu, D., Xu, Y., Fu, H., and Li, J. 2016. Cardiomyocyte specific deletion of PP2A causes cardiac hypertrophy. *Am J Transl Res* 8:1769-1779.